Effects of Transcranial Direct Current Stimulation on Neural Activity in the Primate Brain

By

STACEY SEIDL

DISSERTATION

Submitted in partial satisfaction of the requirements for the degree of

DOCTOR OF PHILOSOPHY

in

NEUROSCIENCE

in the

OFFICE OF GRADUATE STUDIES

of the

UNIVERSITY OF CALIFORNIA DAVIS

Approved:

_____

Jochen Ditterich, Chair

_____

Silvia Bunge

_____

Steven J Luck

_____

Charan Ranganath

_____

W. Martin Usrey, Advisor

Committee in Charge 2021

Acknowledgements

Firstly, I would like to express my sincere gratitude to my advisors Dr. Evan Antzoulatos and Dr. W. Martin Usrey for their continuous support over the course of my Ph.D. They both helped guide my research and provided support and encouragement. I thank them for their patience, motivation, and immense knowledge.

Besides my advisor, I would like to thank the rest of my thesis committee: Dr. Jochen Ditterich, Dr. Steven J Luck, Dr. Charan Ranganath, and Dr. Silvia Bunge for their insightful discussions, comments, and continuous encouragement. Their assistance was invaluable, and I greatly appreciate their constructive criticism and friendly advice. My sincere thanks also goes to my previous academic and research advisors Dr. Gene Gurkoff, Dr. Kia Shahlaie, Dr. Dorothy Kozlowski, Dr. Judith Potashkin, and Dr. Jessica Pamment, who provided me an opportunity to join their teams as a trainee, gave me access to their classrooms, laboratories and research facilities, and have been with me since the beginning. Without their inspiration and precious support, I would have not embarked on this journey in the first place - I am sincerely grateful.

I thank my fellow lab mates for the stimulating discussions, advice and support through the years. I will never forget all the sleepless nights we were working together in the lab and all the laughs and fun times we have had. Additionally, I thank my neuroscience cohort of 2014 for going on and completing this journey together – we did it!

There are also a lot of people in my personal life I would like to thank, including my best friends Lillian Perez, Amanda Siekierski, and Caitlin Sullivan who have always

been my cheerleaders and always encourage me to strive to be my best. I would also like to thank all my other friends who continually encouraged my happiness and helped me find work-life balance.

Last but not the least, I would like to thank my family: my parents and my sister for their love and support throughout my thesis and life. They kept me going during every step of the way and this work would not have been possible without them.

Table of Contents

Abstract

Transcranial direct current stimulation (tDCS) is a non-invasive brain stimulation technique that has shown promise in improving cognitive functioning and as a therapy for neurological disorders. Recent studies have shown that it can modulate widespread neural activity; yet these effects are highly variable and depend on the areas being stimulated (montage) and the type of stimulation (polarity and intensity). We tested two tDCS stimulation montages (unilateral and bilateral) targeting the nonhuman primate prefrontal cortex (PFC) and examined their influence on spectral power in scalp-recorded electroencephalogram (EEG) and intracortical recorded local field potentials (LFPs). The effects of polarity (anodal or cathodal) and intensity (0.5-1.5 mA) were also examined. Our results suggest that tDCS with a bilateral montage may be more effective in changing spectral power than unilateral, causing a robust increase in power post-stimulation in frontal scalp electrodes, focused in the lower frequency bands. No effects of polarity were seen, but intensity of stimulation showed a roughly linear effect on power. Minimal EEG power changes were observed in parietal recordings post-stimulation, which tended to show decreases in power. These results highlight the importance of electrode placement and targeting specific brain areas when considering the potential efficacy of tDCS. Furthermore, these data allow a better understand the underlying mechanisms of tDCS and can help translate findings across experimental studies.

List of Abbreviations

ACC	Anterior cingulate
BOLD	Blood-oxygen-level-dependent imaging
CAD	Caudate nucleus
DPM	Dorsal premotor cortex
DTI	Diffusion tensor imaging
EEG	Electroencephalogram
fMRI	Functional magnetic resonance imaging
HD-tDCS	High-definition transcranial direct current stimulation
LFP	Local field potential
LTP	Long-term potentiation
LTD	Long-term depression
MEG	Magnetoencephalography
NHP	Nonhuman primate
PFC	Prefrontal cortex
ROI	Region of interest
tDCS	Transcranial direct current stimulation
tACS	Transcranial alternating current stimulation
tES	Transcranial electric stimulation
tRNS	Transcranial random noise stimulation
TMS	Transcranial magnetic stimulation

Chapter 1: Introduction

Transcranial Electric Stimulation (tES)

tES is a brain stimulation technique that passes electrical current through the brain to modulate brain function. It has gained popularity as a non-invasive, painless, inexpensive, easy to use/administer, and portable technique, allowing the investigation of neural systems and brain-behavior relationships (Paulus, 2011). A partial list of tDCS effects include its ability to regulate neuronal excitability (Nitsche & Paulus, 2000, 2011), entrain spontaneous oscillatory activity (Ali et al., 2013; Helfrich et al., 2014; Ozen et al., 2010), alter cognitive performance (Coffman et al., 2014), and impact pathologic psychiatric processes (Kuo et al., 2014). In general, tES works by passing weak electrical current through the brain via scalp electrodes. However, only a portion of the current applied reaches the brain.

Three main types of tES exist and include: transcranial direct current stimulation (tDCS), transcranial alternating current stimulation (tACS), and random noise stimulation (tRNS). Despite the similarity of electrodes and placement of these techniques, they differ in stimulation pattern and are therefore thought to have unique behavioral and neural outcomes. These contrast to other forms of stimulation like transcranial magnetic stimulation (TMS) or deep brain stimulation in that the currents delivered in tES techniques are weak (subthreshold) and are believed to not be powerful enough to elicit an action potentials (Radman et al., 2009). We will focus on the use and effects of tDCS and less on tACS or tRNS; however a brief introduction to each follows. The use of tACS and tRNS can have advantages, such as reduced cutaneous perception of stimulation by subjects (Ambrus et al., 2012; Paulus, 2011), but

here we will focus on tDCS because it is the most common and well-understood type of tES (for reference on tACS and tRNS please see (Antal & Herrmann, 2016; Reato et al., 2013). Additionally, the proposed experiments in Chapter 2 and 3 explore the effects of tDCS in the brain.

Transcranial Direct Current Stimulation

Direct current electrical stimulation has been around for more than 100 years as a potential therapeutic tool dating back to the 1800s. Although tDCS has changed from electric current derived from animals, to galvanic batteries and transistors, and modern tDCS uses microprocessors and controllers, the same basic setup remains (Sarmiento et al., 2016). Simply, tDCS works by delivering a constant current through scalp electrodes at low intensities (e.g. 0.5–2 mA). Current flows unilaterally from an active electrode through the brain, including the cerebral cortex, before returning through another electrode. The attractiveness of this technique stems from its potential to modulate cortical excitability with the hope to improve cognitive states and behavior (Nitsche & Paulus, 2000). However, the low-intensity electrical fields generated by tDCS are subthreshold, meaning that it is capable of modifying neuronal transmembrane potentials and modulating excitability - bringing neurons closer to their firing threshold without directly eliciting suprathreshold depolarization (Bikson, 2004).

Simply put, tDCS can be described as hooking up a 9V battery to your head. Where the positive terminal on the battery (or anode) goes to one location and the negative terminal (cathode) to another. The electrical connections between the battery terminals are made through wires and conductive contacts (rubber pads, saline soaked

sponges or electrodes) completing a circuit. **Appendix Figure 1** shows a simplified schematic. Commercially available tDCS systems allow you to manipulate several functions, which are described in the section below. Importantly, it allows the user to turn up or down the intensity of current being delivered, ramp up or down the current across time, and maintain constant current flow across changes in resistance. The advantage of having software to ramp the current up and down slowly is that sudden changes in voltage can harm tissue and invoke sensations (and side effects). Most of these devices also pass very small pulses riding on top of the direct current to assess the quality (impedance) of the circuit through the head as stimulation is delivered. With this method, the user can determine if the resistance has become too high in the circuit. Resistance is simply a measure of how much the material in a circuit reduces the flow of electrical current through it.

Transcranial Alternative Current Stimulation

tACS is used to entrain and alter endogenous oscillatory brain activity in a state dependent manner (Silvanto et al., 2008). Electrical current is passed between electrodes which alternates electrode polarity at a specific frequency. Unlike tDCS, tACS does not alter steady levels of neuronal excitability, but entrains the neuronal firing from the large number of underlying neurons to the exogenous frequency (Battleday et al., 2014). Neuronal entrainment is achieved by the applied current altering the transmembrane potential of neurons. The polarization of neurons is reflected by the current applied to it, leading to a time-varying fluctuation (typically sinusodial) in membrane potential. This fluctuation is both frequency dependent and linearly

proportional to the applied current (Kanai et al., 2008); however, lower frequency stimulation induces larger polarization than does higher frequency stimulation (Reato et al., 2010; Tavakoli & Yun, 2017). Importantly, in comparing tDCS and tACS studies, it is difficult to draw general conclusions about efficacy because of the skull working as a low-pass filter (Nunez & Srinivasan, 2006). The skull effectively attenuates more and more of the tACS applied as higher frequencies are used, filtering much of it above 25 Hz (Reinhart et al., 2017).

Transcranial Random Noise Stimulation

tRNS is similar to tACS in that it uses an alternating current; however, instead of stimulating at a fixed frequency throughout the stimulation period, tRNS alternates at a random frequency and amplitude within a defined range. Stimulation frequency for tRNS is normally distributed between 0.1 and 640 Hz (Terney et al., 2008), although it can be divided into low (0.1–100 Hz) or high (101-640 Hz) frequency stimulation (Fertonani et al., 2011). tRNS is thought to induce excitation resulting in plasticity.

General tES Methodologies and Strategies Used for this Study

tES is a technique that delivers weak electric currents to the scalp using conductive rubber electrodes placed in saline-soaked sponges (Bogaard et al., 2019) or Ag/AgCl electrodes applied with conductive paste or EEG gel. tES is used to target specific regions of interest in the brain in aims to induce shifts in neuronal membrane excitability, resulting in secondary changes in cortical activity. Types of tES are now concomitant with EEG monitoring and use, as similar electrodes can be used to both

stimulate and record neuronal activity. These combined systems can provide valuable information on the mechanisms of tDCS. In addition, EEG findings can be an important surrogate marker for the effects of tDCS and thus can be used to optimize its parameters (Schestatsky et al., 2013). General methodologies on tES setups are important as the experiments in Chapter 2 and 3 utilize the NHP as a model system to investigate the effects of tDCS. As no standardized experimental setups exist, it was therefore necessary for us to create a novel setup.

Electrode localization: Strategic placement of scalp electrodes should aim to create the largest current flow between electrodes and reduce shunting across the scalp. Modeling research has shown that a higher percentage of current penetrates the brain if the electrodes (on the scalp) are placed further apart (Miranda et al., 2006). A distance of at least 8 cm when using 35 cm^2 electrodes has been recommended (Wagner et al., 2007). However, large distances may also require higher stimulation intensities in tDCS studies (Moliadze et al., 2010) as current may dissipate. Yet, it has been suggested that if the distance between electrodes is 5 cm or less, the current would be highly susceptible to a shunting effect (Rush & Driscoll, 1968). Generally, large distances between the scalp electrodes, are expected to increase cortical modulation, allowing the current to be drawn through the cortex, rather than shunted across the scalp (Bikson et al., 2010). Although some montages place electrodes closer together, this may allow current to flow through the cerebrospinal fluid (CSF) from one electrode to the other, without stimulating the cortex. This results from CSF being more conductive than brain tissue (Moliadze et al., 2010).

Several methods can be used to localize the placement of scalp electrodes for tES, with the most common being based on the EEG 10-20 EEG system (Klem et al., 1999). This technique is based on measuring the participants head (naison to inion and from left preauricular to right; (Klem et al., 1999)) in order to locate regions of interest. Since regions of interest may be small, head measurements may be used in combination with brain imaging techniques such as fMRI or PET (Nitsche et al., 2008). Alternatively, neuro-navigation software can also be used if a subject has an MRI. Combination techniques or neuro-navigation are more accurate than the 10-20 system because they account for individual brain variability. However, these other techniques are more expensive and are typically less frequently used. Placement of scalp electrodes can also be done based on physiological measures. For example, motor cortex can be mapped using TMS via inducing MEPs to identify this region (e.g., (Nitsche & Paulus, 2000)). However, physiology-based placement is currently limited to only a few cortical areas (Woods et al., 2016). For our studies, we determined scalp electrode placement using the 10-20 EEG system. The experiments described in Chapter 2 and 3 will also explored how changes in electrode location influence neural activity.

Electrode Contact: Most types of electrodes rely on a contact medium to ensure connectivity between the electrode and scalp. While electro-conductive gel or paste is most commonly used, sponge electrodes use saline as a medium. A study by (Dundas et al., 2007) tested the perception of comfort with different saline concentrations. 15 to 140 mM concentration was found to be most comfortable in comparison to 220 mM or

deionized water (Dundas et al., 2007). Choosing one type of medium over another may depend on availability, ease of loading and use, and preference (DaSilva et al., 2011). It is reported that different types of gels influenced cutaneous sensations in participants as well (Fertonani et al., 2015). Importantly, all types of media have the potential to dry out over time and, due to the temperature that the electrode emits, can consequently increase the risk of burns to the scalp (Lagopoulos & Degabriele, 2008). The amount of contact medium should also be monitored, as too much may lead to bridging and changes in current flow (for further discussion see: (Horvath et al., 2014). Since few NHP tDCS studies have been conducted, conductive paste and gel were both tested (Signa). For ease of use loading the electrodes and for more consistent connectivity, the following studies used the gel.

Ensuring electrodes do not move while recording neural activity or during stimulation is important. A study by Woods et al 2015 showed that movement by 5% during tDCS can alter the accuracy and intensity of the current to targeted brain areas. There are many ways electrodes can be secured to the scalp including rubber bands, elastic tubular netting or neoprene caps. Rubber bands are easy to visualize but are narrow and if not placed correctly, cannot ensure full contact with the scalp. Elastic tubular netting can also be used for securing electrodes, however, it is important that the material it is made of does not absorb saline, as this could cause impedance errors and unwanted dispersal of the current flow across the scalp. With this caveat in mind, netting is easy to use and maintains uniform electrode-skin contact, by allowing the electrodes to adhere to the shape of the head (Fertonani et al., 2015). Neoprene caps are also more secure, and they allow better contact with the scalp, although placing the

electrode accurately may be slightly harder than other methods. In our studies, custom neoprene caps designed to fit each NHP were used as animals had different head size and shape.

Target Stimulation: Stimulation can be targeted to a specific area of interest based on the location of the electrodes and the task. If electrodes are placed incorrectly, different brain areas or networks may be stimulated (Nitsche et al., 2008). Furthermore, specific tasks may also be expected to recruit neurons in the target region, leading to stimulation-related changes in behavior.

Typically, targeted regions are on the cortical surface, as it is unclear how stimulation affects deep brain regions. A study by Opitz et al. (2016) has shown that electrical field was strongest at superficial brain regions. Modeling studies have demonstrated that the distribution of the current can vary across subjects, even when the electrode montage is kept consistent, due to anatomical features such as skull thickness and composition (Opitz et al., 2015). Current flow may also be influenced by brain abnormalities and lesions common in clinical cases (Datta et al., 2011). A more detailed description of inter and intra subject variability with tES is described below. The use of neuro-navigational software can help identify these differences. Importantly, tES techniques are not focal and surrounding regions may also receive stimulation, potentially causing unspecified changes to task performance. In our experiments, we targeted PFC to see if we could elicit changes in activity. Our experimental setup also allowed us to examine neighboring brain regions (frontal and parietal regions on the

scalp and ACC/DPM intracortically) and subcortically (in the CAD) allowing us to further explore the spread and extent tDCS could impact whole brain activity.

Reference: In scalp EEG recordings, voltages recorded at each 'active' electrode are computed with 'reference' to another electrode (Steven J. Luck, 2014). Ideal reference locations should be electrically neutral. Placement of reference electrodes is important impacting not only the amplitude of the recorded potential but also its temporal structure. Examples of locations commonly used for scalp EEG are: the vertex (Cz electrode), nose, linked mastoids (behind the ear) or ears. Reference electrodes can also be placed extracephalically on the neck, shoulders or upper arm (more information on reference electrodes can be found in Fischer et al., 2017). In our experiments, we used the single mastoid referencing for scalp EEG in both NHPs. Linked mastoid references were explored and showed minimal change in scalp EEG activity (data not shown).

In scalp EEG experiments labeling electrodes as 'active' and 'reference' are arbitrarily, as the electrodes participate equally (Steven J. Luck, 2014). In tDCS experiments, scalp electrodes can be referred to as 'target' and 'reference' (Thair et al., 2017). Here, the target electrode is the region of interest (ROI), and the reference is based off the direction of current flow, participant comfort, and safety. Reference electrode distance is greatest at extracephalic locations, such as areas contralateral to the ROI. An important advantage of extracephalic electrode set-up is that it helps to exclude the effect of the reference electrode on cortical modulation (Nitsche & Paulus, 2011). A study by (Imburgio & Orr, 2018) showed that using an extracranial shoulder

reference yielded a larger and more consistent effect size than studies using a cranial reference.

Determining where reference electrodes are placed can also impact current direction. For example, in extracephalic electrode placement, switching between placement on the contralateral upper arm instead of the forearm could shift the current flow to travel across parietal regions rather than frontal (Bikson et al., 2010). Similarly, cephalic electrode placements can also show this affect (Bikson et al., 2010; Datta et al., 2011). One study by Reinhart et al. (2017) found that the reference electrode on the opposite hemisphere of the PFC interfered with the stimulating electrode during prefrontal cortical-administered tDCS.

When combining scalp EEG and tDCS setups, the nomenclatures mentioned above don't neatly apply. We refer to active scalp EEG electrodes, during stimulation, that pass current as 'stimulating' and 'return' or according to the polarity of current (i.e., 'anode' and 'cathode'). Consistency in the nomenclature across studies and when combining techniques is very important, and as scalp EEG and tDCS experiments are emerging in animal models, careful consideration of electrode placement when planning experiments in vital.

Sham and Controls: Sham stimulation is a generic term to indicate an inactive form of stimulation (e.g. a very brief or weak one) that is used to control for placebo effects. The subject believes they are being stimulated normally, but there should not be any real effects. Sham stimulation is administered in order to mimic cutaneous perceptions (e.g., itching, tingling) that tend to be reported within the first few moments of tDCS (Gandiga

et al., 2006) when current levels are changing. This brief stimulation period does not change cortical excitability (Nitsche et al., 2008). Sham tDCS is easy to administer and involves three steps. First, a period of "ramping up" is administered, in which the stimulator gradually reaches the maximum programmed current (e.g., 1 second to reach 1 mA). Ramping up is then followed by a short stimulatory period, in which the participant receives stimulation for a few seconds. Finally, "ramping down" involves the current gradually being switched off. This replicates the same cutaneous sensations that are associated with changing current. Note the longer the ramp up time, the less cutaneous sensations associated with changing current. There are other sham techniques, including using an alternative electrode montage that does not stimulate the ROI (Boggio et al., 2008), or stimulating at an extremely low current (e.g., 0.1 mA with 11 cm^2 electrode sizes) for the same amount of time as "real" stimulation (Miranda et al., 2009). However, the traditional method of ramping up/down is by far the most popular method of sham control (Ambrus et al., 2012).

Control Site. There are many tES experiments in which stimulation of a site is compared with sham stimulation and the conclusion is that a particular area is important for a function. We would suggest that stimulation versus no stimulation is the weakest form of control conditions and suggest that all experiments include a control site. Control polarity may be sufficient here, as it would allow experimenters to claim site specificity. However, there may also be interactions between polarity and task characteristics (Antal et al., 2004; Parkin et al., 2015).

Control Task. As with TMS experiments, every tES experiment requires a control task as well as a control stimulation condition. Just as one needs a control site to make

claims about the effects of stimulating a specific brain region, so too there is a need to show that effects are specific to tasks or task components. As an example, consider that there are effects of tDCS on, say, decision making following stimulation of the DLPFC. The DLPFC is involved in several functions, including working memory. As a minimum case, then, one would need to establish that the effects on decision making are separate from any possible effects on working memory, and to do this would require a working memory control task. It is surprising how often task controls are either non-existent or functionally irrelevant.

Sham tDCS is generally regarded as an effective blinding technique, especially for those who have never experienced tDCS before (Ambrus et al., 2010, 2012; Gandiga et al., 2006). For people familiar with tDCS, blinding is more difficult to achieve and may not be overcome (Ambrus et al., 2012) especially at high current strengths (Russo et al., 2013). Double-blind experiments are usually ideal for experimental control; however, no behavioral differences have been observed between single-blind and double-blind tDCS experiments (Coffman et al., 2012).

In our experiments, we compared the influence of tDCS relative to no stimulation and sham tDCS. Sham stimulation trials were randomly interleaved into experiments to decrease experimenter bias. For comparisons of the effects of sham stimulation see **Supplemental Figure 2.6,3.1.**

*Size of Electrodes***:** Electrodes and pads come in various sizes with benefits to each size. Smaller electrodes are thought to be more efficacious, due to more focal impact and less cross-network influence. However, a larger electrode ensures that the entirety

of the ROI is being stimulated (Datta et al., 2009) and smaller electrode sizes have been correlated with larger shunting effects (Wagner et al., 2007). The most common electrode size used is 20– 35 cm^2 for sponges (Moreno-Duarte et al., 2014) and 5x7 cm for metal electrodes. Although the size of electrodes can vary based on the type and spread of stimulation desired. Because stimulation produces a diffuse effect, high-definition stimulation electrodes, which are smaller in size, are now available. These electrodes are thought to target more specific brain regions and reduce the amount of current spread. However, smaller electrode surface area may produce more adverse side effects such as pain or burning. In our studies we focused on using high definition PISTIM electrodes from Neuroelectrics. Furthermore, size of electrodes was important as the NHP brain is smaller than humans where surface area is more limited.

Electrical Brain Stimulation: A Method of Modulating Neural Activity

tDCS offers a non-invasive means to examine the relationships between neural communication and processing underlying perceptual, cognitive, and motor functions. There are two main polarities of tDCS stimulation: anodal and cathodal. Anodal stimulation is believed to increase the excitability of neurons, while cathodal stimulation is reported to have the opposite effect (Nitsche & Paulus, 2000; Priori et al., 1998). Animal studies have shown that anodal tDCS of the cortex has been linked with facilitation of unconditioned responses (Morrell, 1962). In humans, anodal tDCS has been shown to influence various motor, visual, and somatosensory cortical functions (Been et al., 2007). In contrast, fewer studies have focused on the effects of cathodal stimulation due, in part, to the view of it having a hyperpolarizing effect (Jacobson,

Koslowsky, et al., 2012; Miniussi & Ruzzoli, 2013; Nitsche et al., 2008). However, recent studies have suggested that cathodal stimulation may act as a noise filter, decreasing global neural activity (Antal et al., 2004; Dockery et al., 2009; Weiss & Lavidor, 2012). The ability to selectively modulate neural activity makes tDCS attractive for studying various processes in the brain. In our experiments, we tested the extent to which tDCS can influence neural activity locally (at the intracortical level) and globally (on the scalp).

If tDCS can change neural activity, it holds promise to impact behavior and cognitive function, making it a promising therapeutic method. Yet, the behavioral and cognitive measures accompanying tDCS have shown mixed results in both healthy subjects and patient populations (Agarwal et al., 2013; Flöel, 2014; Hoy et al., 2013; Kuo et al., 2014; Smith et al., 2015). The inconsistency in behavioral outcomes associated with tDCS may stem from our lack of understanding the mechanisms underlying tDCS or the use of sub-optimal stimulation parameters. The observable effects of tDCS depend on the intensity, duration, and/or timing of stimulation (Batsikadze et al., 2013; Pirulli et al., 2013, 2014; Teo et al., 2011). Previous studies have shown that the position of the return electrode may influence the effects of tDCS, and that tDCS montages can also influence the uniformity of current distributed and field strength (Parazzini et al., 2014; Woods et al., 2016). Although similar stimulation parameters have been used in most cognitive tDCS studies (e.g., 35 cm^2 rectangular electrodes, a supraorbital reference electrode, current strength between 1–2 mA), no unitary stimulation protocol has been agreed upon (Coffman et al., 2014). Our study systematically examined the effects of different stimulation parameters on neural activity.

Oscillatory Brain Activity

*Rhythmic Neural Oscillations***.** Neural tissue can produce oscillatory activity driven either by mechanisms localized within individual neurons or by feedback interactions among populations of neurons (i.e., the interplay of excitatory and inhibitory feedback). Three different levels of oscillatory activity have been recognized: microscopic, mesoscopic, and macroscopic (Haken, 1996). At the microscopic level, individual neurons display rhythmic patterns of spiking activity. The Mesoscopic levels reflects summed neuronal activity or LFPs, and the macroscopic scale shows neural activity from multiple brain regions. Studies of single neurons, LFPs, EEG and MEG, have collectively characterized neural oscillations based on their frequency components: delta (1-4 Hz), theta (4-8 Hz), alpha (8-12 Hz), beta (12-30 Hz) and gamma (30-80 Hz) (Puig et al., 2014; Puig & Miller, 2012). Oscillatory rhythms are widespread, and rhythmic activity of the same frequency can often be observed over a wide range of cortical and subcortical regions. Neural oscillations and their synchronization have been linked to many cognitive functions such as perception, motor control, and memory (Fell & Axmacher, 2011; Fries, 2005; Schnitzler & Gross, 2005). Furthermore, the dynamic interactions between local and distant neuronal assemblies are thought to underlie cortical processing and cognition. In our study, two electrophysiological techniques are used to examine the influence of tDCS on neural activity – intracortical LFP's and scalp EEG.

*Dysfunction of Neural Oscillations***.** Cognitive and behavioral functioning is highly dependent on coordinated spatiotemporal neural activity within and between brain networks. By entraining multiple neurons in a coordinated fashion, neural oscillations

form a critical interface between cellular activity and large-scale systemic functions (Buzsáki, 2004; Buzsáki & Draguhn, 2004). It is likely that neurodegenerative disorders show characteristic changes in coordinated network activity, which may account for both cognitive and behavioral dysfunction. However, our knowledge about the pathophysiology of network oscillations in neurodegenerative diseases is surprisingly incomplete, and increased research efforts are urgently needed.

It is unclear if neural oscillations are the cause or an effect of brain dysfunction in neurological disorders. The functional state of networks is often defined by neuromodulatory systems where a change in activity or integrity of these systems can affect the occurrence, strength, and coherence of rhythmic brain activity (Nimmrich et al., 2015). Additionally, the synchronization of neuronal networks at a given frequency depends on the recruitment of specific neuronal subtypes, which are often highly specialized. Loss of selective types may therefore cause selective disruption of specific patterns of oscillatory activity (Nimmrich et al., 2015).Therefore, neural oscillations are speculated to have a key role in both normal and diseased states.

There is a large literature on changes in neural activity of tDCS assessed with EEG (Boonstra et al., 2016) and MEG (Hanley et al., 2016; Marshall et al., 2016; Wilson et al., 2018) where specific changes in oscillatory activity can be explored. For example, selective changes to gamma oscillations have been seen over frontal cortex using anodal tDCS paired with a cognitive control task (Boudewyn et al., 2019). A number of studies have also reported changes to theta oscillations during a variety of cognitive tasks following tDCS (Choe et al., 2016; McDermott et al., 2019; Reinhart et al., 2015). Given the crucial role that neural oscillations play in cognition, both in “local” regional

cortical dynamics and in long-distance communication across regions in a neural network, the impact of tDCS on neural oscillations may make this method uniquely poised to influence cognition (as opposed to methods that influence spiking directly such as TMS). Although we do not study neural oscillations in the diseased state, our transcranial stimulation experiments may shed on how it can change oscillatory activity which can be further translated to functional and clinical domains.

Experimental Goals

tDCS is a promising brain-stimulation technique to modulate cortical excitability, presumably with faciliatory or inhibitory effects, for experimental and therapeutic goals. However, conflicting, and inconsistent results among previous studies hinder the interpretability of polarity-specific and intensity-dependent effects of tDCS. Furthermore, we know little about the mechanisms by which tDCS might work, and, more specifically, how it affects neurophysiology. Our study set out to test the following questions to resolve the apparent inconsistency and non-homogeneous effects that have been reported. (1) Can tDCS stimulation penetrate the brain to influence neural activity, (2) Does tDCS have local or global effects (including an influence in neighboring not directly targeted and subcortically), (3) How do simulation parameters (polarity and intensity) influence oscillatory brain activity, (4) How does unilateral and bilateral electrode montage impact neural activity and the surrounding areas, and (5) can tDCS produce long lasting changes in neural activity. To address these questions, our experiments paired scalp EEG with simultaneous multi-electrode intracranial recordings of LFP in awake NHP during tDCS. LFP power spectra was compared from frontal and

parietal scalp sites and intracortically in the PFC, ACC, DPM, and CAD. Together, these results can help shed light onto the effectiveness of tDCS to modulate neuronal activity and functional connectivity.

Chapter 2: Investigating the Neural Effects of Bilateral Transcranial Electrical Brain Stimulation in the Primate Brain

Introduction

tDCS delivers a constant, low intensity current through the head via scalp electrodes and has been shown to modulate neuronal activity by inducing intracerebral current flow; consequently, either increasing or decreasing neural activity depending on the specific area(s) being stimulated and on the type of stimulation being used. There are two types of tDCS stimulation: anodal and cathodal. In general, anodal stimulation excites neuronal activity while cathodal stimulation inhibits or reduces neuronal activity (Bindman et al., 1964; Nitsche, Liebetanz, Lang, et al., 2003; Nitsche & Paulus, 2000; Purpura & McMurtry, 1965). It is thought that tDCS works on a local scale affecting membrane polarization; however, recent fMRI studies reported that tDCS can influencing resting-state functional connectivity in distinct functional networks (Keeser et al., 2011). Studies like this suggest tDCS may also modulate activity over a long range and may even play an important role in neural oscillations (Filmer et al., 2014). For instance, anodal tDCS was found to increase baseline alpha power and gamma power in response to visual stimuli, markers of cortical inhibition and excitation respectively (Wilson et al., 2018). Additionally, anodal tDCS was found to increase low-frequency oscillations in the underlying tissue without increasing firing rates (M. R. Krause et al., 2017). However, these effects may largely depend on a variety of factors including brain anatomy and stimulation parameters, among other factors.

Despite accumulating evidence supporting the efficacy of tDCS as a treatment option, many questions about its effects and use remain. The current study set out to test how prefrontal tDCS with a bilateral montage affects neural activity at the

population level (as assessed with scalp EEG electrodes and intracortical recording electrodes), to determine the effects of varying stimulation polarity (anodal and cathodal) and intensity (0.5-1.5 mA). We made simultaneous multi-electrode intracranial recordings and scalp EEG recordings in awake NHPs during prefrontal tDCS. We compared the effects of stimulation on scalp EEG power in frontal and parietal electrodes and intracortically recorded local field potential (LFPs) power in the PFC, ACC, DPM and the CAD. Increasing our understanding of how tDCS influences neighboring and subcortical areas will ultimately improve our understand of the underlying mechanisms of tDCS and allow this therapy to be used optimally.

Research Methods

Animals and surgical procedures: Experiments were performed on two adult macaque monkeys (*Macacca mulatta*). All procedures used conformed to NIH guidelines and were approved by UC Davis IACUC. Both NHPs were surgically implanted with a head restraint post and a recording chamber located over the principle and arcuate sulcus. A schematic of animal C and Z's intracortical and scalp electrophysiological setup is shown in **Figure 2.1.** Animal C had recording chamber on left side hemisphere, while animal Z the had recording chamber on right side.

Passive Behavior: Animals were seated in front of a monitor where they were allowed to passively view a grey screen monitor. Eye position was monitored by an infrared video eye tracker (Applied Science Laboratories, Bedford, MA), although no behavioral task was employed.

Transcranial direct current stimulation: tDCS was performed using the commercially available Neuroelectrics system Starstim (Neuroelectrics Instrument Controller, v1.0; Rev 2012-08-01, Neurolelectrics, Barcelona, Spain) with the program NIC. The Neuroelectrics Starstim system is a HD-tDCS generator, allowing for more focal current delivery. This system is commonly used in human studies and the 8-electrode setup was used in our NHP recordings, where 5-6 1 cm radius Ag/AgCl electrodes (PISTIM, Neuroelectrics) were used along with 1 ear clip (CMS/DRL). Contact between electrodes and the scalp was made with Signa conductive gel (Parker Laboratories). Scalp EEG data was collected at 500 Hz and analyzed offline. Electrode impedance at the start of every recording session was 0-10 kΩ, signals >15 kΩ the were automatically aborted.

NHPs had their hair trimmed and were each fitted individually with a customized EEG cap each day of recording. Scalp electrode locations were approximated from a scaled down 10-20 mapping system (**Appendix Figure 1**). Electrodes were placed over frontal (F7 and F8) and parietal brain areas (P7 and P8) with reference electrodes positioned behind the ear as mastoid references (TP9 and TP10). tDCS was administered through F7 and returned through F8, depending on polarity. Parameters being studied included polarity (anodal and cathodal stimulation) and intensity (0.5, 1, 1.5 mA). Electrode placement mimicked a bilateral montage commonly seen in human studies, where current flow crosses both hemispheres (**Figure 2.1**). Raw tDCS intensity values are shown in **Appendix Table 1**. The Neuroelectrics system is capable of simultaneously administering tDCS and recording EEG, however not in stimulating

electrodes. Therefore, scalp EEG during stimulation is only reported for parietal scalp electrodes.

Each day of recording began with a start and end baseline (120 seconds each) and 80 blocks of stimulation (22 seconds) separated by blocks of EEG recording (20 seconds each). For stimulation, current was ramped up to the desired intensity over 1 second, and then maintained at a constant level for 20 seconds, before being ramped down over 1 second for each stimulation trial. Two or three stimulation intensities and both polarities of stimulation were randomly assigned to each trial on a given day. For example, on days when 2 intensities were used,17-21 trials per intensity and polarity were delivered. On days where sham tDCS was delivered, 16 stimulation trials of each condition were randomly re-assigned as sham. Sham stimulation consisted of 1 second ramp up followed by a brief 5 second stimulation, then a 1 second ramp down. At the end of the 20 second of sham tDCS, there is another 1 second ramp up and down (**Supplemental Figure 2.5**).

Two different datasets were collected in both animals. The first included scalp EEG recordings during tDCS. The second included scalp EEG recordings along with simultaneous intracortical recordings during tDCS. Animal C had an additional third dataset, which included scalp EEG in combination with sham tDCS during tDCS.

Neural Recordings: Simultaneous multi-electrode recordings were made from the PFC, CAD, ACC, and DPM with 8-16 tungsten electrodes (FHC, Bowdoin, ME) in both animals (**Supplemental Table 2,1**). Neural recordings were collected through a Plexon headstage (x1) and preamplifier (x1000 gain, band-pass filtering the signal at 0.7 Hz-6

kHz). Broadband signals were collected at 20 kHz through a 1401 data acquisition system in conjunction with Spike2 software (Cambridge Electronic Design, Cambridge, UK). Electrodes were inserted into the brain every day of recording and guided by each animals MRI images. Electrode location and identification was referenced with a Paxinos brain atlas. Our analysis of PFC included both regions of the lateral PFC and caudal PFC (posterior to area 8A including the frontal eye fields). Striatal recordings included the head and body of the caudate nucleus.

Data Analysis: Scalp EEG data was analyzed offline using custom written code in MATLAB (Mathworks, Natick MA). Signals were low-pass filtered using a 10^{th} order Butterworth filter (high cut freq: 250 Hz) and 60 cycle noise was removed (10^{th} order bandstop filter 59-61 Hz). Mastoid references on analysis are TP10 for both animals unless otherwise noted. The signals were then decomposed into their spectral components using a MATLAB-based wavelet analysis toolbox (Torrence and Compo, 1998) through their convolution with a Morlet wavelet, at 6 octaves (2:0.1:128 Hz). The wavelet transform supplies both the amplitude and the phase of the signal at each time point. Quantification of power was made using custom MATLAB code and is reported as the average across days +/- SEM.

To relate intracortical data with scalp EEG, Spike2 recordings were time stamped to NIC software using a TTL trigger adapter (Neuroelectrics, Cambridge MA). Offset between intracortical and scalp EEG data was corrected manually. Intracortical data was analyzed in a similar fashion offline. Signals were low-pass filtered using a 10^{th} order Butterworth filter to separate local field potentials (LFP) from spiking activity (high-

cut freq: 300 Hz). Analysis focused on LFP data, where the signal was further filtered to remove 60 cycle noise (10^{th} order bandstop filter 59-61 Hz) and down sampled to 500 Hz to match the scalp EEG. LFP data was then decomposed using a wavelet analysis. Data are reported as average across electrodes +/- SEM.

Analysis focused on the time and frequency dependence of oscillations in multiple brain areas. Three epochs of electrophysiological data were examined: (i) pre-tDCS to determine baseline physiology, (ii) during tDCS to identify ongoing changes associated with tDCS delivery, and (iii) post-tDCS to evaluate the short and long-term after-effects induced by tDCS. Note on one EEG trial (20 seconds), the beginning of this time frame is analyzed as the post-stimulation (5 seconds) of the previous stimulation trial, and the end of it is the baseline (5 seconds) for the next stimulation trial. Due to the large stimulation artifact seen during the ramp up and down of stimulation (as see in the filtered LFP **Figure 2.2**), this time period was removed from analysis in both scalp EEG and intracortical data. Additionally, a 2 second buffer before and after the artifact peak was removed as the effect of it smeared into the time surrounding it due to wavelet decomposition. Therefore, 16 seconds of data was analyzed during stimulation.

Results

Previous studies report mixed results in the effectiveness of using tDCS as a therapeutic tool. Some studies have shown behavioral enhancement following stimulation while others show no effect at all (Harris et al., 2019)(London & Slagter, 2021) and further question the ability of low current penetrating the brain (Vöröslakos et al., 2018). Here we investigated if bilateral tDCS can causes changes in scalp EEG and intracortical LFPs in the NHP model (**Figure 2.1**), by systematically examining different

stimulation parameters including polarity (anodal V+, cathodal V-) and intensity (0.5, 1, 1.5 mA).

tDCS Leads to a Broadband Change in Scalp EEG Power.

First, we confirmed that tDCS was visible in the scalp EEG in the NHP. An example of three filtered scalp EEG trials during stimulation are shown in **Figure 2.2.** The scalp electrode (P8) shows anodal stimulation across three trials with different intensities (green: 0.5 mA, red: 1 mA, blue: 1.5 mA) from animal C. Time series of the trials shows a 1 second ramp up and down with 20 seconds of stimulation (highlighted in grey).

We examined the spectral power across the frequency spectrum during stimulation to confirm current penetrates the brain and produces changes in neural activity. A large artifact during the ramping phases in the power spectra was seen; therefore, a 2 second buffer was applied for all analysis after the ramp up and before the ramp down during stimulation. A total of 16/20 second of stimulation was analyzed.

tDCS induced a broadband change in EEG power; however, differences in spectral amplitudes of power were seen between both animals **(Figure 2.3)**. For this reason, the effects of tDCS on both animals is plotted separately. Comparisons of the effects of tDCS on brain activity were therefore done within and not between animals.

tDCS Increase Parietal Scalp EEG Power During Stimulation.

The effects of tDCS on the parietal scalp EEG (electrodes P7 and P8) show an overall increase in power during stimulation compared to baseline in both animal C and Z (**Figure 2.4 and 2.5**). Effects of tDCS are focused on the low frequency range, predominately in the delta band (1-4 Hz) **Figure 2.4A and 2.5A**. Table 1 shows the

mean ± SEM and P-values of delta band power during stimulation for animal C and Z (paired t-test, FDR corrected), respectively. No strong differences were seen between polarity; however, a trend towards an increase in intensity and power can be seen. A large deviation in 1.5 mA stimulation for animal C (**Figure 2.4, 2.6**) was apparent; however, this may reflect noise in the recording. No differences were seen between parietal electrodes within each animal, suggesting a lack of hemispheric differences.

Prolonged Effects of tDCS on Scalp EEG Delta Band Power.

Profiles of each animal's power spectra post stimulation can be found in **Figure 2.6** and **2.7**. Since the largest effects during stimulation were seen in low frequency bands, analysis post-stimulation focused on the delta band. Post-stimulation was defined as 2-7 seconds after stimulation (5 seconds total) and followed a 2 second buffer to avoid any ramp-down artifacts. Interestingly current increases during stimulation showed the opposite effect post-stimulation, and not all stimulation parameters that displayed significant changes during stimulation showed changes post-stimulation. Animal C showed prolonged decreases in power in recordings from parietal electrodes post-stimulation in P7 and P8 after anodal 1 mA ($p = 7.2e-7$ and $p = 0.0071$), and cathodal 0.5 mA ($p = 0.0023$ and $p = 0.003$) and 1 mA ($p = 7.5e-8$ and $p = 8.8e-9$) stimulation (**Figure 2.8**). Animal Z only showed a decrease in power in recordings from P8 electrodes (**Figure 2.9**) after anodal 1.5 mA stimulation ($p = 0.022$). Mean ± SEM and P-values for delta band power post-stimulation are reported from a paired t-test (FDR corrected) found in **Table 2.2.**

Scalp EEG was examined post-stimulation for recordings from frontal scalp electrodes, as scalp EEG could not be recorded simultaneously with current delivery. Anodal stimulation showed increases in power post-stimulation at all intensities (**Figure 2.10,2.11**), in a dose dependent manner. See **Table 2.3** for mean ± SEM and FDR corrected paired t-test p-values of delta band power. Cathodal stimulation caused mixed results in relation to current flow and intensity. Animal C showed decreases in the percent change of power relative to baseline in recordings from electrodes F7 and F8 during 1 mA stimulation (-29.52% and -41.58%), and also during 0.5 mA in recordings from electrode F7 (-39.57%) (**Figure 2.10**). Animal Z showed a decrease in power during cathodal 0.5 mA stimulation in recordings from electrode F8 (-33.26%) (**Figure 2.11**). Effects of anodal and cathodal stimulation trend to support polarity specific effects in animal Z.

The Influence of tDCS on Local Field Potentials.

Since tDCS produced significant changes in scalp EEG power we further examined how tDCS impacts neural activity on a finer scale. To achieve this, we simultaneously recorded LFPs during tDCS. We focused on how tDCS impacted cortical regions (PFC, ACC, DPM) during and after stimulation, and compared the effects of tDCS on a cortical (PFC) vs. subcortical (CAD) areas. The PFC and CAD were chosen because they are directly connected through the frontostriatal network. This network has shown to be involved in many different cognitive and behavioral studies and therefore is a great system to examine for modulatory effects (Antzoulatos & Miller, 2014). Next, we further dove into the frontostriatal network to examine specific oscillatory changes (beta band)

inherent to the network and how those were impacted following tDCS. The recording chambers were over different hemispheres in animals C and Z; hemispheric differences were not anticipated.

To confirm low levels of stimulation were reaching the brain, we first confirmed a stimulation artifact was present in the LFP, as was seen with scalp EEG. **Figure 2.2B** shows an example of a filtered LFP from the PFC, including periods of tDCS ramp up and down and stimulation period (highlighted in grey). Interestingly, the profile of the voltage does not stay elevated in the LFP as seen in the scalp EEG, despite similar processing technqiues.

tDCS Produces Broadband Changes in Spectral Power Intracortically.

Effect of tDCS, collapsed across intensity and polarity, included broadband changes in power compared to baseline (**Figure 2.12A, 2.13A**). Strongest and most wide band effects were seen in the PFC and CAD in both animals. Mean ± SEM and p-values are reported from a two-sample t-test and shown in **Table 2.4 and 2.5**. In general, animal C showed decreased changes in power during stimulation, except in the gamma band (**Figure 2.12A**). Animal Z showed similar trends, where higher frequency bands showed increased power, except in CAD which showed effects in all bands (**Figure 2.13A**). A wider view of the spectral profile of tDCS broken down by polarity and intensity are shown in **Figure 2.12C, 2.13C**. ACC, DPM and PFC all show different profiles in spectral power despite their proximity to the stimulating electrode and being superficial cortical areas. This is consistent with each area having distinct local networks and effects of tDCS. All intracortical areas showed strong intrinsic beta band activity.

Changes in PFC power spectra did not align with similar changes in the CAD. Therefore, it is unclear if changes in the CAD result from global changes in the electric field or through network properties.

tDCS Shows Mixed Intracortical Delta Band Power Effects.

To relate the changes in spectral power observed in scalp EEG, we focused our data analysis of intracortically recorded LFP also in the delta band. Animal C and Z both showed mixed effects of beta band power intracortically; however, both show the most widespread effects in the PFC (**Figure 2.14, 2.15**). Animal C shows no changes in ACC. Animal C showed a decrease in delta band power during cathodal 1.5 mA stimulation in DPM ($p = 0.042$) and CAD ($p = 0.0022$). The strongest effects were seen in the PFC during cathodal stimulation of 1 mA ($p = 0.0087$) and 1.5 mA ($p = 6.7e\text{-}5$). Similarly, animal Z showed the least effects in ACC, with only 0.5 mA anodal stimulation being different from baseline ($p = 0.035$). CAD showed significant effects only with anodal 1.5 mA stimulation ($p = 0.0074$). The strongest and most widespread change for animal Z was in DPM and PFC. Anodal and cathodal 0.5 mA in the DPM ($p = 2.4e\text{-}6$ and $p = 0.00062$) and PFC (0.0072 and 0.021), and 1.5 mA in PFC of both (7.7e-5 and 4.8e-5). Changes were also seen in cathodal 1 mA stimulation in DPM ($p = 0.0015$). P-values are reported from a two-sample t-test.

tDCS Produces Limited Changes in Delta Band Power Post-stimulation.

We focused post-stimulation effects in areas that showed significant changes during stimulation. Few areas that showed differences during stimulation had prolonged

effects. Animal C showed long-term effects after 1.5 mA cathodal stimulation in the PFC (0.019) and CAD (0.0010) (**Figure 2.16**). Animal Z showed no changes in baseline post-stimulation in any area (**Figure 2.17**). Interestingly, brain areas became significant different from baseline post-stimulation that did not show significant increases during stimulation, including anodal 1 mA stimulation ($p = 0.035$) in animal C and anodal 0.5 mA ($p = 2.4e-5$) and 1 mA ($p = 0.0015$) in animal Z (data not shown). P-values are reported from a two-sample t-test.

Discussion

Previous studies have shown that the effects of tDCS can be significantly altered by a large number of methodological decisions (Bastani & Jaberzadeh, 2013; Moliadze et al., 2010). Our study is the first to systematically examine multiple dimensions of tDCS parameters in a NHP model of prefrontal tDCS. While other NHP tDCS papers exist, their studies are limited in the brain areas recorded from and stimulation parameters used (Bogaard et al., 2019; Datta et al., 2016; M. R. Krause et al., 2017, 2019). With mixed literature on the neurophysiological effects of tDCS (López-Alonso et al., 2014) we sought to get a wider view of what happens to neural activity under tDCS with a bilateral montage by testing different polarities (anodal/cathodal) and intensities (0.5,1,1.5 mA). Our results show mixed effects of tDCS across scalp recorded EEG and intracortically recorded LFP based on stimulation parameters.

Our results show a global and broadband increase in scalp EEG power in parietal scalp electrodes during stimulation, trending in a dose dependent manner with intensity. Changes in power were the strongest in the lower frequency bands

(Jacobson, Ezra, et al., 2012; M. R. Krause et al., 2017), specifically in the delta band (Wu et al., 2021). However, we cannot eliminate the possibility that these broadband effects are a result of contamination form stimulation artifact emanating from the stimulating electrodes. Nonetheless, it is important information to visualize what these signals look like and highlight the diffuse form of even HD-tDCS systems. This data does however provide evidence of stimulation delivery (with the Neuroelectrics system) and may also be valuable in monitoring afferent effects of stimulation (i.e., potential seizure like activity).

Changes in scalp EEG power seen during stimulation in parietal electrodes were not consistently maintained post-stimulation. In fact, decreases in delta band power were seen (Cai et al., 2019). In contrast, frontal scalp electrodes did show prolonged effects of tDCS power trending with intensity, suggest a more localized effects of tDCS once stimulation is turned off. Animal C also showed increases in power post anodal stimulation and decrease in power with cathodal, in support of polarity specific changes (**Figure 10**). More information on the individualized effects of tDCS can be found in the General Discussion.

The influence of tDCS on intracortical neural activity both during and post-stimulation was less clear, as tDCS parameters had varying results. The strongest intracortical effects were seen in the PFC in animal C during stimulation, which is consistent with the PFC as our main target. A study by Krause et al 2017 also showed the largest tDCS induced changes in single and multiunit activity in the PFC compared to inferior temporal cortex, however they reported increases in activity. All three cortical areas recorded from (PFC, ACC, DPM) showed unique spectral profiles in response to

tDCS in our study. Varying responses of tDCS based on brain regions have been hypothesized to stem from many factors such as cell morphology, cell type, orientation, and much more (Bikson et al., 2004; Bogaard et al., 2019; Kabakov et al., 2012; Radman et al., 2009). Factors influencing tDCS can be found in greater detail in the General Discussion, Chapter 4.

Interestingly, areas that showed significant changes during tDCS did not always show changes post-stimulation. In fact, animal Z showed no significant changes in power intracortically in the delta band post-stimulation (**Figure 2.17**). This may stem from the short stimulation interval used (20 seconds) and account for the short-term effects of tDCS. Longer stimulation intervals could lead to longer lasting post-stimulation effects (Sánchez-León et al., 2020).

It is thought that tDCS influences areas directly under the stimulating electrodes; yet, recent research has demonstrated that tDCS may also exert changes in neuronal activity in deeper brain structures (Chib et al., 2013). Our intracortical CAD data does show large changes in power in both animals, and the direction of change is opposite in both. Mechanistically, it is unclear if these changes arise from network properties or global changes in electric fields (see Chapter 4 General Discussion).

To support the role of tDCS being a form of diffuse stimulation, more global and larger effects were seen with the scalp EEG than with the intracortical LFP. This could stem from the scalp EEG casting a wider net and picking up the summated influence of stimulation. In contrast, it is possible that tDCS induced changes could be more drastically seen on a single neuron level than population, highlighting how scope and study design can influence the interpretability of tDCS studies.

Animals C and Z were statistically different from each other, yet the trends of tDCS influence of tDCS in both animals were similar (**Figure 2.3**). This is consistent with human studies showing individualized effects of tDCS and may be explained by several factors including brain size, anatomy, etc. (Datta et al., 2009; B. Krause & Cohen Kadosh, 2014; Opitz et al., 2015; Russell et al., 2013). More information on individualized differences can be found in the General Discussion.

Three different stimulation intensities were used in the following study: 0.5, 1, and 1.5 mA. These intensities were used as they are commonly tested in human studies. However, 2 mA stimulation was eliminated from the present study early on as the animal's showed discomfort. tDCS related side effects are most reported during the ramping periods where current levels change and can include sensations such as tingling, warmth, and skin discomfort. The ramp times in the present study were 1 second long, whereas human tDCS experiments this is on a longer time scale (e.g., 30 second). It is possible that longer ramp times may alleviate any ramping induced side effects and the large artifact seen in both the scalp EEG and intracortical LFP (**Figure 2.2**).

The mechanism of action of tDCS is thought to arise from altering resting membrane potentials (Lang et al., 2005; Nitsche & Paulus, 2001) where anodal stimulation leads to an increase in neuronal activity and cathodal stimulation inhibits it (Monte-Silva et al., 2013). Our data did not show strong polarity induced effects during stimulation or post-stimulation. Furthermore, human studies of bilateral tDCS have shown evidence of increasing cortical excitability in one hemisphere while causing a

decrease in the contralateral hemisphere (Mordillo-Mateos et al., 2012). However, we do not see this teeter totter effect either.

Conclusion

In conclusion, the effects of scalp EEG in the NHP are mixed, where changes in power were variable in relation to the different stimulation parameters used and the time periods examined. Trends of Intensity and polarity induced changes were reported throughout yet were not consistent. Further studies will need to be done to better relate local changes in neural activity to scalp EEG. Despite these results, there is still promise that specific combinations of tDCS parameters may influence frequency specific changes in power in some individuals. Future experiments will need to address longer stimulation times, repeated stimulation, the influence of tDCS on behavior, and more. Gaining a better mechanistic view of the effects of tDCS and reducing intra-individual variability can further progress its use a method of modulating neural activity and as a therapeutic intervention (Ezzyat et al., 2018).

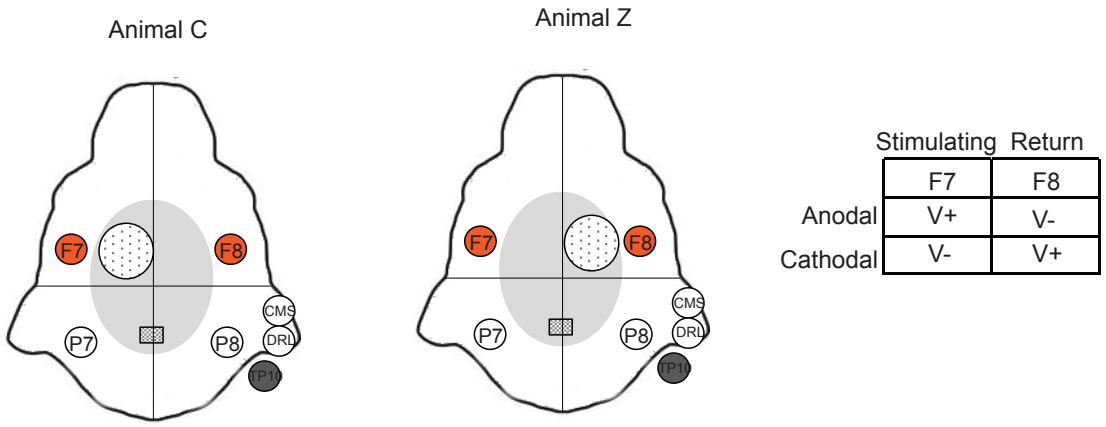

Figure 2.1: Bilateral Stimulation tDCS Montage Setup. Approximate location of stimulating electrodes (orange), recording scalp electrodes (white) and reference (grey) in both animals C and Z. Current flows from stimulating (F7) to return electrode (F8). Anodal and cathodal stimulation represent the charge of current (V+ and V-) in reference to F7.

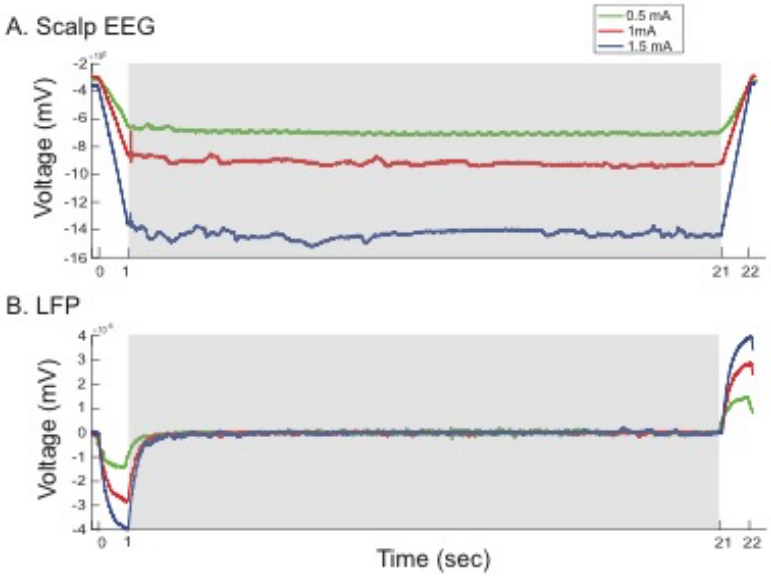

Figure 2.2: tDCS Artifact in LFP and Scalp EEG. Example of pre-processed scalp EEG (A) and LFP (B) data from one recording day showing 3 anodal stimulation trials across intensities (green: 0.5 mA, red: 1 mA, blue: 1.5 mA). Three time epochs are focused on: ramp up (0-1 seconds), stimulation (1-21 seconds), and ramp down (21-22 seconds). Stimulation is highlighted in grey.

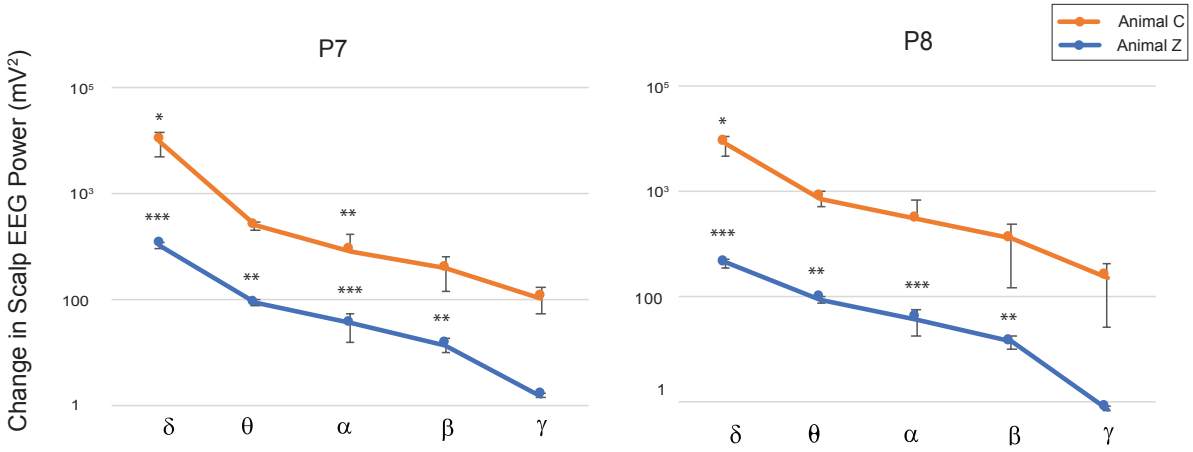

Figure 2.3: Change in tDCS Scalp EEG Power Across Frequency Bands. tDCS causes changes in parietal scalp EEG power compared to baseline in animal C (orange) and Z (blue). Frequency bands are designated as Delta (δ; 1-4 Hz), Theta (θ; 4-8 Hz), Alpha (α; 8-12 Hz), Beta (β; 12-30 Hz), and Gamma (γ; 30-128 Hz). Animal C and Z show similar changes in spectral power, with animal C ~100 folder higher. Data is collapsed across polarity and intensity and reported as mean ± SEM: *= p<0.05; ** = p<0.01; *** = p<0.001 (two sample t-test).

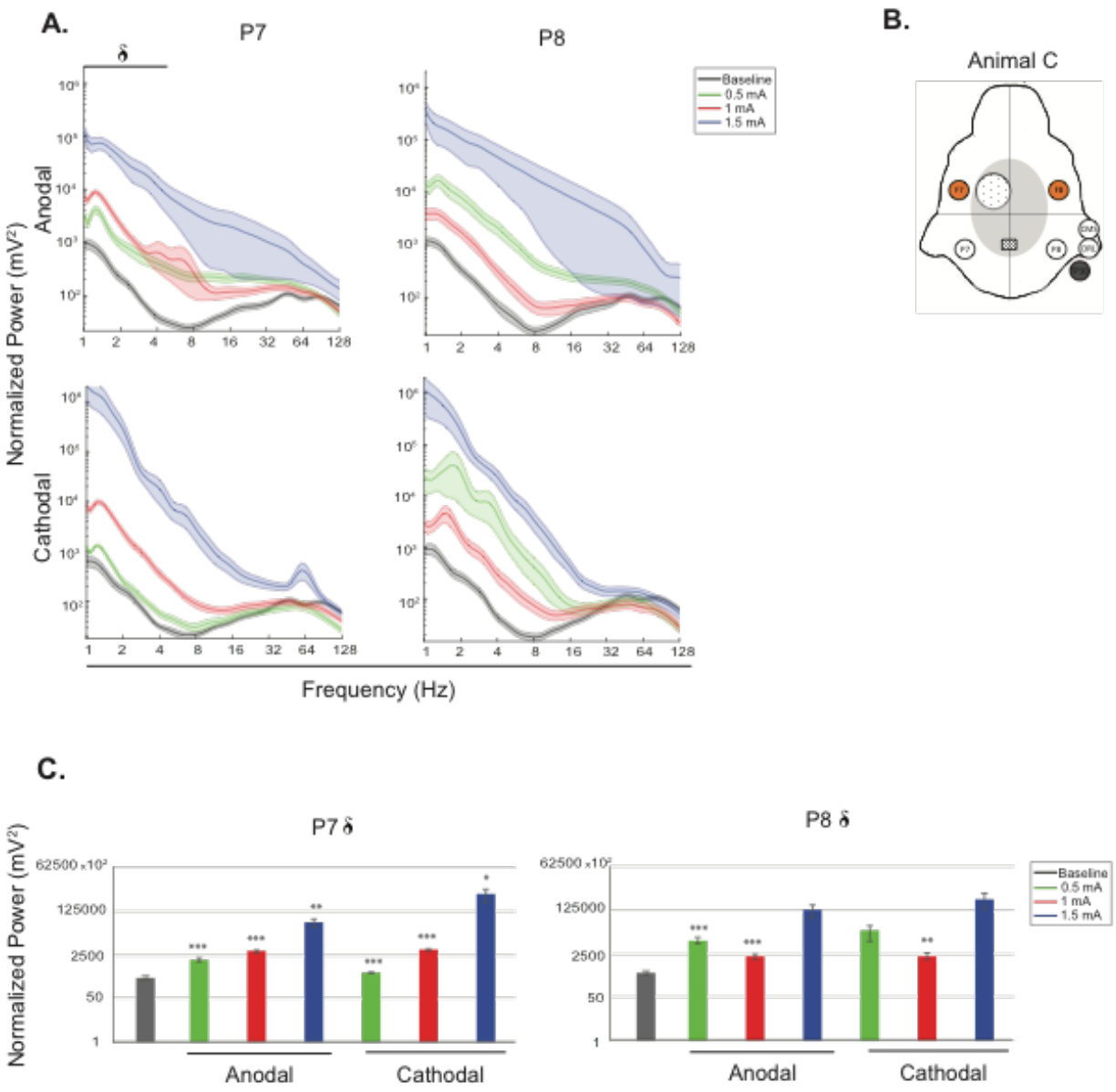

Figure 2.4: The Effects of tDCS on Scalp EEG During Stimulation in Animal C. Power spectra of parietal scalp electrodes during anodal (top) and cathodal (bottom) stimulation with a bilateral montage (A). Three different stimulation intensities (green: 0.5 mA, red: 1 mA, blue: 1.5 mA) are superimposed on each panel along with baseline (black). Power has been normalized for correction of power-law decay and is plotted on a log scale. Strongest effects are seen in the low frequency bands, highlighted in the delta band (δ; 1-4 Hz). Inset of animal C with a bilateral tDCS montage, scalp electrodes (orange) and reference (grey). Delta band effects of tDCS relative to baseline of each stimulation condition in parietal electrodes (C). Baseline is specific for each area, collapsed across intensity and polarity. Data is reported as mean ± SEM: *= $p<0.05$; ** = $p<0.01$; *** = $p<0.001$ (two sample t-test, unequal variance; FDR corrected).

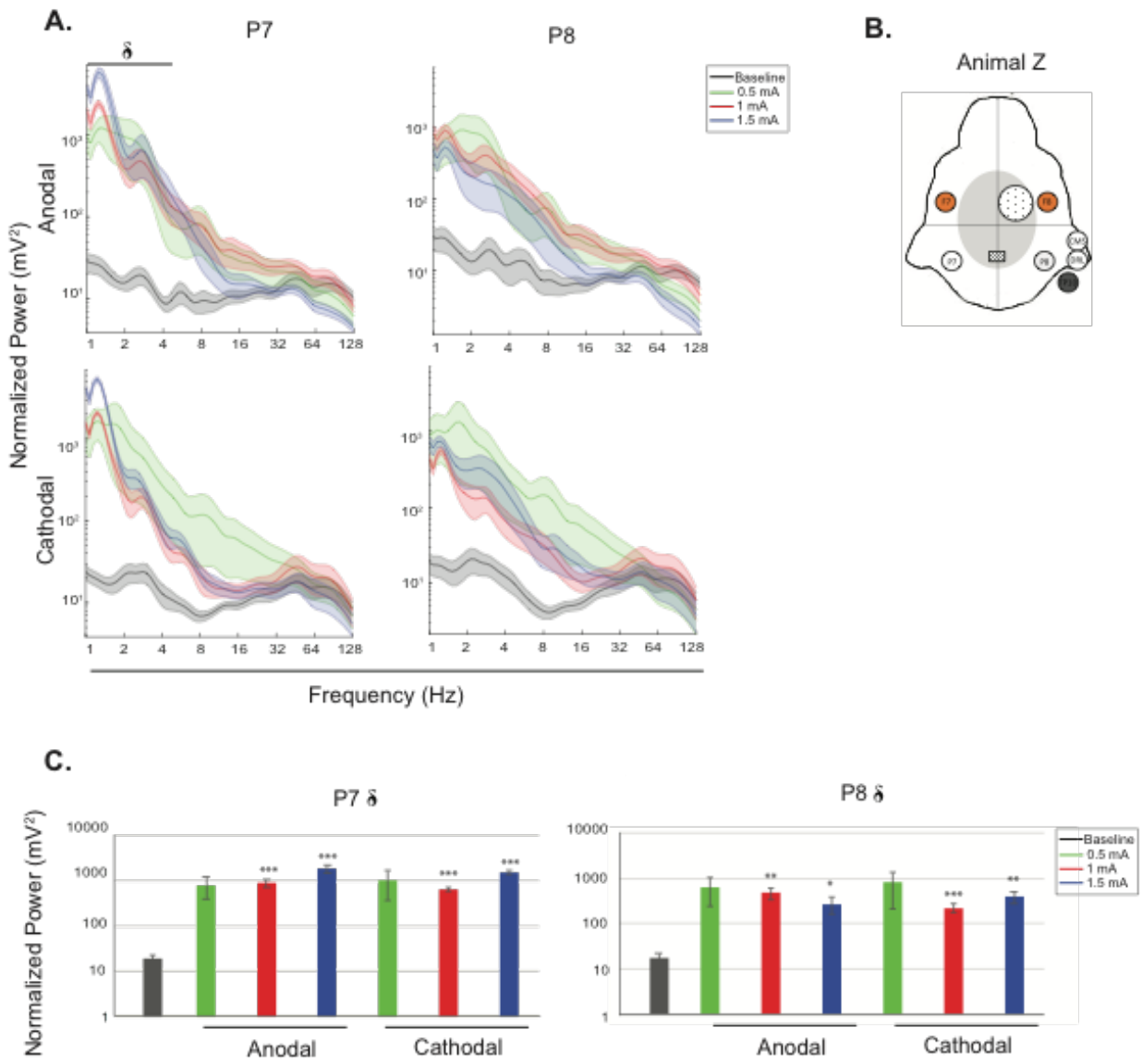

Figure 2.5: The Effects of tDCS on Scalp EEG in Animal Z. Power spectra of parietal scalp electrodes with a bilateral montage during anodal and cathodal stimulation (A). Superimposed on each panel are three different stimulation intensities (green: 0.5 mA, red: 1 mA, blue: 1.5 mA) and baseline (black). Power is plotted on a log scale and has been normalized for correction of power-law decay. Strongest effects are highlighted in the delta band (δ; 1-4 Hz). Inset of animal Z with a bilateral montage (B) highlighting stimulating (orange) electrodes and reference (grey). Stimulation effects of tDCS in the delta band on parietal electrodes relative to baseline across conditions (C). Baseline is specific for each area, collapsed across polarity and intensity. Data is reported as mean ± SEM: *= p<0.05; ** = p<0.01; *** = p<0.001 (two sample t-test, unequal variance; FDR corrected).

A. P7

		Animal C		Animal Z	
	Intensity (mA)	Stimulation	p-val	Stimulation	p-val
Baseline	--	309.97 ± 44.88	--	19.39 ± 2.91	--
Anodal	0.5	1574.38 ± 249.85	4.1e-6	801.60 ± 411.78	0.15
	1	3478.21 ± 382.03	4.8e-12	874.48 ± 156.56	1.6e-6
	1.5	46641.06 ± 14480.44	0.0027	1819.65 ± 391.54	7.6e-5
Cathodal	0.5	498.23 ± 30.45	0.0011	1015.01 ± 652.83	0.23
	1	3943.13 ± 395.70	2.5e-12	647.94 ± 62.74	9.2e-15
	1.5	584035.78 ± 302561.16	0.075	1528.02 ± 131.74	3.0e-16

B. P8

		Animal C		Animal Z	
	Intensity (mA)	Stimulation	p-val	Stimulation	p-val
Baseline	--	443.08 ± 59.86	--	17.90 ± 4.41	--
Anodal	0.5	8549.47 ± 2229.16	0.0023	642.44 ± 394.98	0.20
	1	1998.35 ± 437.79	0.0026	485.38 ± 137.90	0.0061
	1.5	131295.52 ± 72275.13	0.12	269.62 ± 110.56	0.064
Cathodal	0.5	19658.17 ± 11714.30	0.12	812.82 ± 595.18	0.25
	1	2016.71 ± 543.26	0.011	225.88 ± 46.86	0.00038
	1.5	349692.27 ± 207679	0.12	397.41 ± 121.59	0.011

Table 2.1: Bilateral Stimulation Scalp EEG P-values. Power spectra from parietal scalp electrodes, P7 (A) and P8 (B), across polarity and intensity in animal C and Z. Stimulation data mean ± SEM (paired t-test of unequal variance, FDR corrected).

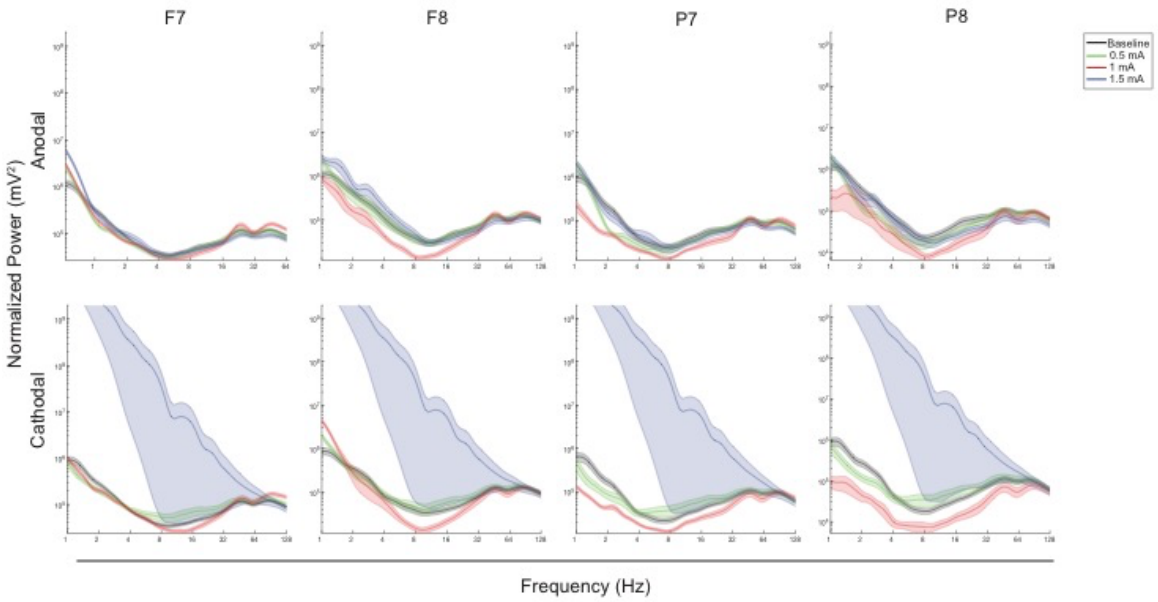

Figure 2.6: Post-stimulation Power Spectra in Animal C. Frontal and parietal scalp EEG with a bilateral montage during anodal and cathodal stimulation. Superimposed on each panel are three different stimulation intensities (green: 0.5 mA, red: 1 mA, blue: 1.5 mA) and baseline (black). Power has been normalized for correction of power-law decay.

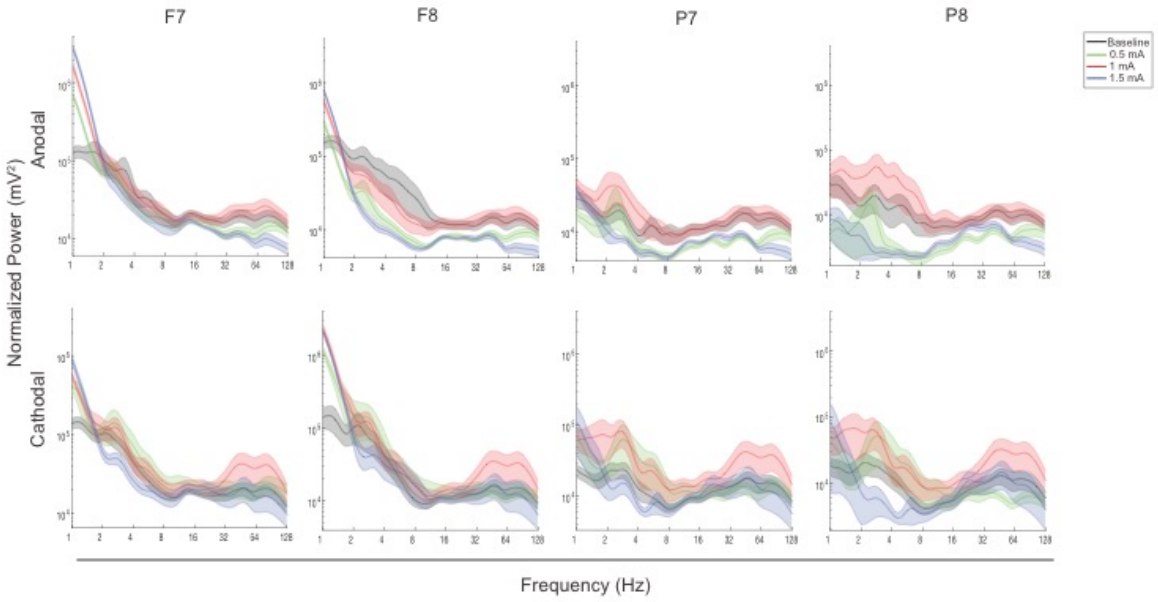

Figure 2.7: Post-stimulation Power Spectra in Animal Z. Frontal and parietal scalp EEG with a bilateral montage during anodal and cathodal stimulation. Superimposed on each panel are three different stimulation intensities (green: 0.5 mA, red: 1 mA, blue: 1.5 mA) and baseline (black). Power has been normalized for correction of power-law decay.

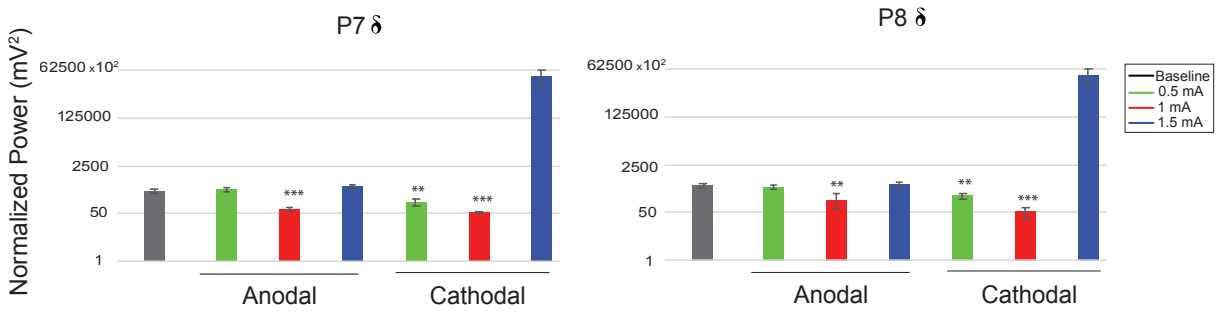

Figure 2.8: Post-stimulation in Parietal Areas in Animal C. Power spectra from parietal scalp EEG in the delta band during anodal and cathodal stimulation. Superimposed on each panel are three different stimulation intensities (green: 0.5 mA, red: 1 mA, blue: 1.5 mA) and baseline (black). Significant decreases in power can be seen in both P7 and P8 5 seconds after stimulation.

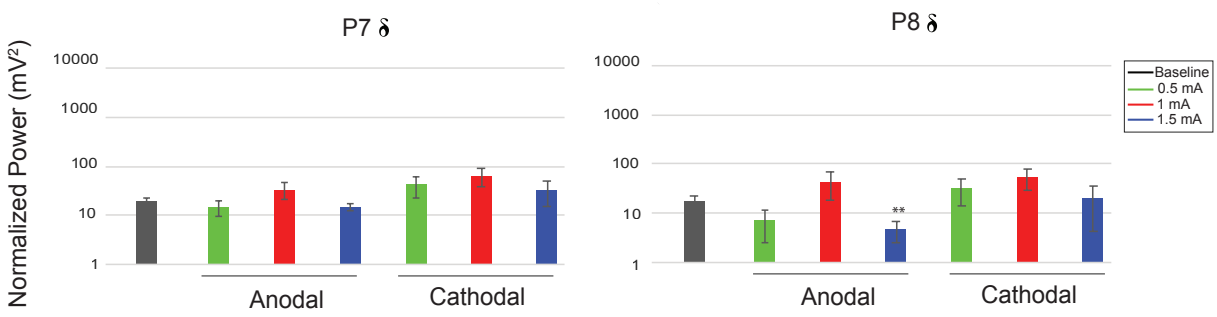

Figure 2.9: Post-stimulation in Parietal Areas in Animal Z. Delta band power from parietal scalp EEG during anodal and cathodal stimulation. Superimposed on each panel are three different stimulation intensities (green: 0.5 mA, red: 1 mA, blue: 1.5 mA) and baseline (black). Significant decreases in power can be seen in both P7 and P8 5 seconds after stimulation.

A. P7

		Animal C		Animal Z	
	Intensity (mA)	Post-stimulation	p-val	Post-stimulation	p-val
Baseline	--	309.97 ± 44.88	--	19.39 ± 2.91	--
Anodal	0.5	354.83 ± 73.41	0.60	14.73 ± 5.03	0.46
	1	69.58 ± 10.40	7.2e-7	33.62 ± 12.96	0.34
	1.5	430.45 ± 96.58	0.28	14.73 ± 2.19	0.30
Cathodal	0.5	128.77 ± 33.95	0.0023	42.10 ± 19.67	0.34
	1	53.52 ± 3.77	7.5e-8	64.84 ± 26.38	0.18
	1.5	3811013.22 ± 2316462.65	0.12	32.41 ± 17.46	0.46

B. P8

		Animal C		Animal Z	
	Intensity (mA)	Post-stimulation	p-val	Post-stimulation	p-val
Baseline	--	443.08 ± 59.86	--	17.90 ± 4.41	--
Anodal	0.5	402.52 ± 74.96	0.67	7.07 ± 4.49	0.17
	1	143.27 ± 79.74	0.0071	42.98 ± 24.36	0.38
	1.5	500.39 ± 113.57	0.67	4.65 ± 2.22	0.022
Cathodal	0.5	196.57 ± 45.19	0.003	32.29 ± 18.09	0.48
	1	52.51 ± 18.12	8.8e-9	54.02 ± 25.53	0.25
	1.5	3799195.94 ± 2301897.55	0.12	20.21 ± 15.82	0.89

Table 2.2: Bilateral Post-stimulation Scalp EEG P-values Animal C and Z. Power spectra from parietal scalp electrodes, P7 (A) and P8 (B), across polarity and intensity in both animals during post-stimulation. Post-stimulation data mean ± SEM (paired t-test of unequal variance, FDR corrected).

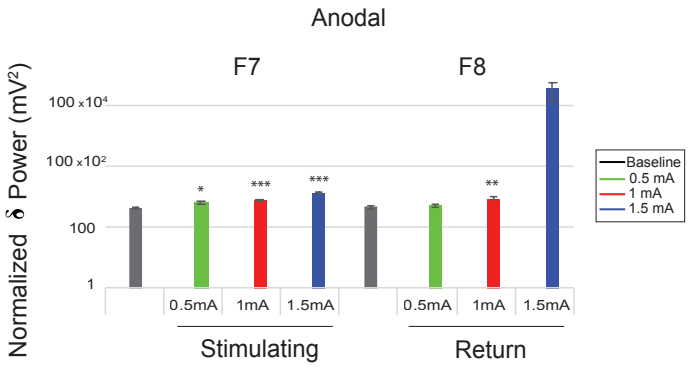

Animal C

% Change δ PWR Post Stim

	F7	F8
0.5mA	49.27	9.16
1mA	69.69	84.50
1.5mA	223.87	783946.30

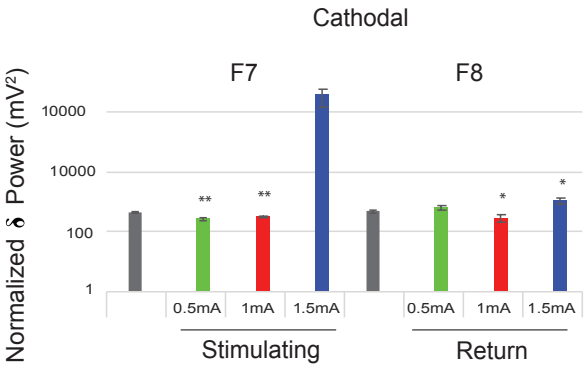

% Change δ PWR Post Stim

	F7	F8
0.5mA	-39.57	28.59
1mA	-29.52	-41.58
1.5mA	863917.60	124.96

Figure 2.10: Post-stimulation Effects of tDCS in Frontal Regions in Animal C. Normalized delta band power during baseline and post-stimulation in frontal scalp electrodes. Power is broken down by polarity and intensity across frontal areas. Percent decrease from baseline (red) and increase (green). Baseline is specific for each area, collapsed across polarity and intensity. Data is reported as mean ± SEM: *= p<0.05; ** = p<0.01; *** = p<0.001 (two sample t-test, unequal variance; FDR corrected).

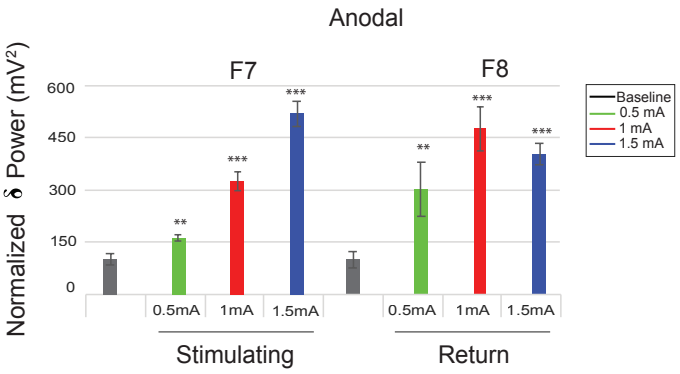

Animal Z

% Change δ PWR Post Stim

	F7	F8
0.5mA	62.53	197.18
1mA	69.33	368.91
1.5mA	420.99	298.01

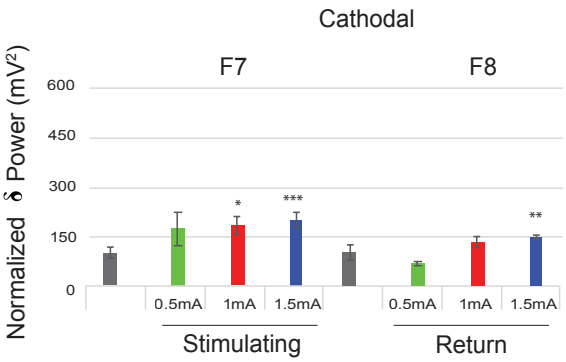

% Change δ PWR Post Stim

	F7	F8
0.5mA	72.36	-33.26
1mA	82.65	30.14
1.5mA	99.34	46.08

Figure 2.11: Post-stimulation Effects of tDCS in Frontal Regions in Animal Z. Normalized delta band power during baseline and post-stimulation in frontal scalp electrodes. Decrease in percent change from baseline broken down by polarity and intensity (red) and increase (green). Baseline is specific for each area, collapsed across polarity and intensity. Data is reported as mean ± SEM: *= p<0.05; ** = p<0.01; *** = p<0.001 (two sample t-test, unequal variance; FDR corrected).

A. Anodal

		Animal C		Animal Z	
	Intensity (mA)	Post-stimulation	p-vals	Post-stimulation	p-vals
F7	0.5	655.66 ± 75.53	0.017	162.67 ± 9.13	0.0018
	1	745.36 ± 37.84	7.9e-7	326.38 ± 26.51	4.9e-11
	1.5	1422.56 ± 109.54	3.1e-13	521.43 ± 36.58	7.0e-16
F8	0.5	526.28 ± 67.06	0.61	302.97 ± 77.64	0.031
	1	889.48 ± 114.06	0.010	478.05 ± 63.90	8.0e-7
	1.5	3779836 ± 2278172.42	0.15	405.77 ± 31.36	6.1e-12

B. Cathodal

		Animal C		Animal Z	
	Intensity (mA)	Post-stimulation	p-vals	Post-stimulation	p-vals
F7	0.5	265.42 ± 32.91	0.0036	172.51 ± 51.70	0.19
	1	309.54 ± 20.56	0.013	182.81 ± 28.71	0.017
	1.5	3795130.85 ± 2297997.85	0.10	199.51 ± 21.76	0.00081
F8	0.5	619.94 ± 122.28	0.35	68.04 ± 7	0.19
	1	281.65 ± 77.04	0.067	132.68 ± 17.27	0.29
	1.5	1084.54 ± 234.65	0.041	148.93 ± 8.13	0.084

Table 2.3: Bilateral Post-stimulation Frontal Scalp EEG P-values Animal C and Z. Power spectra from scalp electrodes during anodal and cathodal F7 stimulation. F7 is the stimulating electrode and F8 is the return, animal C's baseline power is 439.24 ± 44.62 and 482.09 ± 53.17 respectively. Animal Z's baseline powers as 100.08 ± 16.84 and 101.95 ± 23.18 respectively. Post-stimulation data mean ± SEM (paired t-test of unequal variance, FDR corrected).

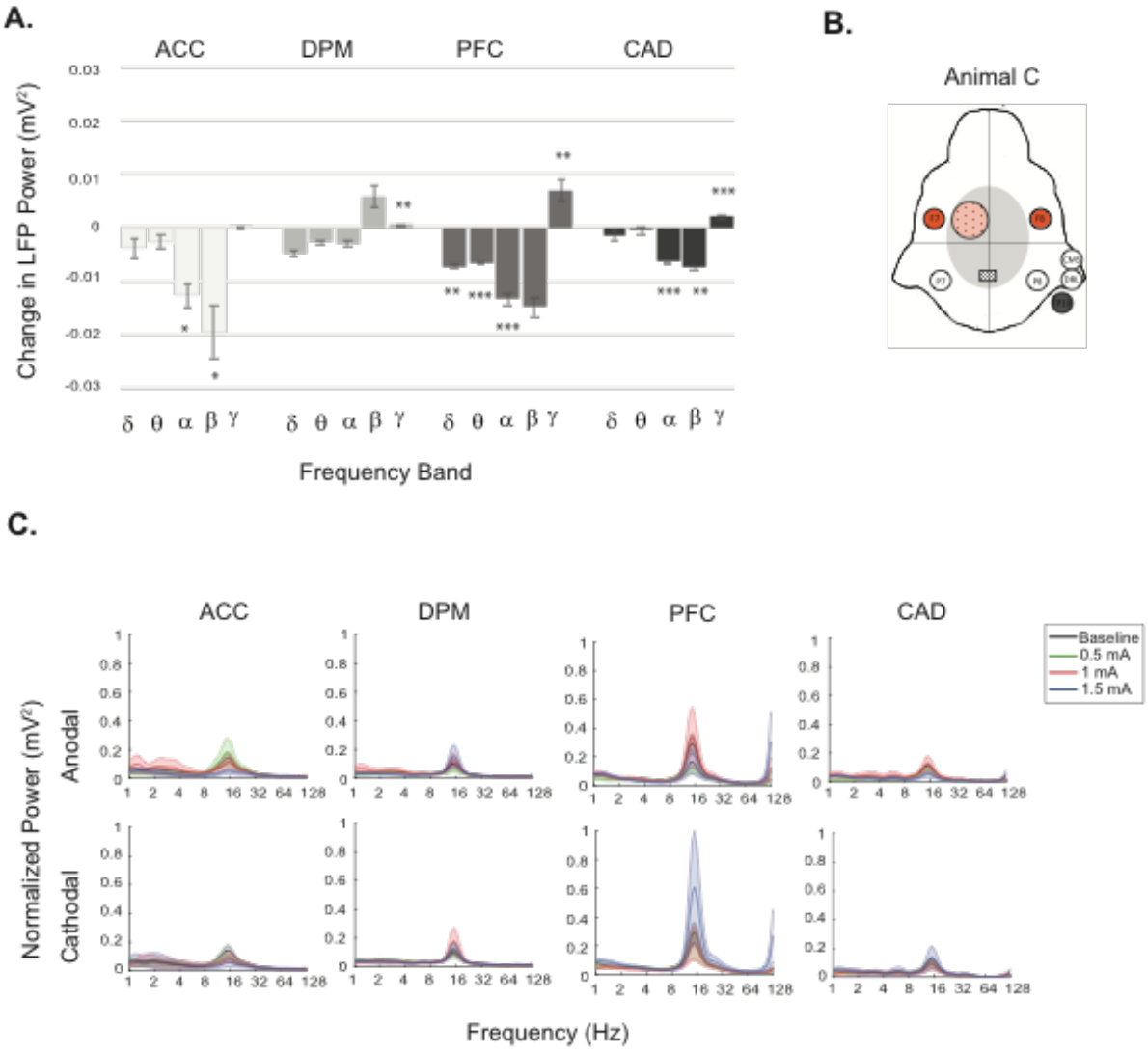

Figure 2.12: The Influence of tDCS on Intracortical Brain Regions in Animal C. LFP data from ACC, DPM, PFC, and CAD recorded simultaneously during tDCS. Change in LFP power spectra collapsed across polarity and intensity in each location (A). Stimulation effects are seen across frequency bands Delta (δ; 1-4 Hz), Theta (θ; 4-8 Hz), Alpha (α; 8-12 Hz), Beta (β; 12-30 Hz), and Gamma (γ; 30-128 Hz). Approximate location of intracortical electrodes (light orange) and stimulating (orange) and reference (grey) scalp electrodes (B). Full power spectrum broken down by polarity (anodal and cathodal) and three different stimulation intensities (green: 0.5 mA, red: 1 mA, blue: 1.5 mA) are shown along with baseline (black). Power has been normalized for correction of power-law decay. Baseline is specific for area. Data is reported as mean ± SEM: *= $p<0.05$; ** = $p<0.01$; *** = $p<0.001$ (paired t test).

A. ACC

	Baseline	Stimulation	p-val
δ	0.058 ± 0.011	0.054 ± 0.013	0.66
θ	0.037 ± 0.0057	0.034 ± 0.0072	0.56
α	0.063 ± 0.01	0.050 ± 0.0079	0.024
β	0.084 ± 0.015	0.064 ± 0.01	0.029
γ	0.016 ± 0.0017	0.016 ±0.0017	0.91

B. DPM

	Baseline	Stimulation	p-val
δ	0.042 ± 0.0043	0.037 ± 0.0048	0.2
θ	0.031 ± 0.0023	0.028 ± 0.0026	0.13
α	0.039 ± 0.0036	0.036 ±0.003	0.14
β	0.05 ± 0.0061	0.056 ± 0.0081	0.19
γ	0.011 ± 0.0008	0.012 ± 0.0008	0.0088

C. PFC

	Baseline	Stimulation	p-val
δ	0.058 ± 0.0038	0.051 ± 0.0034	0.005
θ	0.04 ± 0.0025	0.033 ± 0.0023	9.10e-06
α	0.081 ± 0.0097	0.068 ± 0.0086	0.00034
β	0.14 ± 0.026	0.12 ± 0.025	0.089
γ	0.021 ± 0.0025	0.028 ± 0.0045	0.0075

D. CAD

	Baseline	Stimulation	p-val
δ	0.034 ± 0.0036	0.032 ± 0.0045	0.52
θ	0.029 ± 0.0040	0.028 ± 0.0049	0.77
α	0.042 ± 0.0043	0.036 ± 0.0043	0.00089
β	0.055 ± 0.0074	0.047 ± 0.0071	0.0018
γ	0.0066 ± 0.00081	0.0087 ± 0.0012	0.00035

Table 2.4: Bilateral Stimulation Intracortical P-values Animal C. Power spectra from ACC (A), DPM (B), PFC (C), and CAD (D) collapsed across polarity and intensity by frequency band. Data presented as mean ± SEM (two sample t-test).

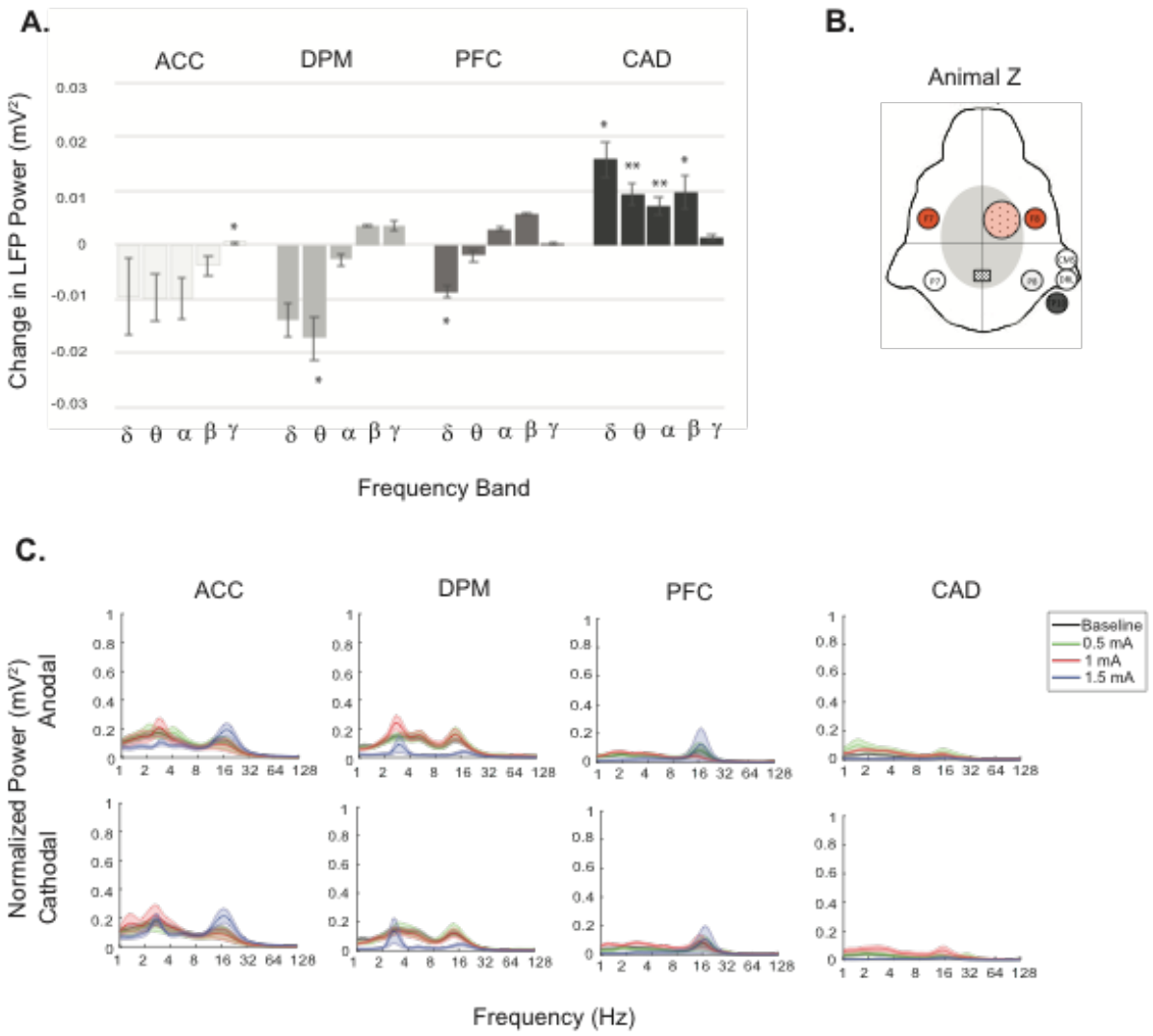

Figure 2.13: The Influence of tDCS on Intracortical Brain Regions in Animal Z. LFP data from ACC, DPM, PFC, and CAD recorded simultaneously during tDCS. Change in LFP power spectra collapsed across polarity and intensity in each location (A). Stimulation effects are seen across frequency bands Delta (δ; 1-4 Hz), Theta (θ; 4-8 Hz), Alpha (α; 8-12 Hz), Beta (β; 12-30 Hz), and Gamma (γ; 30-128 Hz). Approximate location of intracortical electrodes (light orange) and stimulating (orange) and reference (grey) scalp electrodes (B). Full power spectrum broken down by polarity (anodal and cathodal) and three different stimulation intensities (green: 0.5 mA, red: 1 mA, blue: 1.5 mA) are shown along with baseline (black). Power has been normalized for correction of power-law decay. Baseline is specific for area. Data is reported as mean ± SEM: *= $p<0.05$; ** = $p<0.01$; *** = $p<0.001$ (paired t test).

A. ACC

	Baseline	Stimulation	p-val
δ	0.14 ± 0.022	0.13 ± 0.015	0.55
θ	0.11 ± 0.013	0.097 ± 0.0083	0.31
α	0.09 ± 0.011	0.08 ± 0.007	0.094
β	0.088 ± 0.014	0.084 ± 0.012	0.21
γ	0.0091 ± 0.0013	0.0097 ± 0.0012	0.013

B. DPM

	Baseline	Stimulation	p-val
δ	0.11 ± 0.012	0.098 ± 0.0085	0.081
θ	0.11 ± 0.015	0.097 ± 0.011	0.029
α	0.081 ± 0.01	0.079 ± 0.0091	0.47
β	0.071 ± 0.008	0.074 ± 0.0081	0.20
γ	0.0061 ± 0.0011	0.0097 ± 0.002	0.076

C. PFC

	Baseline	Stimulation	p-val
δ	0.046 ± 0.0058	0.0375 ± 0.0047	0.044
θ	0.035 ± 0.0055	0.033 ± 0.0044	0.62
α	0.03 ± 0.0065	0.033 ± 0.0062	0.30
β	0.044 ± 0.014	0.005 ± 0.014	0.091
γ	0.0036 ± 0.0009	0.0039 ± 0.0083	0.72

D. CAD

	Baseline	Stimulation	p-val
δ	0.032 ± 0.055	0.048 ± 0.0088	0.031
θ	0.019 ± 0.0028	0.0288 ± 0.0048	0.0048
α	0.016 ± 0.0023	0.023 ± 0.0039	0.0056
β	0.015 ± 0.0025	0.0248 ± 0.0056	0.023
γ	0.0028 ± 0.0008	0.0042 ± 0.0014	0.21

Table 2.5: Bilateral Stimulation Intracortical P-values Animal Z. Change in power spectra in ACC (A), DPM (B), PFC (C), and CAD (D) across frequency bands, collapsed by polarity and intensity. Data presented as mean ± SEM (two sample t-test).

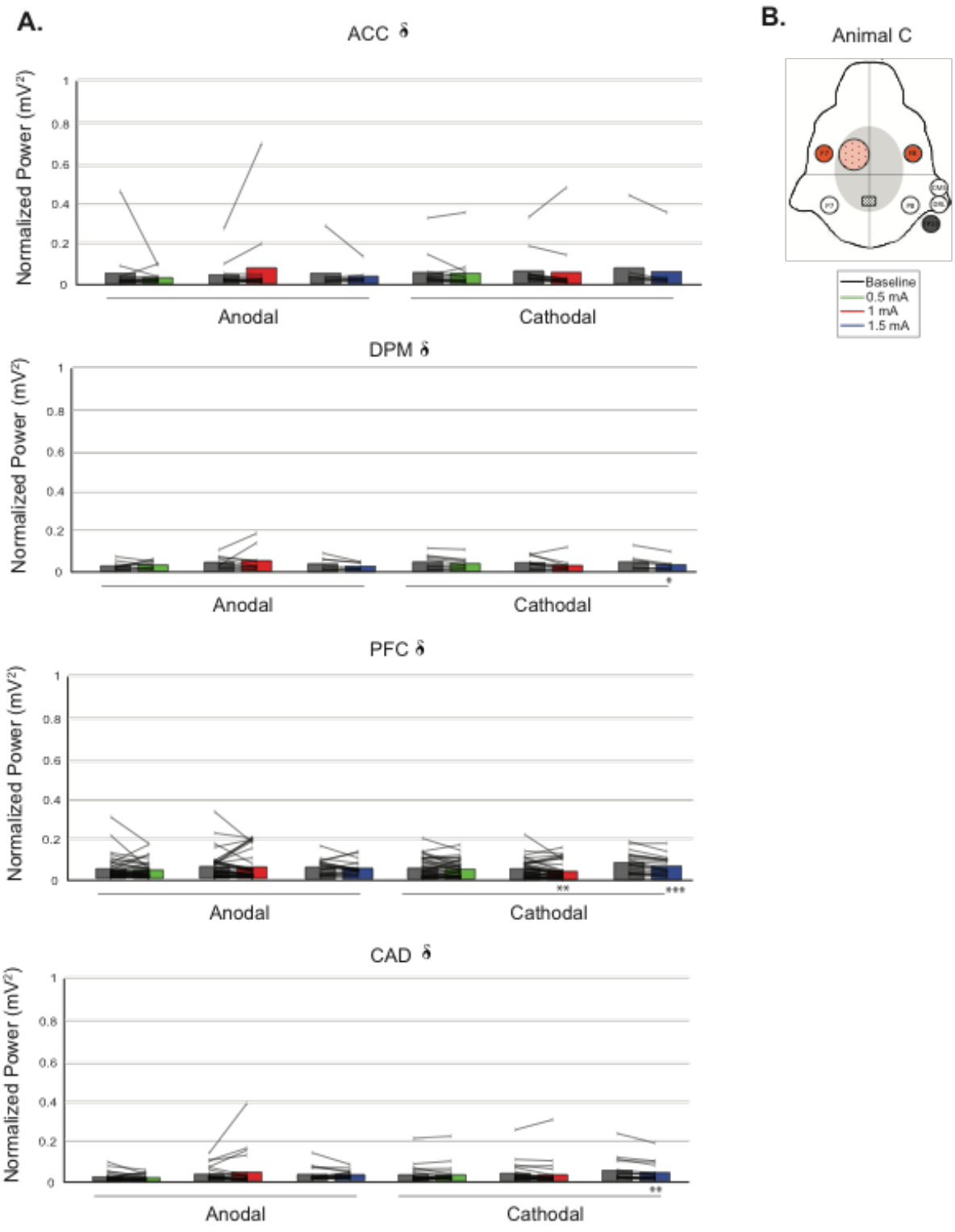
A.
ACC δ
Normalized Power (mV²)
Anodal
Cathodal
DPM δ
PFC δ
CAD δ
B.
Animal C
Baseline
0.5 mA
1 mA
1.5 mA

Figure 2.14: Intracortical Delta Band Power During Stimulation in Animal C. Normalized delta band power broken down by polarity (anodal and cathodal) and intensity (green: 0.5 mA, red: 1 mA, blue: 1.5 mA) compared to baseline (dark grey). Bars represent average mean, lines denote individual electrodes. Data is reported as mean ± SEM: *= $p<0.05$; ** = $p<0.01$; *** = $p<0.001$ (paired t test).

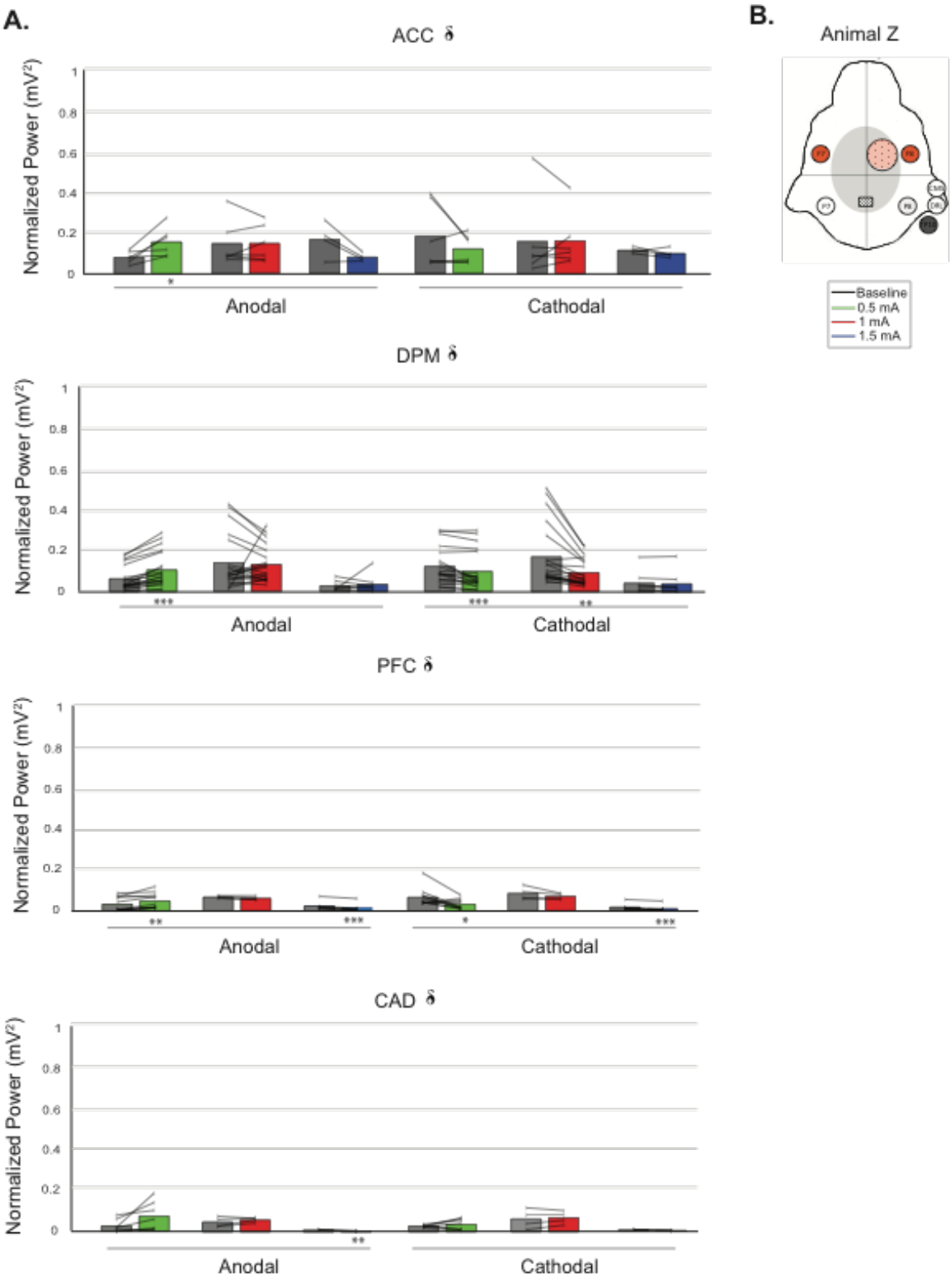
A.
ACC δ
Normalized Power (mV²)
Anodal
Cathodal
DPM δ
PFC δ
CAD δ
B.
Animal Z
Baseline
0.5 mA
1 mA
1.5 mA

Figure 2.15: Intracortical Delta Band Power During Stimulation in Animal Z. Normalized delta power broken across polarity (anodal and cathodal) and intensity (green: 0.5 mA, red: 1 mA, blue: 1.5 mA). Power compared to baseline (dark grey). Bars represent average mean, lines denote individual electrodes. Data is reported as mean ± SEM: *= $p<0.05$; ** = $p<0.01$; *** = $p<0.001$ (paired t test).

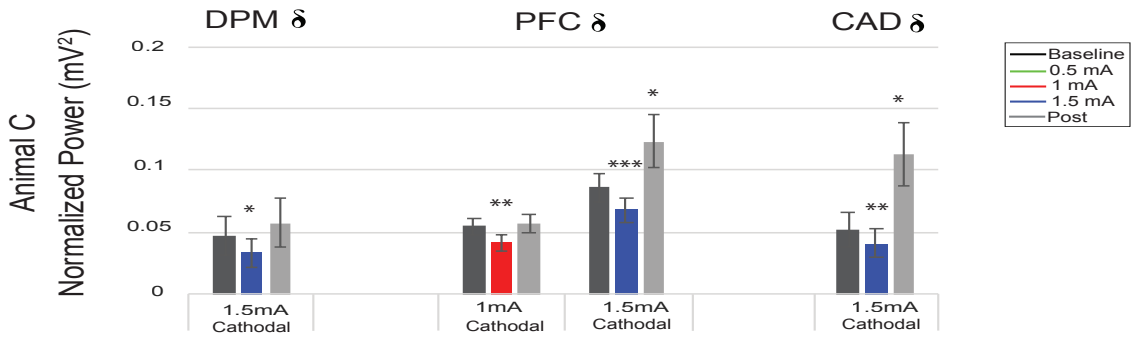

Figure 2.16: Intracortical Post-stimulation Delta Power in Animal C. Intracortical areas with significant increases in power during stimulation compared to post. Post-stimulation is 2—7 seconds after stimulation is turned off, to exclude ramp down effects. Changes in delta power during stimulation are not seen post-stimulation except in Cathodal 1.5 mA in the CAD. Data is reported as mean ± SEM: *= $p<0.05$; ** = $p<0.01$; *** = $p<0.001$ (paired t test).

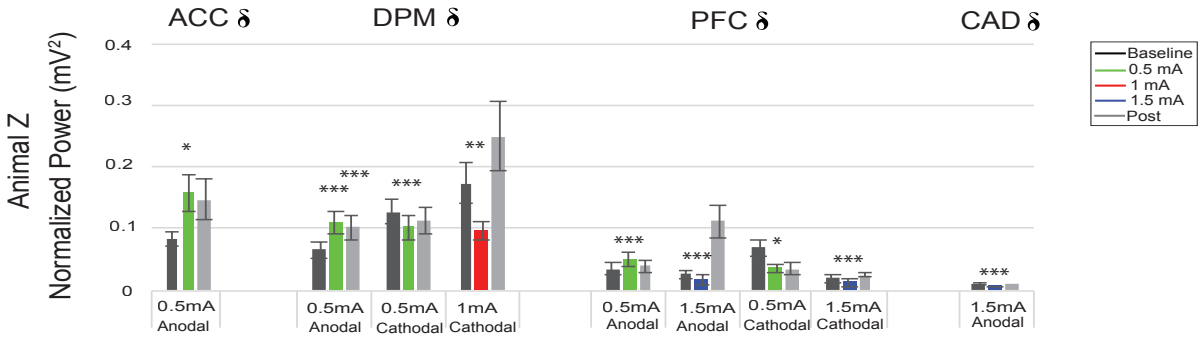

Figure 2.17: Intracortical Post-stimulation Delta Power in Animal Z. Intracortical areas with significant increases in power during stimulation compared to post. Post-stimulation is 2—7 seconds after stimulation is turned off, to exclude ramp down effects. Changes in delta power during stimulation are not seen post-stimulation except in Anodal 0.5 mA in the CAD. Data is reported as mean ± SEM: *= $p<0.05$; ** = $p<0.01$; *** = $p<0.001$ (paired t test).

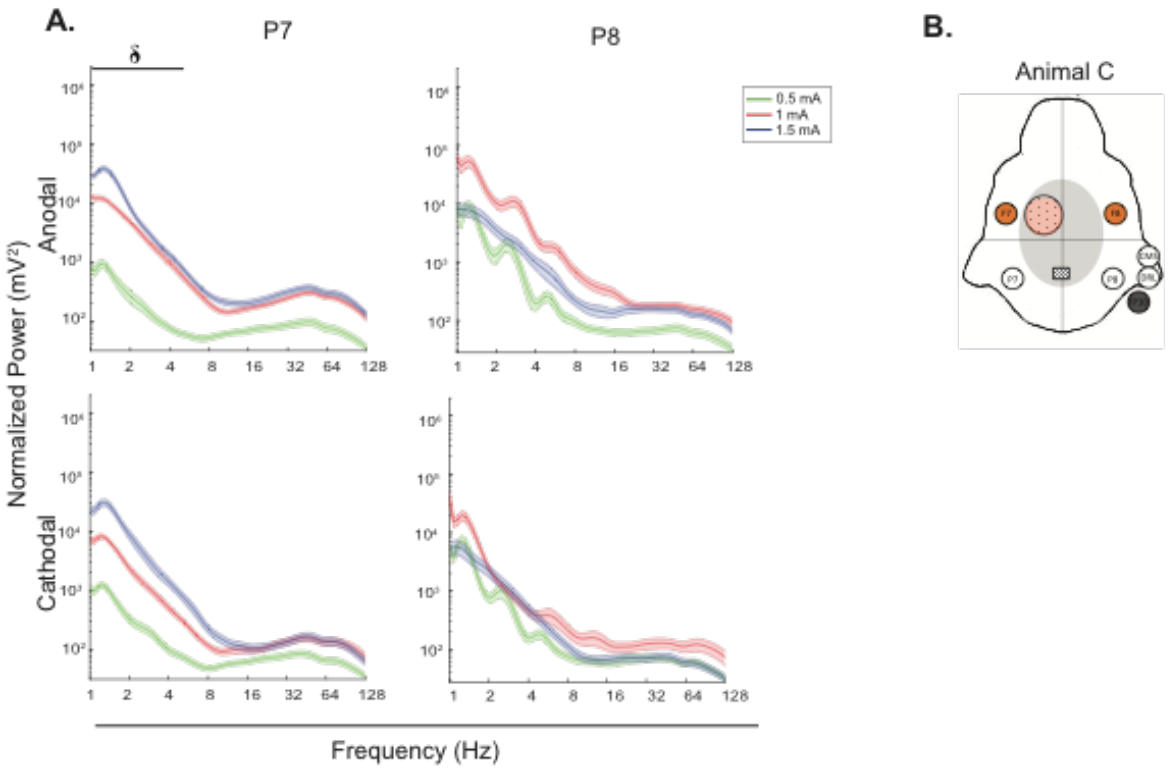

Supplemental Figure 2.1: The Effects of tDCS with Intracortical Electrodes Inserted on Scalp EEG in Animal C. Power spectra of parietal scalp electrodes during anodal (top) and cathodal (bottom) stimulation with intracortical electrodes in place (A). Three different stimulation intensities (green: 0.5 mA, red: 1 mA, blue: 1.5 mA) are superimposed on each panel. Power has been normalized for correction of power-law decay and is plotted on a log scale. Inset of animal C with a bilateral tDCS montage, stimulating scalp electrodes and recording chamber (orange) and reference scalp electrode (grey). Intracortical electrodes were inserted into the PFC, ACC, DPM, and CAD.

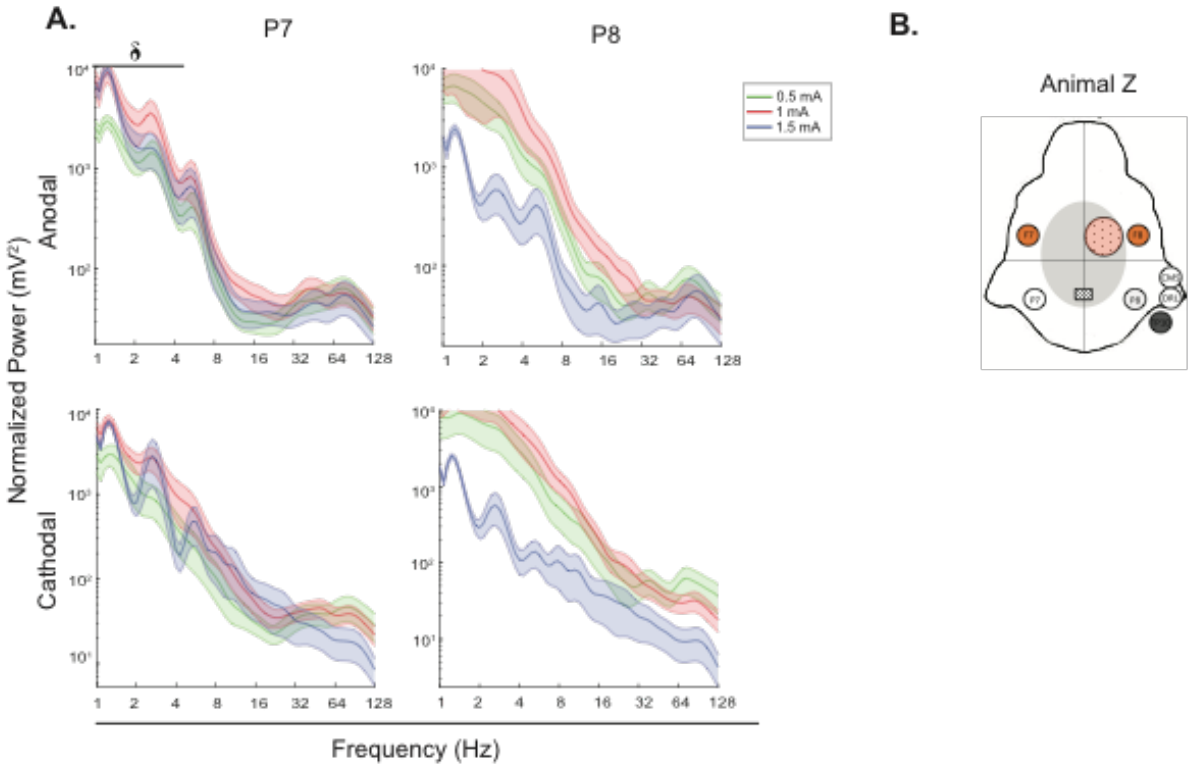

Supplemental Figure 2.2: The Effects of tDCS with Intracortical Electrodes Inserted on Scalp EEG in Animal Z. Power spectra of parietal scalp electrodes during anodal and cathodal stimulation with intracortical electrodes present (A). Intracortical electrodes were inserted into the PFC, ACC, DPM, and CAD. Superimposed on each panel are three different stimulation intensities (green: 0.5 mA, red: 1 mA, blue: 1.5 mA). Power is plotted on a log scale and has been normalized for correction of power-law decay. Location of stimulating scalp electrodes and recording chamber (orange) and scalp EEG reference (grey) (B).

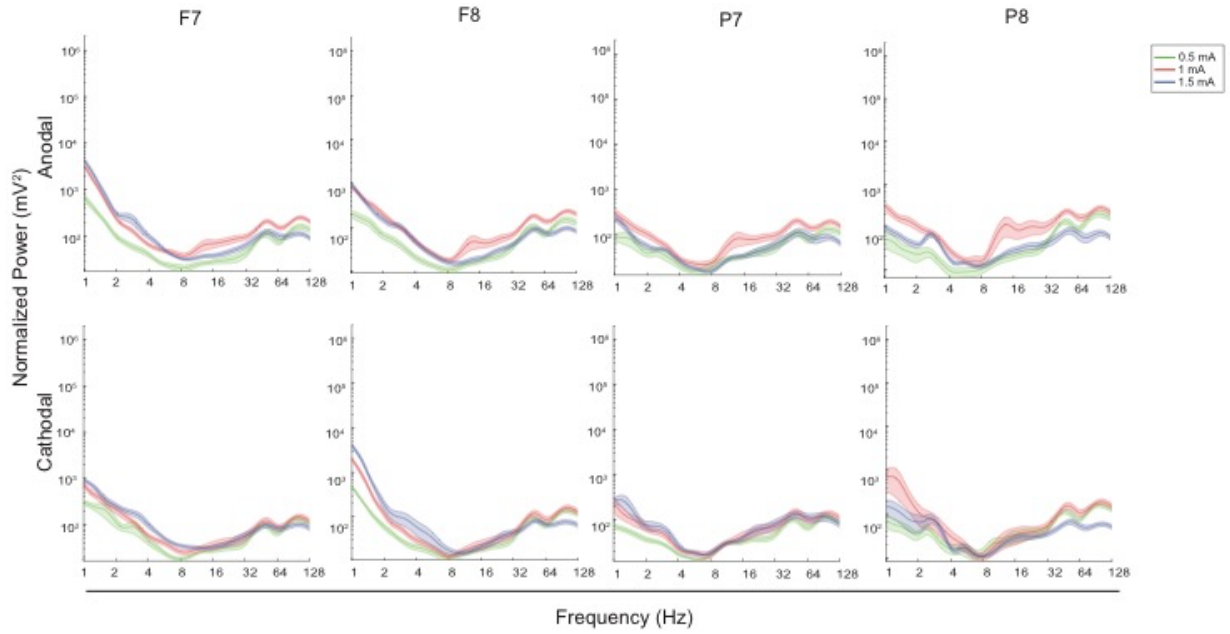

Supplemental Figure 2.3: Post-stimulation Scalp EEG Power Spectra in Animal C with Intracortical Electrodes Inserted. Frontal and parietal scalp EEG during anodal and cathodal stimulation with intracortical electrodes. Intracortical electrodes were inserted into the PFC, ACC, DPM, and CAD. Superimposed on each panel are three different stimulation intensities (green: 0.5 mA, red: 1 mA, blue: 1.5 mA). Power has been normalized for correction of power-law decay.

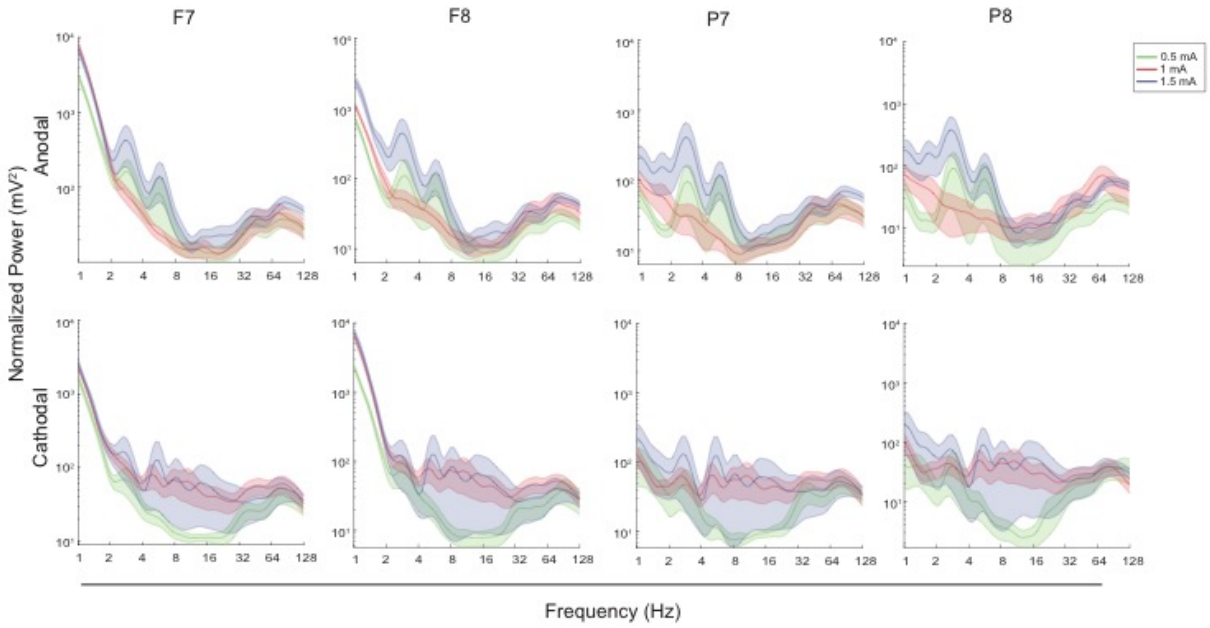

Supplemental Figure 2.4: Post-stimulation Scalp EEG Power Spectra in Animal Z with Intracortical Electrodes Inserted. Frontal and parietal scalp EEG during anodal and cathodal stimulation with intracortical electrodes inserted into the PFC, ACC, DPM, and CAD. Superimposed on each panel are three different stimulation intensities (green: 0.5 mA, red: 1 mA, blue: 1.5 mA). Power has been normalized for correction of power-law decay.

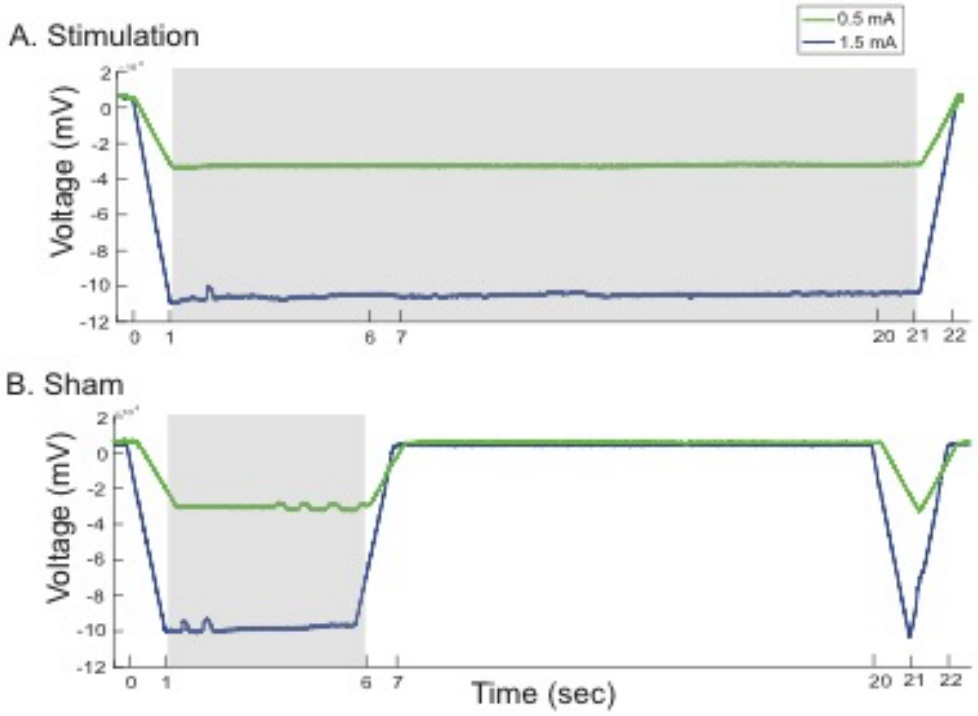

Supplemental Figure 2.5: EEG of tDCS and Sham tDCS Trial. Example of a pre-processed scalp EEG channel from one recording day showing 2 anodal stimulation trials (A) and 2 anodal sham tDCS trials (B). Two intensities are shown at 0.5 mA (green) and 1.5 mA (blue). Stimulation (1-21 seconds) and sham tDCS (1-6) time segments are highlighted in grey.

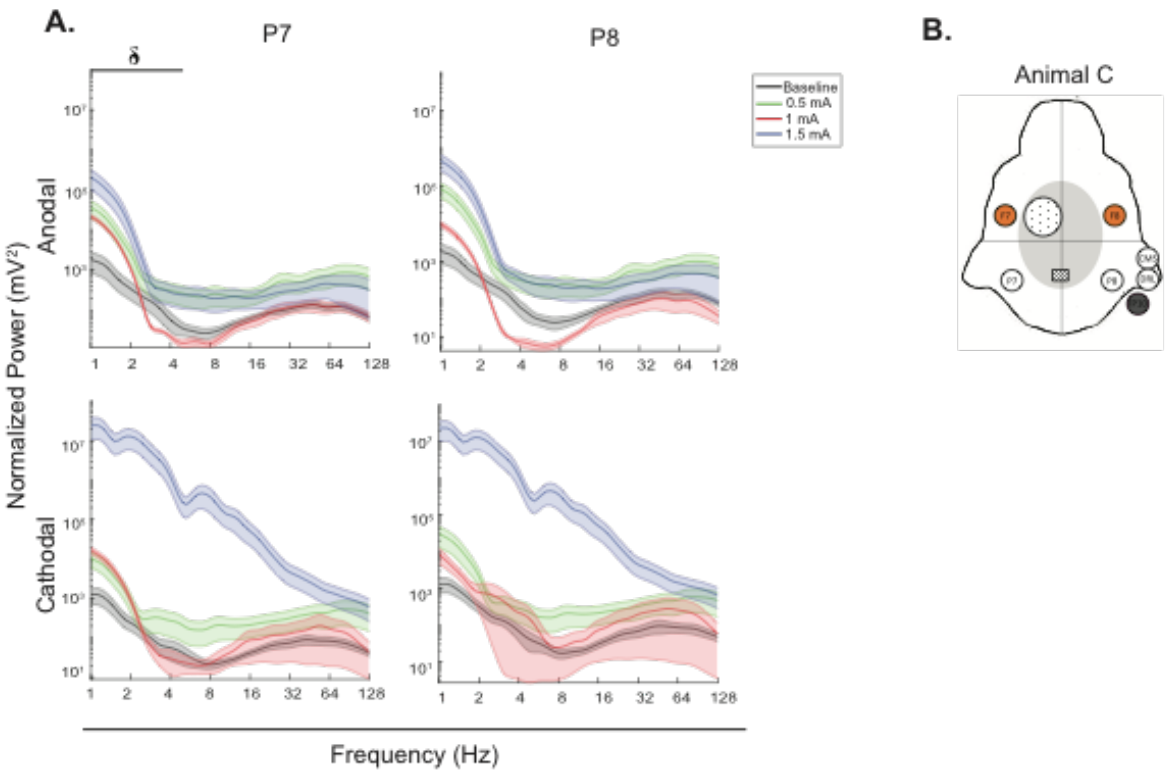

Supplemental Figure 2.6: Power Spectra During Shortened Duration Stimulation in Animal C. Power spectra of parietal scalp electrodes during a brief 5 second anodal (top) and cathodal (bottom) stimulation, also referred to as sham stimulation (A). Three stimulation intensities (green: 0.5 mA, red: 1 mA, blue: 1.5 mA) are superimposed on each panel. Power has been normalized for correction of power-law decay and is plotted on a log scale. Inset of animal C with a bilateral tDCS montage, stimulating scalp electrodes (orange) and reference scalp electrode (grey).

Bilateral Montage

	PFC	ACC	DPM	CAD
Animal C	41	14	13	25
Animal Z	11	8	24	7

Supplemental Table 2.1: Identity and Number of Intracortical Electrodes with Bilateral tDCS Montage. Number of intracortical electrodes per area in animal C and Z that data was collected and analyzed from.

Chapter 3: The Influence of Unilateral Transcranial Electric Brain Stimulation on Neural Activity in the Primate Brain

Introduction

tDCS is a form of neuro-stimulation that has gained popularity as a clinical tool for the treatment of neuropsychiatric disorders. Despite growing interest in this technique, we know little about the mechanisms by which tDCS might work. There is considerable controversy as to whether or how tDCS affects neural activity (Vöröslakos et al., 2018), and understanding the potential effects is complicated by stimulation parameters including electrode montage, polarity, and intensity of stimulation (Bastani & Jaberzadeh, 2013; Moliadze et al., 2010). Previous studies have suggested that tDCS can modulate cortical excitability in a polarity-dependent fashion (Sánchez-León et al., 2021), such that anodal stimulation is thought to increase cortical excitability, whereas cathodal stimulation may decrease it (Bindman et al., 1964; Nitsche, Nitsche, et al., 2003; Nitsche & Paulus, 2000; Purpura & McMurtry, 1965). Furthermore, placement of scalp electrodes is thought to change current flow and the areas being impacted. Therefore, there is a growing demand to understand the underlying mechanisms of this technique in aims to further optimize stimulation paradigms as a therapeutic target.

In the experiments described below, we explore the parameter space of tDCS by identifying changes in spectral power following tDCS in the NHP. We systematically break down different stimulation parameters (including polarity and intensity) to identify their neurophysiological effects more clearly by pairing multi-electrode intracranial recordings with tDCS. tDCS was targeted over the PFC via scalp electrodes using a unilateral montage, where current from stimulating to return electrode flowed within the

same hemisphere. Scalp EEG and intracortical LFP data were simultaneously collected to assess effects both during and post-stimulation.

Research Methods:

Animals and surgical procedures: Experiments were conducted on one female (animal C) and one male (animal Z) adult macaque monkey (*Macacca mulatta*). Both NHP were surgically implanted with a head restraint post and a recording chamber located over the principle and arcuate sulcus**.** All surgical procedures used conformed to NIH guidelines and were approved by UC Davis IACUC.

Passive Behavior: NHPs did not perform a behavioral task but were seated in front of a monitor where there were allowed to passively view a grey screen monitor. No visual stimuli were presented on the screen. Eye position was monitored by an infrared video eye tracker (Applied Science Laboratories, Bedford, MA).

Transcranial direct current stimulation: tDCS was performed using the 8 electrode Neuroelectrics Starstim setup (Neuroelectrics Instrument Controller, v1.0; Rev 2012-08-01, Neurolelectrics, Barcelona, Spain) in conjunction with the program NIC. Five-six 1cm radius Ag/AgCl electrodes (PISTIM, Neuroelectrics) were used with Signa conductive gel (Parker Laboratories). An earclip was used for CMS/DRL. Scalp EEG data was collected at 500 Hz and analyzed offline. Electrode impedance at the start of every recording session was 0-10 kΩ, signals >15 kΩ were automatically aborted.

Scalp electrode locations were approximated from a scaled down 10-20 mapping system and both NHPs were fitted with custom scalp EEG caps. NHP hair was trimmed

before each recording session. Electrodes were placed over frontal (F7 and F8) and parietal brain areas (P7 and P8) with reference electrodes positioned behind the ear as mastoid references (TP9 and TP10). A unilateral stimulation montage was used, where the stimulating electrode and return was on the same hemisphere. The stimulating electrode was F7 in animal C and F8 in animal Z, as their recording chambers are on opposite hemispheres. tDCS stimulation parameters examined include polarity (anodal and cathodal stimulation) and intensity (0.5, 1, 1.5 mA). Scalp electrodes were not able to simultaneously record EEG during active current delivery, therefore, the effects of tDCS on scalp EEG during stimulation are examined in recordings from 2 electrodes while baseline and post-stimulation effects were examined in recordings from all 4. A breakdown of stimulating electrodes in each animal according to montage is shown in **Figure 3.1**. Mastoid references used in analysis are TP10 for both animals unless otherwise noted.

A combination of stimulation protocols was used, where 2-3 stimulation intensities and both polarities of stimulation were randomly assigned to each trial on a given day. Trials began with a start and end baseline (120 seconds each) and 80 blocks of stimulation (22 seconds) separated by blocks of EEG recording (20 seconds each). Stimulation ramp-up and ramp-down was 1 seconds. On days where sham tDCS was delivered, 16 stimulation trials of each condition were randomly re-assigned as sham. Two different datasets were collected: scalp EEG only and scalp EEG with intracortical LFPs. Sham stimulation data was only collected in animal C and consisted of the same ramp up and down time but consisted of a brief 5 second stimulation period.

Neural Recordings: Simultaneous multi-electrode recordings were made from the PFC, CAD, ACC, and DPM with 8-16 tungsten electrodes (FHC, Bowdoin, ME). Total number of electrodes in each recording site can be found in **Supplemental Table 3.1**. Broadband signals were collected at 20 kHz through a Plexon headstage (x1) and preamplifier (x1000 gain, band-pass filtering the signal at 0.7 Hz-6 kHz) via a 1401 data acquisition system and Spike2 software (Cambridge Electronic Design, Cambridge, UK). Electrodes were lowered into different sites every day of recording and were guided by each animals MRI images. Our analysis of PFC included both regions of the lateral PFC and caudal PFC (posterior to area 8A including the frontal eye fields) and CAD included both the head and body.

Data Analysis: Scalp EEG and intracortical LFP data were analyzed offline using custom written code in MATLAB (Mathworks, Natick MA). Signals were low-pass filtered using a 10^{th} order Butterworth filter (high cut freq: 300 Hz for LFP and 250 Hz for scalp EEG) and 60 cycle noise was removed (10^{th} order bandstop filter 59-61 Hz). LFP data was down-sampled to 500 Hz to match the scalp EEG. Both signals were decomposed into their spectral components using a MATLAB-based wavelet analysis toolbox (Torrence and Compo, 1998) through their convolution with a Morlet wavelet, at 6 octaves (2:0.1:128 Hz).

Analysis focused on power across multiple brain areas during 3 epochs: (i) pre-stimulus baseline, (ii) during stimulation, and (iii) post-tDCS. Scalp EEG power is reported across days and LFP is across electrodes, data is presented as mean ± SEM.

Due to the large stimulation artifact seen ramping periods, this time period (with a 2 second buffer around it) was removed from all analyses.

Results

It is unclear how different stimulation parameters influence the effectiveness of tDCS and further limiting its potential as a therapeutic tool (Harris et al., 2019; London & Slagter, 2021). In the following experiments we investigated unilateral tDCS to determine whether it causes changes in scalp EEG and intracortical LFPs in the NHP model (**Figure 3.1**), and whether any effects depend on stimulus polarity (anodal V+, cathodal V-) and/or intensity (0.5, 1, 1.5 mA).

Animal Specific Effects are Seen in Scalp EEG Power During Stimulation.

First, we wanted to know if both animals displayed similar responses to tDCS, as human studies have shown individualized effects (López-Alonso et al., 2014). In line with the human literature, animals C and Z displayed different spectral profiles in response to stimulation (**Figure 3.2**). Animal C showed minimal changes in broadband scalp EEG power during stimulation over the non-stimulated hemisphere (**Figure 3.3A**). In contrast, animal Z showed large changes at <16 Hz (**Figure 3.4A**). Animals received tDCS stimulation over the PFC; yet stimulation was delivered on opposite hemispheres in each animal (**Figure 3.1A, 3.1B**). Animal C received stimulation on the left hemisphere, with the stimulating electrode F7 and return P7. Animal Z's received stimulation on the right side from scalp electrodes F8 for stimulating and P8 for return. We do not anticipate hemispheric differences, yet the influence of tDCS on both animals are plotted separately and stimulation related effects should be done within animal.

As stimulation showed the largest effects in the lower frequency bands, analysis focused on the delta band (1-4 Hz). Animal C showed no changes in delta band power during stimulation (**Figure 3.3C**); yet, animal Z showed the largest effects of tDCS on scalp EEG in the delta band (**Figure 3.4C**). No effects of polarity were seen in either animal. Animal Z shows larger changes in scalp EEG power for 1.5 mA than 1 mA stimulation. However, no 0.5 mA stimulation data was collected and therefore we cannot conclude any linear effects of intensity. See **Table 3.1** for a breakdown of mean power and SEM for each animal.

tDCS Increases Scalp EEG Power Post tDCS at Stimulated Sites.

It is thought that tDCS can have both immediate and long term effects on neural activity (Sánchez-León et al., 2020). Therefore, we further examined how long changes of power lasted post stimulation. For analysis, we added a 5 second buffer following the termination of stimulation, as similar ramp up and down artifacts were seen as reported in Chapter 2. Broadband spectral profiles of scalp recorded EEG sites are found in **Figures 3.5 and 3.6**. No large broadband changes in scalp EEG were seen post-stimulation in animal C, except in 1.5 mA P8 stimulation (**Figure 3.5**). This decrease in power persisted through post-stimulation in the delta band (**Figure 3.7**). Qualitatively, animal Z shows broadband increases in scalp EEG post anodal 1.5 mA stimulation across all scalp EEG sites (**Figure 3.6**). However, animal Z did not show long lasting changes in power post-stimulation in the delta band (**Figure 3.8**). A breakdown of mean power and SEM for each animal can be found in **Table 3.2**.

As our system does not allow us to simultaneously record scalp EEG and deliver current from stimulating electrodes; we could only examine post stimulating effects on stimulated sites. Stimulating electrodes in animal C was F7 with a return in P7, and F8 to P8 in animal Z (**Figure 3.1**). Analysis showed an increased scalp EEG power at stimulated sites in both animals (**Table 3.3**). Animal C showed increased power in both F7 and P7 after tDCS. No polarity specific effects were seen (**Figure 3.9**). Increases in intensity trended to increase with delta band power post-stimulation in animal C. Animal Z showed similar results, where F8 and P8 both shows increased power post-stimulation (**Figure 3.10**). Not enough data was available for conclusions on polarity and intensity related effects. Overall, these data show that tDCS related effects were not strong or maintained post-stimulation in site distal to stimulation but were at areas directly involved in current delivery.

Local Field Potential Show Varying Results with tDCS.

Intracortical recordings were paired with tDCS stimulation to examine the influence of stimulation parameters directly on neurons. Areas recorded from included cortical (ACC, DPM, PFC) and subcortical areas (CAD). Spectral profiles of each area recorded from can be found in **Fig 3.11C and 3.12C**. These data show that each cortical area recorded from had different levels of power with intrinsically strong frequency bands and peaks. This is consistent with cortical areas having unique connections and network properties.

During stimulation, a broadband decrease in power across all intracortical recordings sites was seen, except ACC delta band in Animal C (mean: 0.045 ± 0.037)

(Figure 3.11A). Figures 3.11A and 3.12A show broadband changes in power across frequency bands in animal C and Z, where intensity and polarity are collapsed. Changes in power observed were focused in the lower frequency bands, below gamma **(Table 3.4).** Animal Z showed similar decreases in the change of power during stimulation, except in fewer frequency bands **(Figure 3.12, Table 3.5).** Similarly, animal Z also showed only one parameter combination that increased power, except it was in the beta band in DPM (mean: 0.012 ± 0.0074) **(Figure 3.12A).** These data support the idea that tDCS can penetrate the brain and cause broadband changes in LFP power, as changes were seen in cortical areas adjacent to the targeted stimulation site (the PFC) and subcortically in the CAD.

Delta Band Activity During Unilateral Stimulation Showed Limited Long-term Effects.

Animal C and Z showed some significant changes in delta band power during stimulation in each intracortical areas recorded from (**Figure 3.13 and 3.14)**. No consistent polarity or intensity related effects were seen. Recordings in animal C show strong outliers in cathodal 0.5 mA stimulation in ACC (**Figure 3.13**) and anodal 0.5 mA PFC in animal Z (**Figure 3.14**). From here we examined if areas that had significant changes in power during stimulation showed longer term effects. Both animals show no changes in delta band power post-stimulation, except for animal C in the PFC following anodal 1 mA stimulation (**Figure 3.15 and 3.16; Table 3.6 and 3.7).** These results highlight the potential transient nature of the stimulation applied.

Discussion:

Previous studies have shown that a variety of stimulation parameters influence the effectiveness of tDCS in modulating neuronal activity and as therapy (Bastani & Jaberzadeh, 2013; Moliadze et al., 2010). This study expands the parameter space further than Chapter 2, by looking at the influence of montage on changes in scalp EEG and intracortical activity in the NHP prefrontal tDCS where current flows in a single hemisphere. In the sections below we re-visit discussion topics similar to Chapter 2 and expand upon some important aspects related specifically to montage.

Our results show animal specific changes in non-stimulated scalp EEG recording sites during stimulation (Hsu et al., 2016; Kim et al., 2014). Animal C showed minimal changes, whereas animal Z had increased scalp EEG power in the lower frequency bands that appear related to intensity. Similar changes in low frequency bands have been reported in similar studies (M. R. Krause et al., 2017). Since only two stimulation intensities were collected in animal Z, therefore intensity related effects are speculative. Despite these effects, we cannot eliminate the possibility that changes in power during stimulation may be due artifact of stimulation, as even HD-tDCS systems have large spread in current. For further explanation on how data during stimulation could include artifact of contamination, see Chapter 2.

Non-stimulated sites show minimal if any changes in power from baseline post-stimulation in scalp EEG. However, stimulated scalp EEG sties showed increases in power post-stimulation that trend dose dependent. Overall, 1.5 mA stimulation elicited the largest response in both animals. No polarity specific effects were seen, as anodal and cathodal both caused increases in power post-stimulation at stimulated sites. These

data support the tDCS having more localized effects, despite it being a diffuse form of stimulation.

Since tDCS passes low current through the brain, it is debated the extent to which it can influence intracortical neuron activity has been the subject of debate (Vöröslakos et al., 2018). We further explored the question of whether stimulation could influence intracortical LFP power. Indeed, we found that stimulation changed LFP power, with both animals showing general decreases in broadband spectral power across all intracortical sites recorded – PFC, ACC, DPM, and CAD. This overall change in spectral power is speculated to be from global electric field changes. Furthermore, as most of these areas are cortical – i.e. they generally have similar cell types and orientation – these observations are consistent with similar effects from *in vitro* studies showing neuronal features important in modulating activity (Bikson et al., 2004; Kabakov et al., 2012; Radman et al., 2009).

From here we focused our analysis on the lower frequency band to see if similar changes in scalp EEG data could be found in LFPs. Increases in delta band power were seen in animals C and Z, although these effects were not as pronounced. Similarly, no polarity or intensity related effects were seen. In fact, changes in LFP power seen in the delta band were not long lasting, as power returned to baseline levels post-stimulation. It is possible that long-term changes in power were not seen due to the shortened time frame of stimulation (20 seconds). It is thought that immediate effects of tDCS on neural activity stem from changes in electric fields, causing membrane polarization via redistribution of charges in the cells (Chan et al., 1988). Yet, after effects observed after stimulation is turn off likely requires several minutes of stimulation to develop and

involve plasticity mechanism (Huang et al., 2017), therefore we would not see these effects. For more information on how duration of stimulation and mechanisms of action for tDCS see Chapter 4.

Conclusion

tDCS is a growing technique that has promise as a therapeutic tool capable of modifying neural activity in the brain. Previous studies have shown that stimulation can cause behavioral and psychological changes; however, much work remains to demonstrate its efficacy and use. To broadly investigate its potential benefit, we examined the large parameter space of tDCS in a NHP model and tested different stimulation parameters. No strong effects of polarity or intensity were seen in either scalp EEG or in intracortical LFPs, providing support for the view that purely hyperpolarizing stimulation does not exist (Liu et al., 2018). However, 1.5 mA stimulation did show the largest changes in power in scalp EEG. Furthermore, scalp EEG results showed more obvious changes in neural activity compared to intracortical LFP results, where numerous factors including cell type, neuron orientation and more must be considered. Taken together, these results show that through two different electrophysiological measures, tDCS can lead to changes in population-level dynamics using specific parameter combinations. More broadly these findings highlight the potential use of tDCS as a noninvasive method of stimulation that can influence brain activity, further highlighting its potential as a therapeutic tool (Reinhart & Woodman, 2015).

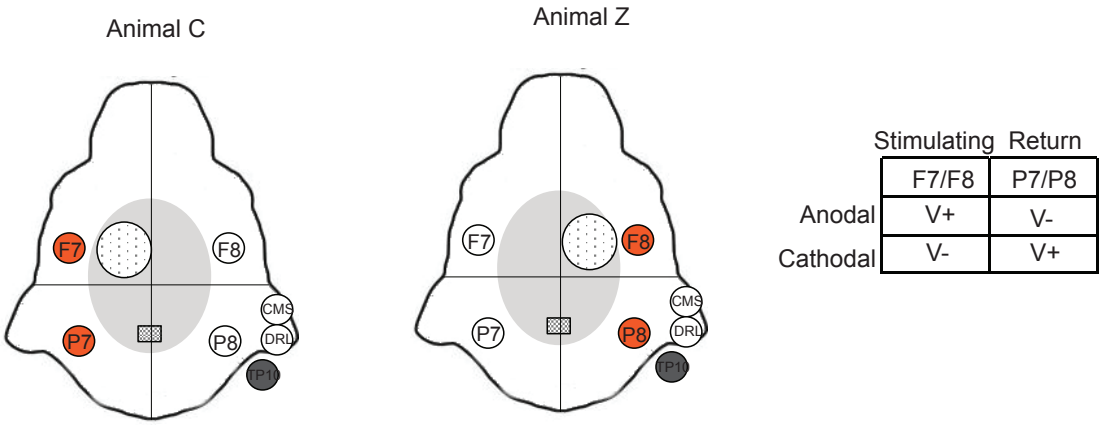

	Stimulating	Return
	F7/F8	P7/P8
Anodal	V+	V-
Cathodal	V-	V+

Figure 3.1: Unilateral Stimulation tDCS Montage Setup. Approximate location of stimulating electrodes (orange), recording scalp electrodes (white) and reference (grey) in both animals C and Z. Current flows within one hemisphere from stimulating (frontal scalp electrode) to return electrode (parietal). Current flows from F7 to P7 in animal C and F8 to P8 in animal Z. Anodal and cathodal stimulation represent the charge of current (V+ and V-) in reference to frontal scalp electrodes.

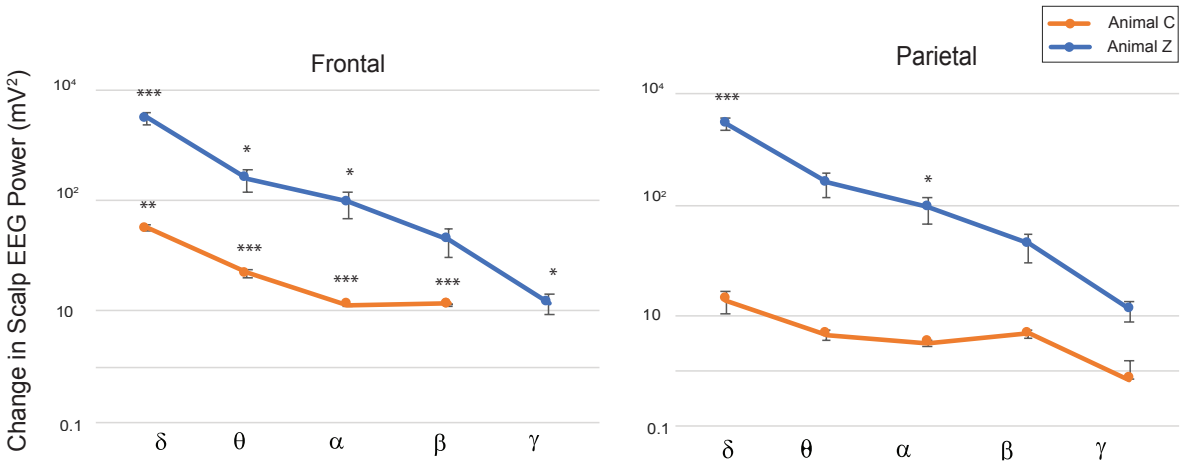

Figure 3.2: Change in tDCS scalp EEG power across frequency bands. tDCS causes changes in frontal and parietal scalp EEG power during stimulation compared to baseline in animal C (orange) and Z (blue). Frontal and parietal scalp recorded site in animal C is F8 and P8, and animal Z is F7 and P7 respectively. Frequency bands are designated as Delta (δ; 1-4Hz), Theta (θ; 4-8Hz), Alpha (α; 8-12Hz), Beta (β; 12-30Hz), and Gamma (γ; 30-128Hz). Animal C and Z show similar changes in spectral power, with animal Z ~100 folder higher. All datapoints are collapsed across polarity and intensity and reported as mean ± SEM: *= p<0.05; ** = p<0.01; *** = p<0.001 (two sample t-test). Gamma band in animal C frontal electrodes is not plotted, as data is plotted on a log scale (-14.41 ± -0.091; ***).

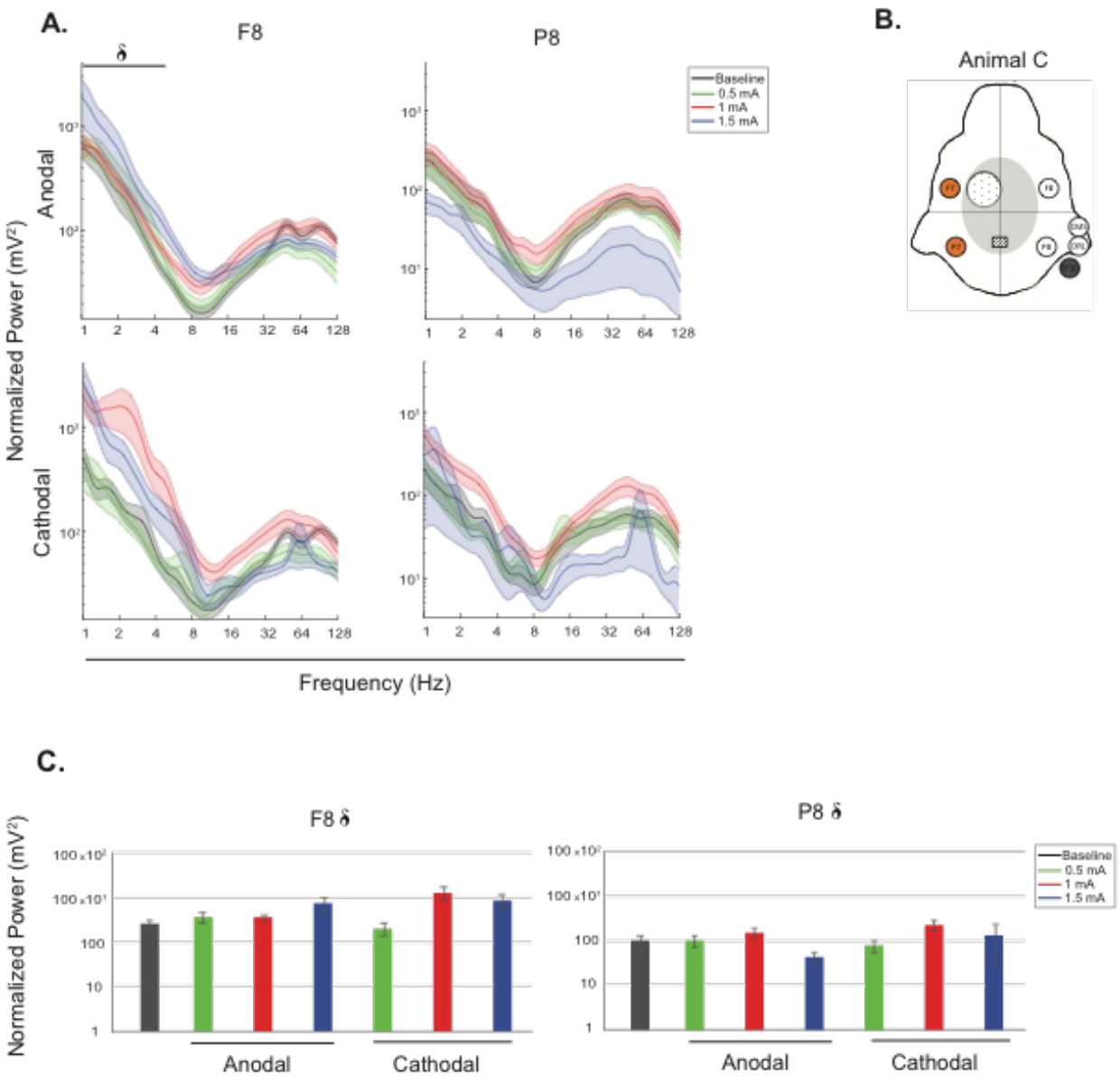

Figure 3.3: The Effects of tDCS on Scalp EEG During Stimulation in Animal C. Power spectra of parietal scalp electrodes during anodal (top) and cathodal (bottom) stimulation with a bilateral montage (A). Three different stimulation intensities (green: 0.5 mA, red: 1 mA, blue: 1.5 mA) are superimposed on each panel along with baseline (black). Power has been normalized for correction of power-law decay and is plotted on a log scale. Strongest effects are seen in the low frequency bands, highlighted in the delta band (δ; 1-4 Hz). Inset of animal C with a unilateral tDCS montage, scalp electrodes (orange) and reference (grey). Delta band effects of tDCS relative to baseline of each stimulation condition in parietal electrodes (C). Baseline is specific for each area, collapsed across intensity and polarity. Data is reported on a log scale as mean ± SEM: *= p<0.05; ** = p<0.01; *** = p<0.001 (two sample t-test, unequal variance; FDR corrected).

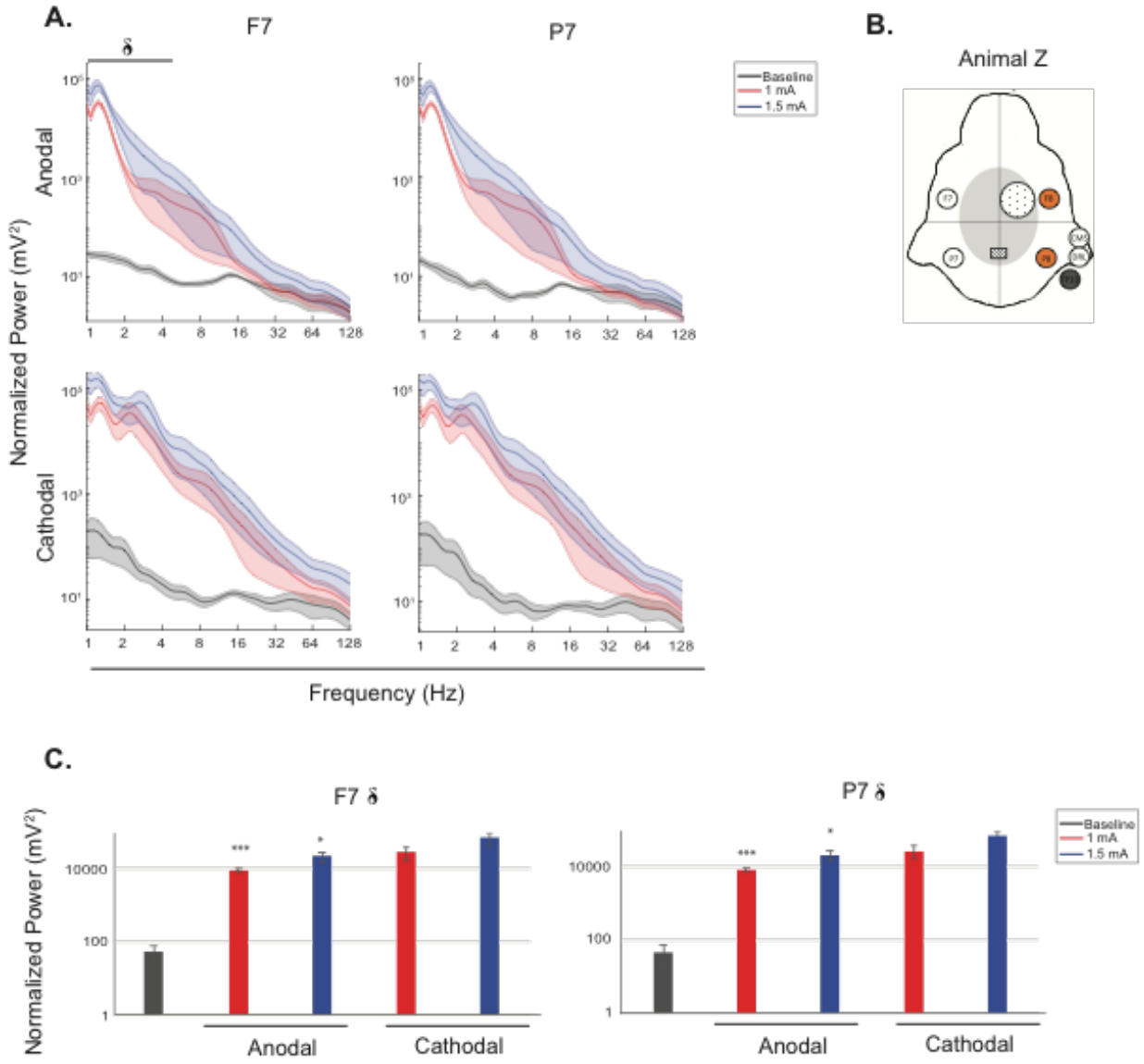

Figure 3.4: The Effects of tDCS on Scalp EEG During Stimulation in Animal Z. Power spectra of parietal scalp electrodes during anodal (top) and cathodal (bottom) stimulation with a umilateral montage (A). Three different stimulation intensities (red: 1 mA, blue: 1.5 mA) are superimposed on each panel along with baseline (black). Power has been normalized for correction of power-law decay and is plotted on a log scale. Strongest effects are seen in the low frequency bands, highlighted in the delta band (δ; 1-4 Hz). Inset of animal C with a bilateral tDCS montage, scalp electrodes (orange) and reference (grey). Delta band effects of tDCS relative to baseline of each stimulation condition in parietal electrodes (C). Baseline is specific for each area, collapsed across intensity and polarity. Data is reported on a log scale as mean ± SEM: *= p<0.05; ** = p<0.01; *** = p<0.001 (two sample t-test, unequal variance; FDR corrected).

C. Frontal

		Animal C (F8)		Animal Z (F7)	
	Intensity (mA)	Stimulation	p-val	Stimulation	p-val
Baseline	--	250.41 ± 42.79	--	52.74 ± 24.36	--
Anodal	0.5	362.57 ± 98.97	0.51	N/A	N/A
	1	345.30 ± 53.25	0.40	8864.19 ± 1110.63	0
	1.5	722.29 ± 299.47	0.40	22229.67 ± 6443.71	0.013
Cathodal	0.5	196.028 ± 62.48	0.63	N/A	N/A
	1	1261.89 ± 406.24	0.18	28030.78 ± 10986.83	0.054
	1.5	823.79 ± 284.72	0.30	70865.59 ± 29355.21	0.055

D. Parietal

		Animal C (P8)		Animal Z (P7)	
	Intensity (mA)	Stimulation	p-val	Stimulation	p-val
Baseline	--	103.27 ± 27.45	--	44.09 ± 25.87	--
Anodal	0.5	98.75 ± 26.71	0.95	N/A	N/A
	1	149.90 ± 39.16	0.66	8455.50 ± 1080.50	0
	1.5	41.48 ± 12.20	0.15	21539.19 ± 6499.66	0.018
Cathodal	0.5	75.41 ± 23.10	0.75	N/A	N/A
	1	225.35 ± 55.91	0.16	27724.73 ± 11038.89	0.058
	1.5	128.16 ± 101.67	0.95	70599.21 ± 29615.74	0.058

Table 3.1: Unilateral Stimulation Scalp EEG P-values. Power spectra from frontal scalp electrodes (A) F8 (animal C) and F7 (animal Z) and parietal electrodes (B) P8 (animal C) and P7 (animal Z). electrodes, Data is shown across polarity and intensity in both animals. Stimulation power data mean ± SEM (paired t-test of unequal variance, FDR corrected) with significant p values in red.

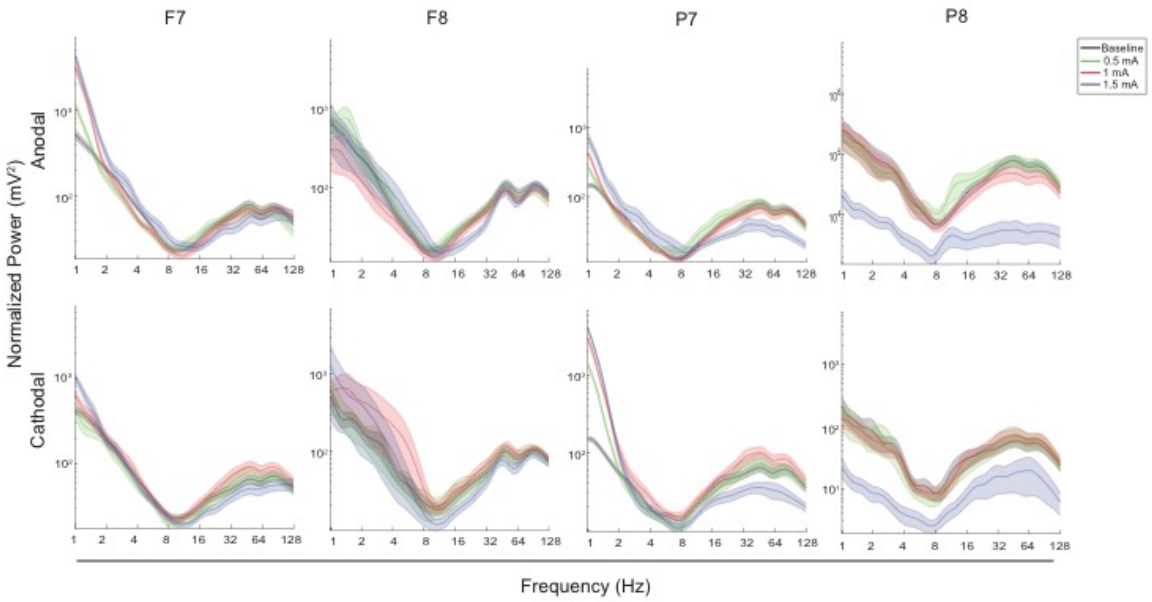

Figure 3.5: Post-stimulation Power Spectra in Animal C. Frontal and parietal scalp EEG with a unilateral montage during anodal and cathodal stimulation in animal C. Stimulated sits were F7 and P7, non stimulated were F8 and P8. Superimposed on each panel are three different stimulation intensities (green: 0.5 mA, red: 1 mA, blue: 1.5 mA) and baseline (black). Power has been normalized for correction of power-law decay. Data is reported on a log scale as mean power at each frequency ± SEM

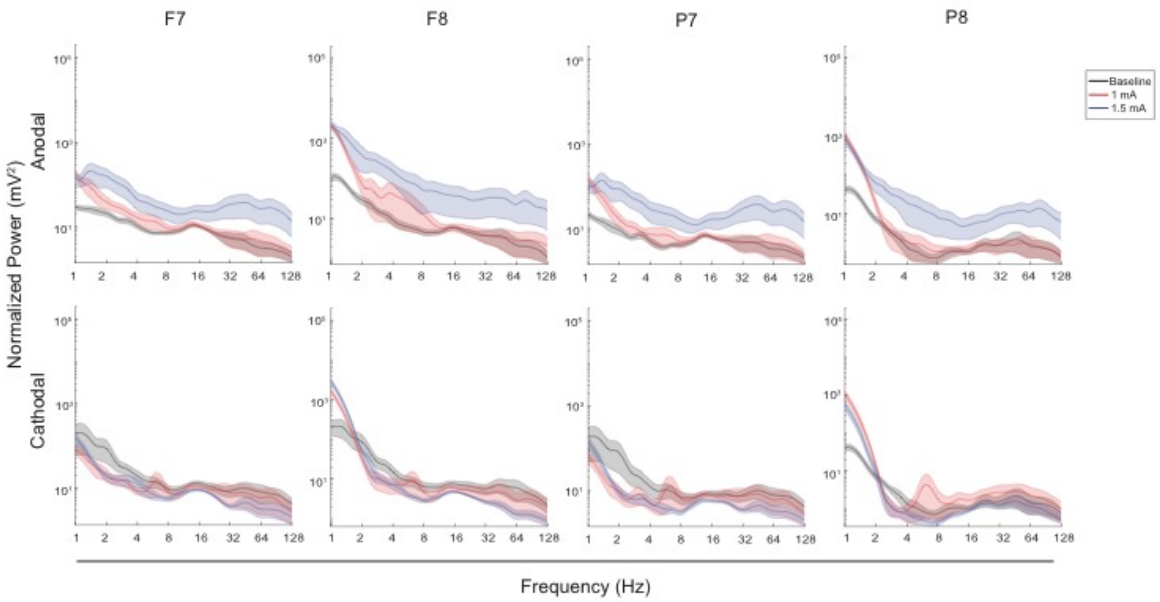

Figure 3.6: Post-stimulation Power Spectra in Animal Z. Frontal and parietal scalp EEG with a unilateral montage in animal Z during anodal and cathodal stimulation. Current was passed between F8 and P8, and non-stimulated sites are F7 and P7. Superimposed on each panel are two different stimulation intensities (red: 1 mA, blue: 1.5 mA) and baseline (black). Power has been normalized for correction of power-law decay and is reported as mean power per frequency ± SEM on a log scale.

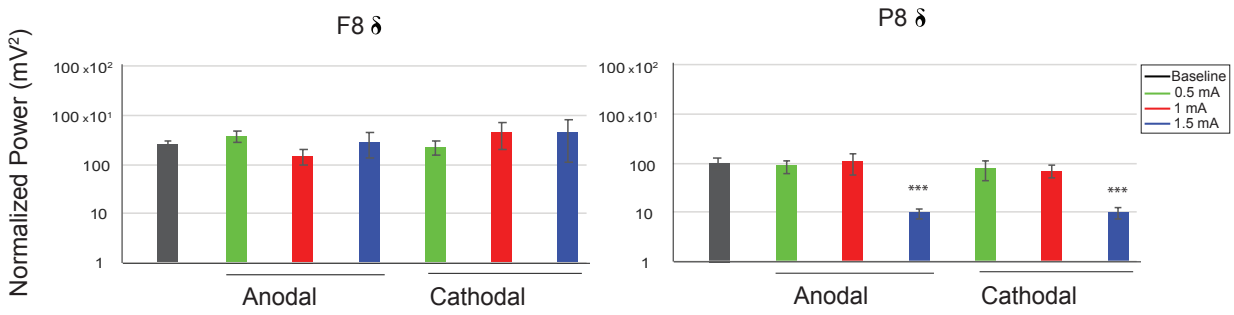

Figure 3.7: Post-stimulation in Non-stimulated Sites in Animal C. Power spectra from parietal scalp EEG in the delta band during anodal and cathodal stimulation. Superimposed on each panel are three different stimulation intensities (green: 0.5 mA, red: 1 mA, blue: 1.5 mA) and baseline (black). Significant decreases in power can be found in P8 during anodal and cathodal 1.5 mA stimulation after 5 seconds. Data is reported as mean delta power per trial ± SEM.

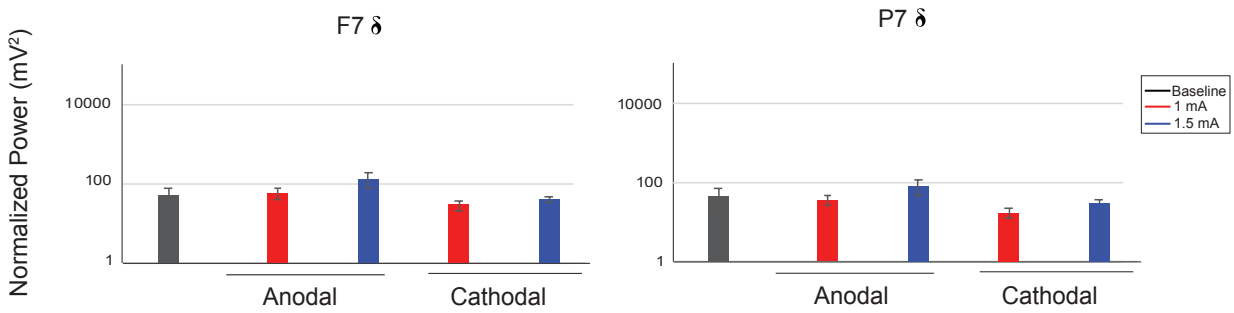

Figure 3.8: Post-stimulation in Non-stimulated Sites in Animal Z. Power spectra from parietal scalp EEG in the delta band during anodal and cathodal stimulation. Superimposed on each panel are two different stimulation intensities (red: 1 mA, blue: 1.5 mA) and baseline (black). No significant decreases in power can be seen in both F7 and P7 5 seconds after stimulation. Data is reported mean delta power per trial ± SEM.

B. Frontal

		Animal C (F8)		Animal Z (F7)	
	Intensity (mA)	Post-stimulation	p-val	Post-stimulation	p-val
Baseline	--	250.41 ± 42.79	--	52.74 ± 24.36	--
Anodal	0.5	383.71 ± 107.06	0.50	N/A	N/A
	1	149.80 ± 55.28	0.40	58.46 ± 16.94	0.85
	1.5	284.12 ± 152.41	0.83	132.24 ± 57.37	0.344
Cathodal	0.5	226.54 ± 74.18	0.83	N/A	N/A
	1	462.97 ± 255.57	0.62	29.27 ± 7.68	0.48
	1.5	465.47 ± 353.51	0.66	40.77 ± 6.58	0.73

B. Parietal

		Animal C (P8)		Animal Z (P7)	
	Intensity (mA)	Post-stimulation	p-val	Post-stimulation	p-val
Baseline	--	103.27± 27.45	--	44.09 ± 25.87	--
Anodal	0.5	85.42 ± 25.67	0.85	N/A	N/A
	1	106.60 ± 48.47	0.95	36.68 ± 9.49	0.79
	1.5	9.76 ± 2.28	0.0044	80.07 ± 33.29	0.53
Cathodal	0.5	77.016 ± 31.64	0.80	N/A	N/A
	1	69.90 ± 19.31	0.66	17.15 ± 4.57	0.49
	1.5	9.71 ± 2.60	0.0045	30.13 ± 6.39	0.69

Table 3.2: Unilateral Post-stimulation Scalp EEG P-values Animal C and Z. Power spectra from frontal scalp electrodes (A) F8 (animal C) and F7 (animal Z) and parietal electrodes (B) P8 (animal C) and P7 (animal Z) after stimulation. Power is reported across polarity and intensity. Post-stimulation data mean ± SEM (paired t-test of unequal variance, FDR corrected) with significant p values in red.

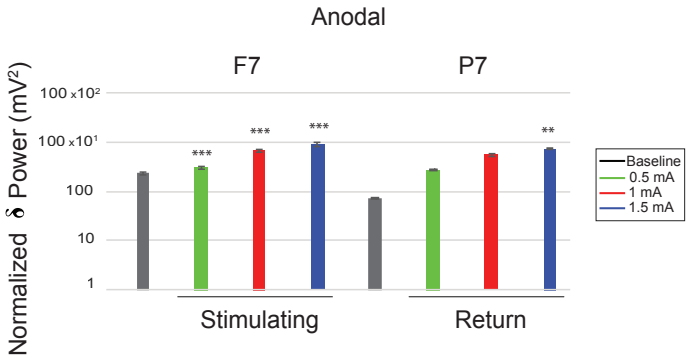

Animal C

% Change δ PWR Post Stim

	F7	P7
0.5mA	32.07	282.77
1mA	191.65	684.71
1.5mA	282.70	925.98

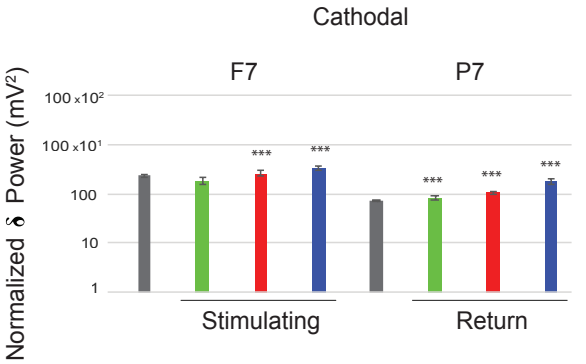

% Change δ PWR Post Stim

	F7	P7
0.5mA	-19.89	16.30
1mA	11.88	49.62
1.5mA	43.34	153.16

Figure 3.9: Post-stimulation Effects of tDCS in Frontal Regions in Animal C. Normalized delta band power during baseline and post-stimulation in frontal scalp electrodes. Power is broken down by polarity and intensity across frontal areas. Percent decrease from baseline (red) and increase (green). Baseline is specific for each area, collapsed across polarity and intensity. Data is reported as mean ± SEM: *= p<0.05; ** = p<0.01; *** = p<0.001 (two sample t-test, unequal variance; FDR corrected).

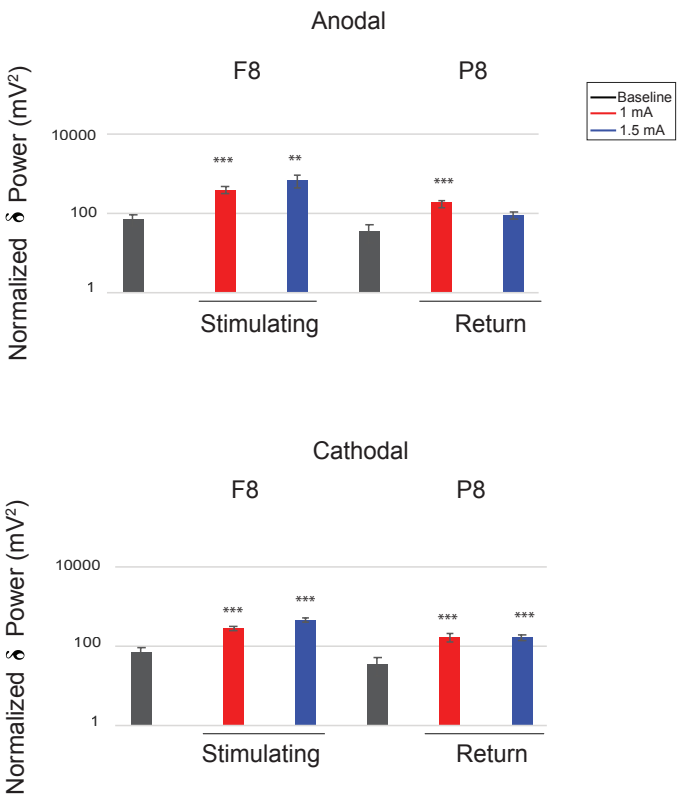

Animal Z

% Change δ PWR Post Stim

	F8	P8
1mA	472.94	405.76
1.5mA	910.36	155.22

% Change δ PWR Post Stim

	F8	P8
1mA	305.32	370.32
1.5mA	589.69	372.01

Figure 3.10: Post-stimulation Effects of tDCS in Frontal Regions in Animal Z. Normalized delta band power during baseline and post-stimulation in frontal scalp electrodes. Power is broken down by polarity and intensity across frontal areas. Percent decrease from baseline (red) and increase (green). Baseline is specific for each area, collapsed across polarity and intensity. Data is reported as mean ± SEM: *= $p<0.05$; ** = $p<0.01$; *** = $p<0.001$ (two sample t-test, unequal variance; FDR corrected).

C. Anodal

		Animal C		Animal Z	
	Intensity (mA)	Post-stimulation	p-vals	Post-stimulation	p-val
Stimulating	0.5	305.96 ± 18.26	0.0021	N/A	N/A
	1	675.63 ± 44.10	7.20E-16	398.50 ± 72.88	0.00021
	1.5	886.54 ± 73.86	1.93E-11	702.75 ± 258.15	0.026
Return	0.5	185.57 ± 27.71	0.16	N/A	N/A
	1	259.19 ± 35.83	0.47	281.92 ± 39.38	0.00010
	1.5	332.05 ± 34.42	0.012	479.71 ± 62.99	0

D. Cathodal

		Animal C		Animal Z	
	Intensity (mA)	Post-stimulation	p-vals	Post-stimulation	p-val
Stimulating	0.5	82.70 ± 6.19	0.096	N/A	N/A
	1	106.39 ± 7.68	5.87E-05	166.74 ± 35.62	0.0028
	1.5	180.01 ± 26.00	0.00014	167.34 ± 32.72	0.0028
Return	0.5	272.16 ± 9.44	8.52E-39	N/A	N/A
	1	557.97 ± 35.34	8.66E-23	179.31 ± 36.11	0.0028
	1.5	729.52 ± 32.17	1.00E-28	90.48 ± 21.56	0.055

Table 3.3: Bilateral Post-stimulation Frontal Scalp EEG P-values Animal C and Z. Power spectra from scalp electrodes during anodal and cathodal stimulation. F7 is the stimulating electrode and P7 is the return, animal C's baseline power is 231.65 ± 12.94 and 71.10 ± 3.14 respectively. Animal Z's stimulating electrode is F8 and return is P8. Baseline power for animal Z is 69.55 ±20.52 for F8 and 35.45±17.72 for P8. Post-stimulation data mean ± SEM (paired t-test of unequal variance, FDR corrected). Significant p-values are shown in red.

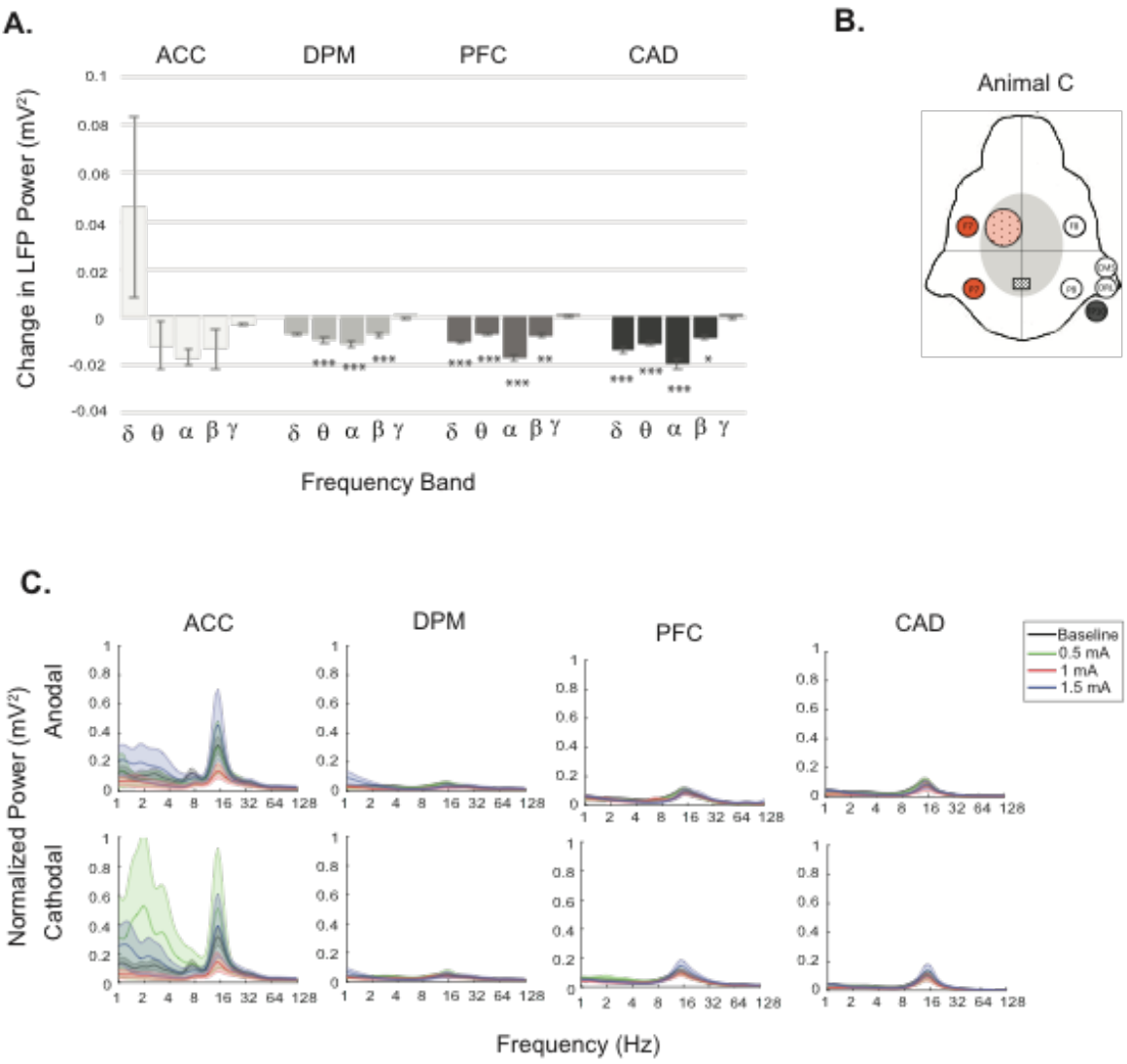

Figure 3.11: The Influence of tDCS on Intracortical Brain Regions in Animal C. LFP data from ACC, DPM, PFC, and CAD recorded simultaneously during tDCS. Change in LFP power spectra collapsed across polarity and intensity in each location (A). Stimulation effects are seen across frequency bands Delta (δ; 1-4 Hz), Theta (θ; 4-8 Hz), Alpha (α; 8-12 Hz), Beta (β; 12-30 Hz), and Gamma (γ; 30-128 Hz). Approximate location of intracortical electrodes (light orange) and stimulating (orange) and reference (grey) scalp electrodes (B). Full power spectrum broken down by polarity (anodal and cathodal) and three different stimulation intensities (green: 0.5 mA, red: 1 mA, blue: 1.5 mA) are shown along with baseline (black). Power has been normalized for correction of power-law decay. Baseline is specific for area. Data is reported as mean ± SEM: *= p<0.05; ** = p<0.01; *** = p<0.001 (paired t test).

E. ACC

	Baseline	Stimulation	p-val
δ	0.11 ± 0.031	0.15 ± 0.068	0.46
θ	0.086 ± 0.018	0.075 ± 0.027	0.67
α	0.11 ± 0.016	0.090 ± 0.019	0.31
β	0.17 ± 0.026	0.15 ± 0.034	0.55
γ	0.033 ± 0.0041	0.030 ± 0.0038	0.051

F. DPM

	Baseline	Stimulation	p-val
δ	0.035 ± 0.0038	0.028 ± 0.0035	0.13
θ	0.028 ± 0.0033	0.018 ± 0.0021	2.67E-05
α	0.039 ± 0.0042	0.028 ± 0.0031	3.16E-05
β	0.042 ± 0.0053	0.035 ± 0.0046	0.00074
γ	0.016 ± 0.0022	0.017 ± 0.0022	0.45

G. PFC

	Baseline	Stimulation	p-val
δ	0.051 ± 0.0026	0.041 ± 0.0030	0.00062
θ	0.040 ± 0.0020	0.032 ± 0.0025	0.00033
α	0.070 ± 0.0046	0.053 ± 0.0035	7.12E-12
β	0.076 ± 0.0063	0.069 ± 0.0056	0.0025
γ	0.015 ± 0.00089	0.016 ± 0.0010	0.057

H. CAD

	Baseline	Stimulation	p-val
δ	0.035 ± 0.0031	0.021 ± 0.0015	1.59E-06
θ	0.025 ± 0.0018	0.015 ± 0.0010	2.22E-08
α	0.055 ± 0.0052	0.036 ± 0.0032	1.26E-06
β	0.059 ± 0.0064	0.051 ± 0.0056	0.022
γ	0.0050 ± 0.00045	0.005 ± 0.00045	0.30

Table 3.4: Unilateral Stimulation Intracortical P-values Animal C. Power spectra from ACC (A), DPM (B), PFC (C), and CAD (D) collapsed across polarity and intensity by frequency band. Data presented as mean ± SEM (two sample t-test), significant p values in red.

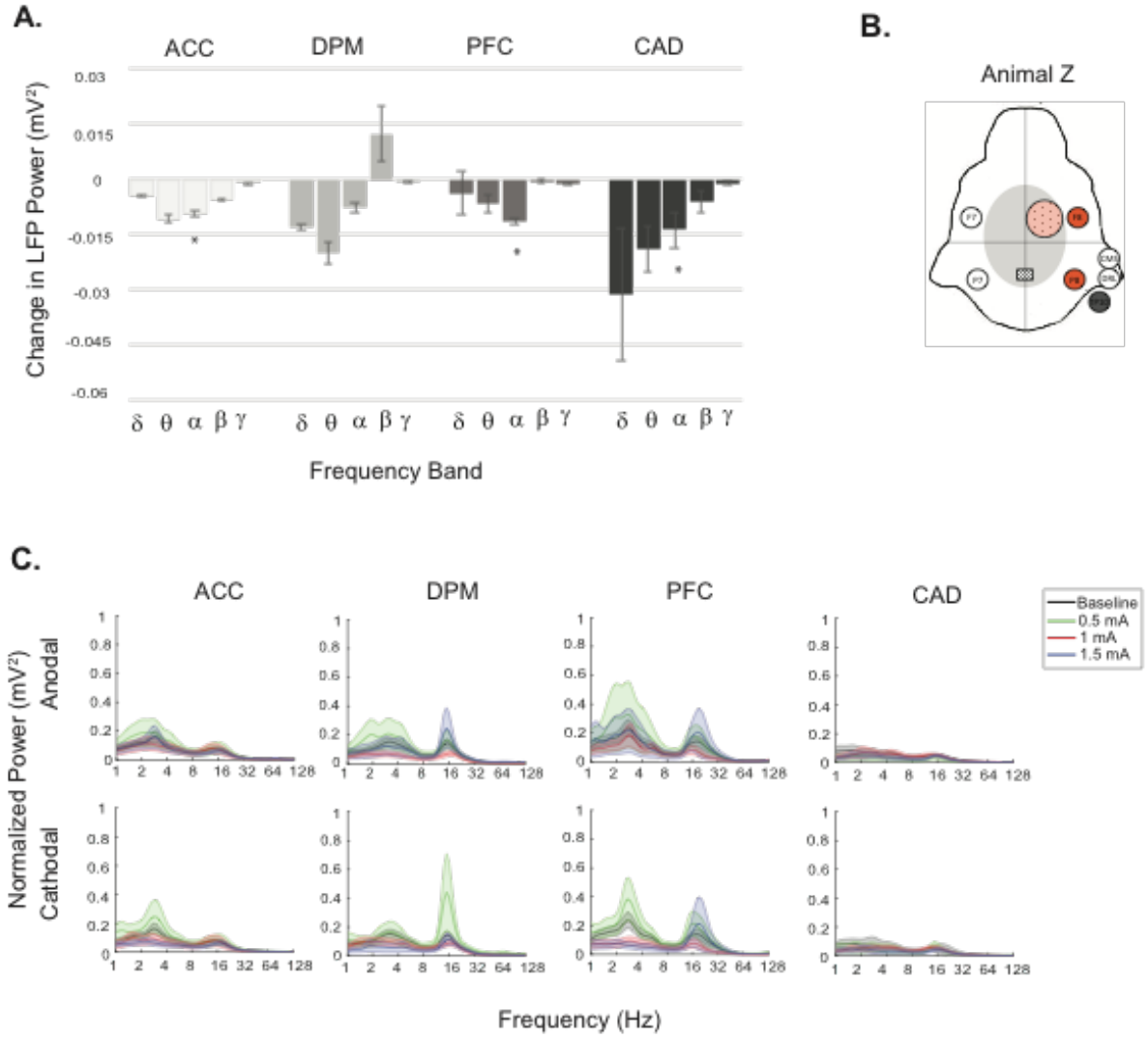

Figure 3.12: The Influence of tDCS on Intracortical Brain Regions in Animal Z. LFP data from ACC, DPM, PFC, and CAD recorded simultaneously during tDCS. Change in LFP power spectra collapsed across polarity and intensity in each location (A). Stimulation effects are seen across frequency bands Delta (δ; 1-4 Hz), Theta (θ; 4-8 Hz), Alpha (α; 8-12 Hz), Beta (β; 12-30 Hz), and Gamma (γ; 30-128 Hz). Approximate location of intracortical electrodes (light orange) and stimulating (orange) and reference (grey) scalp electrodes (B). Full power spectrum broken down by polarity (anodal and cathodal) and three different stimulation intensities (green: 0.5 mA, red: 1 mA, blue: 1.5 mA) are shown along with baseline (black). Power has been normalized for correction of power-law decay. Baseline is specific for area. Data is reported as mean ± SEM: *= $p<0.05$; ** = $p<0.01$; *** = $p<0.001$ (paired t test).

E. ACC

	Baseline	Stimulation	p-val
δ	0.12 ± 0.020	0.11 ± 0.020	0.71
θ	0.078 ± 0.012	0.067 ± 0.011	0.058
α	0.061 ± 0.0094	0.052 ± 0.0083	0.036
β	0.055 ± 0.0085	0.049 ± 0.0083	0.10
γ	0.0063 ± 0.00088	0.0054 ± 0.00078	0.063

F. DPM

	Baseline	Stimulation	p-val
δ	0.11 ± 0.021	0.10 ± 0.021	0.37
θ	0.097 ± 0.017	0.077 ± 0.014	0.13
α	0.067 ± 0.0090	0.059 ± 0.0078	0.16
β	0.083 ± 0.012	0.096 ± 0.019	0.28
γ	0.011 ± 0.0015	0.010 ± 0.0017	0.74

G. PFC

	Baseline	Stimulation	p-val
δ	0.17 ±0.037	0.16 ±0.043	0.88
θ	0.10 ±0.019	0.092 ±0.021	0.60
α	0.067 ±0.0095	0.055 ±0.0087	0.032
β	0.10 ±0.023	0.10 ±0.023	0.96
γ	0.012 ±0.0024	0.011 ±0.0022	0.32

H. CAD

	Baseline	Stimulation	p-val
δ	0.076 ± 0.027	0.045 ± 0.0091	0.20
θ	0.053 ± 0.013	0.034 ± 0.0066	0.061
α	0.041 ± 0.0089	0.027 ± 0.0042	0.039
β	0.037 ± 0.0065	0.031 ± 0.0035	0.27
γ	0.0046 ± 0.00084	0.0036 ± 0.00041	0.093

Table 3.5: Unilateral Stimulation Intracortical P-values Animal Z. Change in power spectra in ACC (A), DPM (B), PFC (C), and CAD (D) across frequency bands, collapsed by polarity and intensity. Data presented as mean ± SEM (two sample t-test) with significant p values in red.

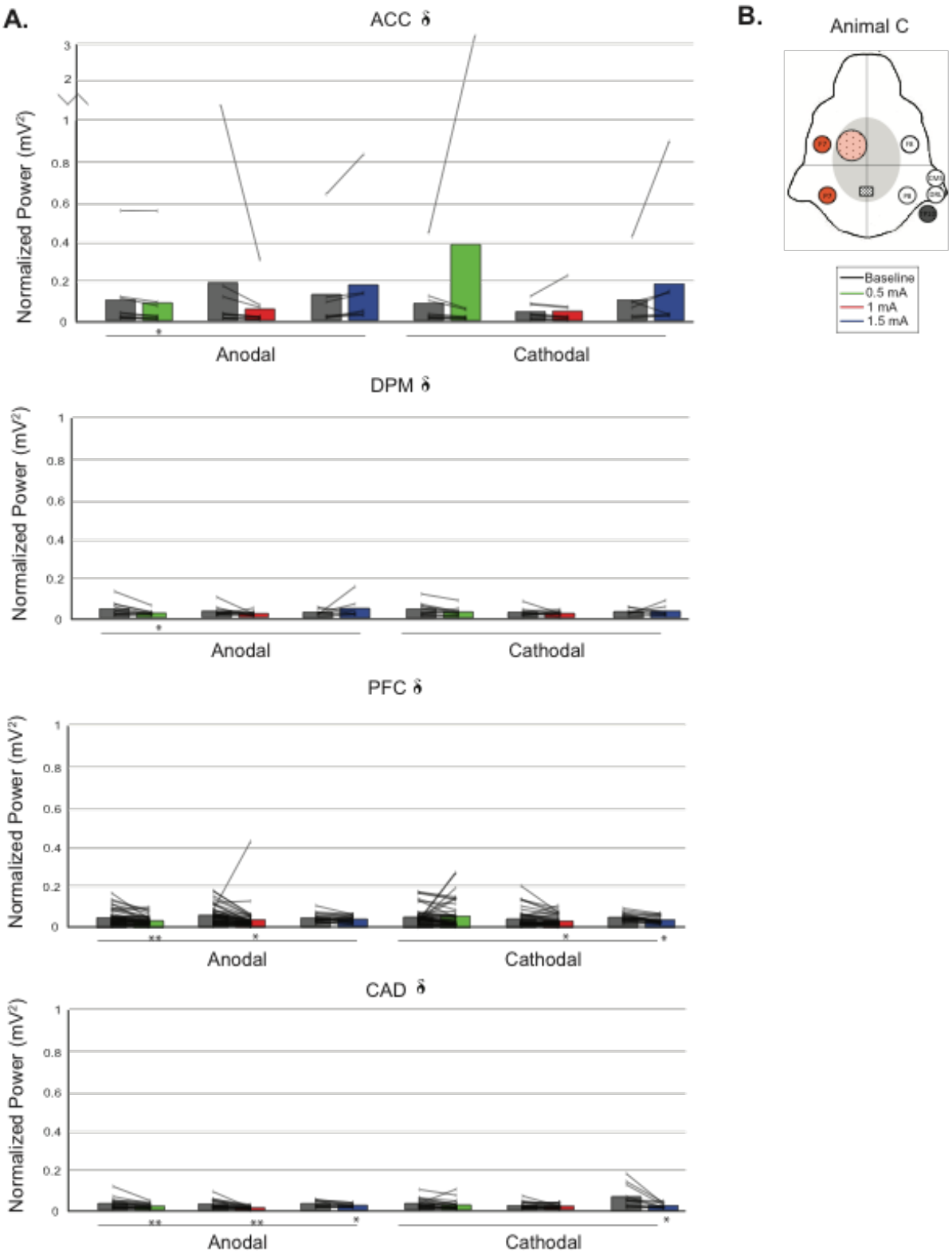
A.
ACC δ
Normalized Power (mV²)
Anodal
Cathodal
DPM δ
PFC δ
CAD δ
B.
Animal C
Baseline
0.5 mA
1 mA
1.5 mA

Figure 3.13: Intracortical Delta Band Power During Stimulation in Animal C. Normalized delta band power broken down by polarity (anodal and cathodal) and intensity (green: 0.5 mA, red: 1 mA, blue: 1.5 mA) compared to baseline (dark grey). Bars represent average mean; lines denote individual electrodes. Data is reported as mean ± SEM: *= $p<0.05$; ** = $p<0.01$; *** = $p<0.001$ (paired t test).

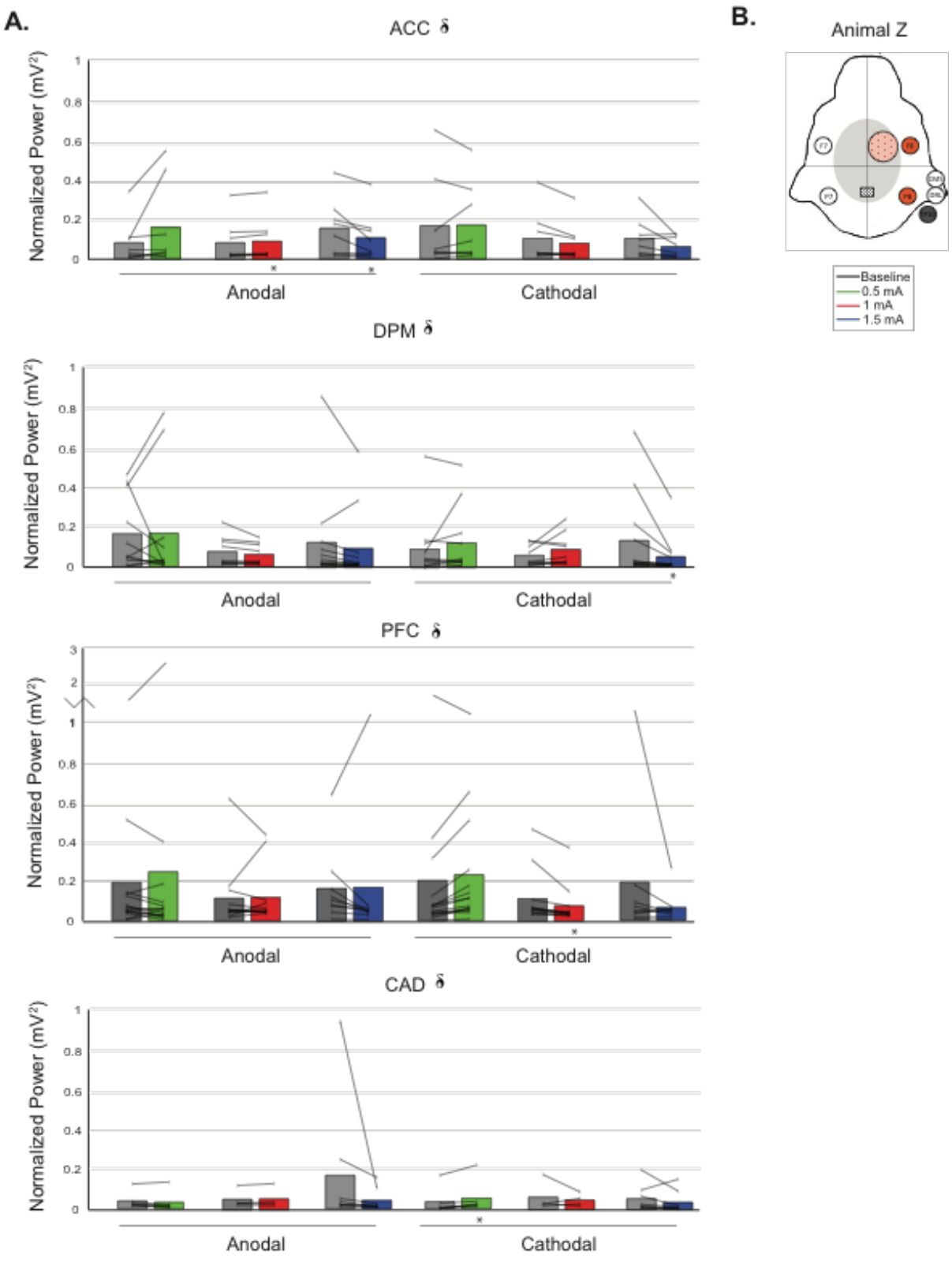
A.
ACC δ
Normalized Power (mV²)
Anodal
Cathodal
DPM δ
PFC δ
CAD δ
B.
Animal Z
Baseline
0.5 mA
1 mA
1.5 mA

Figure 3.14: Intracortical Delta Band Power During Stimulation in Animal Z.
Normalized delta band power broken across polarity (anodal and cathodal) and intensity (green: 0.5 mA, red: 1 mA, blue: 1.5 mA). Power compared to baseline (dark grey). Bars represent average mean; lines denote individual electrodes. Data is reported as mean ± SEM: *= $p<0.05$; ** = $p<0.01$; *** = $p<0.001$ (paired t test).

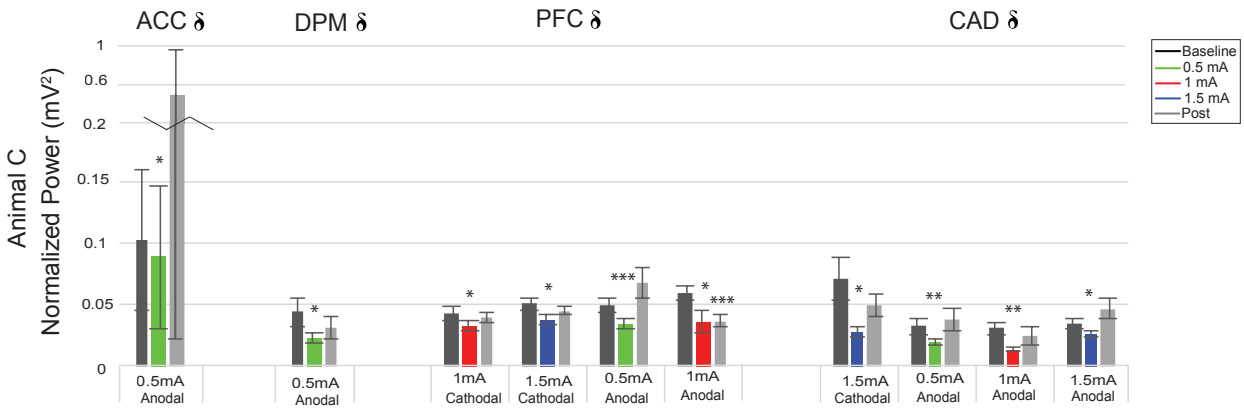

Figure 3.15: Intracortical Post-stimulation Delta Band Power in Animal C. Intracortical areas with significant increases in power during stimulation compared to post. Post-stimulation is 2—7 seconds after stimulation is turned off, to exclude ramp down effects. Changes in delta band power during stimulation are not seen post-stimulation except in anodal 1 mA in the CAD. Data is reported as mean ± SEM: *= $p<0.05$; ** = $p<0.01$; *** = $p<0.001$ (paired t test).

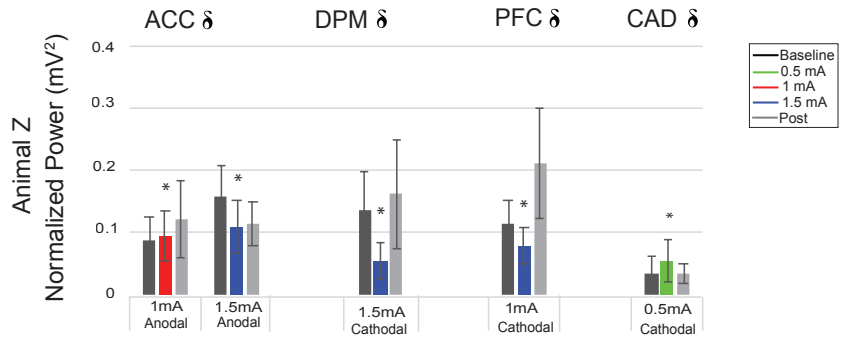

Figure 3.16: Intracortical Post-stimulation Delta Band Power in Animal Z. Intracortical areas with significant increases in power during stimulation compared to post. Post-stimulation is 2—7 seconds after stimulation is turned off, to exclude ramp down effects. Changes in delta band power during stimulation are not seen post-stimulation. Data is reported as mean ± SEM: *= $p<0.05$; ** = $p<0.01$; *** = $p<0.001$ (paired t test).

A. ACC

Polarity	Intensity (mA)	Baseline	Stimulation	p-val	Post-stimulation	P-val
Anodal	0.5	0.10 ± 0.058	0.089 ± 0.058	0.010	0.49 ± 0.47	0.37

B. DPM

Polarity	Intensity (mA)	Baseline	Stimulation	p-val	Post-stimulation	P-val
Anodal	0.5	0.044 ± 0.012	0.023 ± 0.0047	0.019	0.031 ± 0.0096	0.083

C. PFC

Polarity	Intensity (mA)	Baseline	Stimulation	p-val	Post-stimulation	P-val
Cathodal	1	0.042 ± 0.0062	0.033 ± 0.0038	0.022	0.040 ± 0.0047	0.57
	1.5	0.051 ± 0.0045	0.038 ± 0.0040	0.014	0.046 ± 0.0029	0.16
Anodal	0.5	0.050 ± 0.0058	0.035 ± 0.0035	0.00042	0.068 ± 0.013	0.13
	1	0.060 ± 0.0066	0.037 ± 0.0092	0.016	0.037 ± 0.0050	1.56E-05

D. CAD

Polarity	Intensity (mA)	Baseline	Stimulation	p-val	Post-stimulation	P-val
Cathodal	1.5	0.072 ± 0.017	0.028 ± 0.0037	0.019	0.050 ± 0.0091	0.054
Anodal	0.5	0.032 ± 0.0062	0.020 ± 0.0029	0.0052	0.038 ± 0.0090	0.46
	1	0.031 ± 0.0052	0.013 ± 0.0017	0.0010	0.025 ± 0.0069	0.41
	1.5	0.035 ± 0.0047	0.026 ± 0.0026	0.035	0.047 ± 0.0081	0.070

Table 3.6: Unilateral Stimulation and Post-stimulation Intracortical Delta Band P-values in Animal C. Baseline, stimulation and post-stimulation delta band power spectra from intracortical areas ACC (A), DPM (B), PFC (C), and CAD (D). Data presented as mean ± SEM (two sample t-test). Significant effects (red p-vals) during stimulation were not maintained poststimulation.

A. ACC

Polarity	Intensity (mA)	Baseline	Stimulation	p-val	Post-stimulation	p-val
Anodal	1	0.087 ± 0.038	0.095 ± 0.039	0.018	0.12 ± 0.062	0.23
	1.5	0.16 ± 0.051	0.11 ± 0.043	0.035	0.11 ± 0.035	0.21

B. DPM

Polarity	Intensity (mA)	Baseline	Stimulation	p-val	Post-stimulation	p-val
Cathodal	1.5	0.14 ± 0.061	0.054 ± 0.028	0.047	0.16 ± 0.087	0.46

C. PFC

Polarity	Intensity (mA)	Baseline	Stimulation	p-val	Post-stimulation	p-val
Cathodal	1	0.11 ± 0.038	0.079 ± 0.028	0.020	0.21 ± 0.089	0.11

D. CAD

Polarity	Intensity (mA)	Baseline	Stimulation	p-val	Post-stimulation	p-val
Cathodal	0.5	0.035 ± 0.027	0.054 ±n0.033	0.035	0.035 ± 0.016	0.99

Table 3.7: Unilateral Stimulation and Post-stimulation Intracortical Delta Band P-values in Animal Z. Delta band power from intracortical areas ACC (A), DPM (B), PFC (C), and CAD (D) comparing stimulation and post-stimulation to baseline. Data presented as mean ± SEM (two sample t-test). Significant p-values are reported in red. No significant changes were seen in post-stimulation data that were significant during.

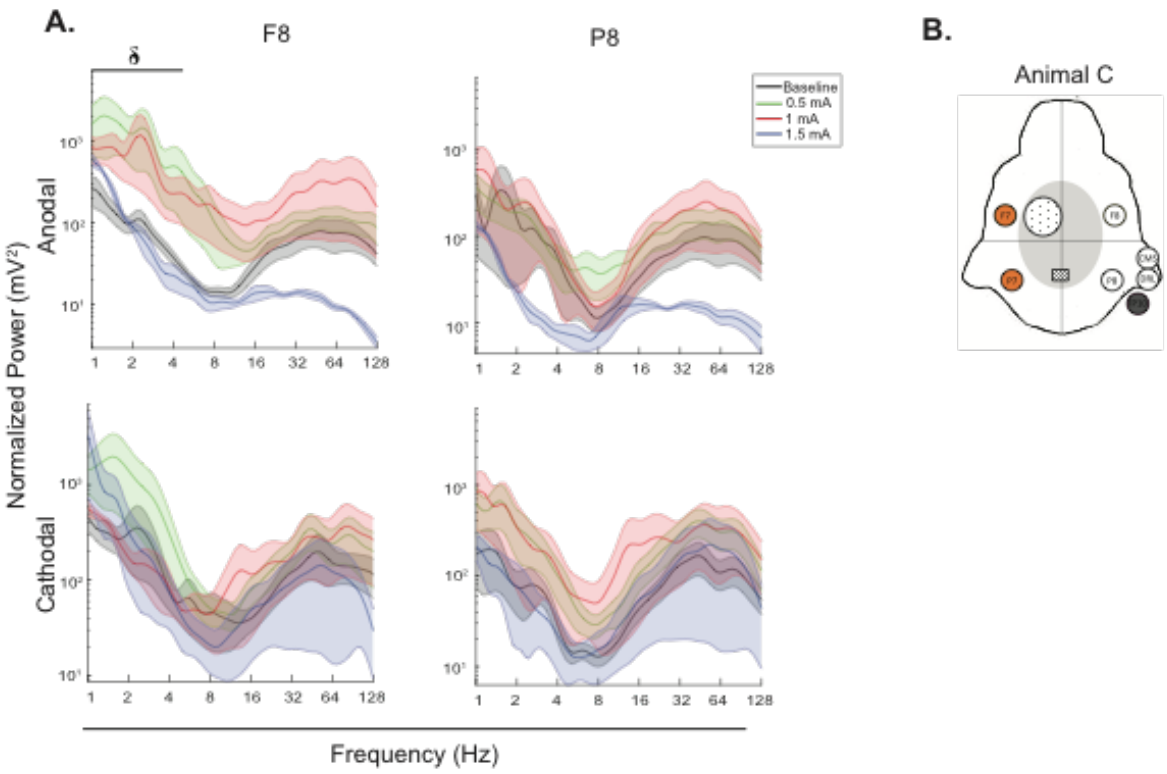

Supplemental Figure 3.1: Power spectra during shortened duration stimulation in animal C. Power spectra of frontal and parietal scalp electrodes during a brief 5 sec anodal (top) and cathodal (bottom) stimulation, also referred to as sham stimulation (A). Three stimulation intensities (green: 0.5mA, red: 1mA, blue: 1.5mA) are superimposed on each panel. Power has been normalized for correction of power-law decay and is plotted on a log scale. Inset of animal C with a unilateral tDCS montage, stimulating scalp electrodes (orange) and reference scalp electrode (grey).

Unilateral Montage

	PFC	ACC	DPM	CAD
Animal C	47	9	7	19
Animal Z	18	12	16	9

Supplemental Table 3.1: Identity and Number of Intracortical Electrodes with Unilateral tDCS Montage. Number of intracortical electrodes per area in animal C and Z that data was collected and analyzed from.

Chapter 4: General Discussion

tDCS Stimulation Parameters and Factors Influencing its Efficacy

Below we break down tDCS stimulation parameters by factors and how they could influence neural activity and ultimately impact its potential as a therapeutic tool. Parameters and topics expanded upon that were investigated in Chapters 2 and 3 include electrode placement, polarity, intensity, and subject variability. Further themes discussed are how tDCS influences and is affected by behavioral state, duration, and repeated stimulation.

Electrode Placement. The PFC is a common target in human studies and shows promise for improving cognitive function and as a therapeutic target for tDCS. It is possible that other electrode locations and montages may better target this region of frontal cortex and show different effects on neural activity. Electrode montages differ between studies and there is no standardized placement, although many are now being explored. Two montages were investigated in Chapters 2 and 3, showing that targeting PFC with two different montages of tDCS differentially influenced spectral power.

Furthermore, electrode placement and its relationship to current is not a trivial and depends on the distance from the current source, which determines the electrical field strength. Factors such as neuronal orientation and morphology of neurons also influence current flow (Das et al., 2016). To address this, we examined the influence of PFC tDCS on cortical areas (PFC, ACC, and DPM), as these are all near/beneath the

stimulating electrode. Our data showed that cortical brain areas showed different spectral profiles in response to tDCS.

It is also thought that tDCS may influence neural activity remotely (through electric fields) or systemically (via neuronal circuitry). Evidence from human electrophysiological and neuroimaging studies suggests that tDCS modulates brain activity in cortical or subcortical areas other than the stimulated site (Antal et al., 2011; Bachmann et al., 2010; Chib et al., 2013; Halko et al., 2011; Lang et al., 2005) potentially through anatomical connections (Selemon & Goldman-Rakic, 1985). Therefore, we further tested the effects of tDCS on the frontostriatal network, to see if stimulation could influence the CAD. Our results show that PFC to CAD had differences in magnitude of power and spectral profiles, where a stronger effect was seen in PFC. However, it is unclear how much of an influence tDCS had on the CAD. Looking at timing of changes with knowledge of circuit properties would help elucidate this. Furthermore, the frontostriatal network contains both excitatory and inhibitory projections (Li et al., 2015) and therefore it might also be possible that tDCS affects extracellular dopamine levels, as previous studies have shown tDCS can affect dopamine release (Tanaka et al., 2013).

Although strong effects of tDCS on power spectra were not seen post-stimulation, this highlights the idea of ‘functional targeting (Bikson & Rahman, 2013). Functional targeting suggests that specific brain networks activated by a task and would be more sensitive to tDCS as they are already active (Jackson et al., 2016). This idea is supported by tDCS producing too low of intensity to influence activity de novo and that only synapses already active would be modulated (Kronberg et al., 2017). Furthermore,

location of the stimulating electrode, as well as the return electrode position is relevant for stimulation effects, determining electrical field orientation and direction of current flow. Collectively, electrode location and montage are crucial factors for the effectiveness tDCS and its influence on other stimulation parameters (Bikson et al., 2010; Moliadze et al., 2010).

Polarity. It is traditionally thought that anodal stimulation causes depolarization and cathodal stimulation causes hyperpolarization of neurons, leading to an alteration of spontaneous neural activity or by bringing neurons closer to their firing thresholds (Bindman et al., 1964; Purpura & McMurtry, 1965). In humans, measurement of motor evoked potentials revealed that anodal tDCS over motor cortex increases cortical excitability and cathodal tDCS decreases it (Nitsche, Nitsche, et al., 2003; Nitsche & Paulus, 2000). Our data does not support this clear influence on the direction of power, where anodal tDCS increases power in scalp EEG or intracortical LFP, and cathodal stimulation decreases it. Importantly, the effects of polarity are not necessarily opposite in direction of excitatory and inhibitory effects (Matsunaga et al., 2004) and depend on other factors including neural morphology (Radman et al., 2009) and current intensity (Batsikadze et al., 2013). Furthermore, the effects of polarity have shown to be more homogenous in motor studies and heterogeneous in cognitive ones (Jacobson, Koslowsky, et al., 2012).

Intensity. tDCS is hallmarked by the delivery of low current ranging from 0 to 2 mA. Our experiments examined three different tDCS stimulation intensities: 0.5 mA, 1 mA, and

1.5 mA. 2 mA stimulation was also originally tested but was stopped as the NHP showed increased arousal during while current was being delivered. The use of anesthetics applied to stimulation sites has been shown to reduce uncomfortable sensations, compared to a placebo (McFadden et al., 2011). However, their use is not advisable as they may mask the sensation of any damage being caused (DaSilva et al., 2011).

With the three intensities tested, we did not find a dose dependent relationship between tDCS intensity and post-stimulation effects on scalp EEG or intracortical data, suggesting intensity does not necessarily translate into a more robust outcome. In some cases, the lowest intensity (0.5 mA stimulation) showed the largest effects, as this may be more physiological. In contrast, since tDCS current can easily be shunted, it is also thought that higher stimulation intensities would result in more current reaching the brain and influencing activity. It is important to note that the amount of current applied to the head is different from the amount of current that reaches the cortex. Electrical currents are known to follow the path of least resistance. The skin and the brain are relatively low resistance; however, the skull is relatively high resistance, meaning a significant amount of the current is shunted through the scalp and does not penetrate the skull.

Influence of tDCS Parameters on Individuality. Many factors influence tES techniques, besides stimulation parameters. This includes participant factors such as age (Leach et al., 2019) and gender (Russell et al., 2017). In fact, between animal C and Z, their spectral profiles and intensity of power varied. Animal C is a younger female macaque

and has a smaller brain, compared to animal Z. Furthermore, no two brains are identical, with variability in brain anatomy and function. Variation between individuals can produce large differences in tES stimulation. Factors affecting tissue composition include idiosyncrasies of gyral/sulcal geometry, white and gray matter architecture (Russell et al., 2013), variations in skull thickness and shunting of current through cerebrospinal fluid, are among many other factors that complicate current flow (Datta et al., 2009; B. Krause & Cohen Kadosh, 2014; Opitz et al., 2015).Other factors that may influence the effects of tDCS include cellular properties such as morphology, orientation, position of soma, and resting membrane potential. This is consistent with modeling studies and a recent study by Bogaard et al. (2019) showing pyramidal cells being more affected by tDCS. It is also important to recognize network level effects, where exciting intermediate inhibitory cells could produce unpredictable and non-specific effects. These effects may help explain why cathodal stimulation can produce excitatory effects (Bogaard et al., 2019).

The issue of individual variability in response to stimulation is important for many tES techniques and applications. Two approaches to help address this include: selecting an appropriate stimulation type (tDCS, tRNS, TMS) or by identifying the optimal stimulation parameters. In addition to anatomical and physiological variables influencing tDCS (Alagapan et al., 2016) intra-individual variability may further stem from brain states (Neuling et al., 2013) and behavior.

Behavioral State. The effects of tDCS have been further shown to depend on behavioral state (Bikson & Rahman, 2013; Petti et al., 2017; Silvanto et al., 2008; Wang et al.,

2018). For example, differences in brain activity during tDCS can be seen during restful wakefulness compared to behavioral tasks (Clemens et al., 2014; Dalong et al., 2021). A study by Li et al. (2019) showed in the absence of a task, the main effect of tDCS accentuate default mode network activation and deactivation in the salience network (SN). In contrast, during task performance, tDCS increased SN activation. In our experiments, the animals were not performing a behavioral task and were allowed to passively view a monitor. Animals were allowed to close their eyes and 'rest' while tDCS protocols were conducted. In addition to behavior, tDCS has also shown to be influenced by psychopathology (depressed or non-depressed), sleep deprivation, etc. Our experiments were conducted in healthy animals on normal sleep and wake cycles. Further experiments to exploring behavioral and mental states are needed.

Duration. Human studies have shown that tDCS can produce effects during stimulation and also afterwards (Bindman et al., 1964). Typical human tDCS paradigms span several minutes (10–20 min) (Aparício et al., 2016; Khadka et al., 2020; Stagg & Nitsche, 2011), and can have changes that persist for more than an hour after the delivery of current (Nitsche, Nitsche, et al., 2003; Nitsche & Paulus, 2001). The duration of the stimulation depends on the aim of the experimental approach, and in our experiments, we chose to do shorter duration stimulation trials (20 seconds) to see instantaneous effects on neural activity. Our data did not show prolonged effects of tDCS in a time dependent manner (data not shown) and effects of post-stimulation were only examined for 5 seconds after ramp down. Increasing the duration of stimulation has shown to have longer duration after-effects. However, one study has shown that

increasing duration led to a reversal of plasticity related effects of tDCS. The authors hypothesized that this non-linearity of prolonged stimulation duration might activates counter-regulatory mechanisms to prevent excessive brain excitation (Hassanzahraee et al., 2020). Overall, we do not see a strong time dependence of stimulation regardless of parameters.

Repeat Stimulation. Repeated sessions of tDCS are increasingly used for therapeutic applications The majority of clinical trials do apply multiple sessions of tDCS (around 5–30 sessions)(Herrera-Melendez et al., 2020). However, it is unclear how timing of repeated stimulation (i.e., the number of sessions and spacing) are related to desired outcomes. It is possible that the effects of tDCS can be additive over consecutive stimulation sessions, and that the duration of effects increases after a series of consecutive stimulation sessions (Nitsche, Liebetanz, Antal, et al., 2003; Nitsche & Paulus, 2001; Rostami et al., 2013). Effects of timing in regard to when tDCS should be applied - before or during behavioral paradigms – also need to be further explored. Yet, many studies have shown that repeated tDCS may influence behavioral outcomes, including improving spatial working memory (Wu et al., 2017). Studies have also examined the safety and efficacy of adverse events associated with repeated sessions, showing little evidence to suggest that repeated sessions of active tDCS pose increased risk to participants. For a systematic review of multiple tDCS sessions see Nikolin et al. (2018).

Animal Models of tDCS

In vivo studies with animals may only be indirectly applicable to humans. Animal models have different anatomy including skull thickness and musculature that can influence tDCS stimulation parameters, shunting the signal or changing its properties. Work with human cadavers and monkey skulls shows that approximately 45% of the current that tDCS electrodes deliver to the scalp makes it through the skull to the brain (Burger & Milaan, 1943; Rush & Driscoll, 1968). More recent studies examining the scalp in rodents and brains of human cadavers, have even estimated that ~75% of scalp-applied currents are attenuated by soft tissue and skull (Vöröslakos et al., 2018), and it is thought that >1 mV of current reaches the brain. Therefore, shunting of current may have account for null or inconsistent results of tDCS on scalp EEG and intracortical data.

Furthermore, changes in current flow in the present studies may be due to factors relating to the simultaneous intracortical recordings. Various head hardware and alterations needed for the experiments, including the cranial implant, the recording chamber, and the craniotomy may account for differences in tDCS results. Still, we expect these differences to be consistent as they do not change across tDCS session. To account for tungsten recording electrodes, we examined the influence of tDCS with and without them being present. Data shows that they do impact the spectra profiles and intensity of spectral power during stimulation **(Supplemental Figure 2.1,2.2)** and post stimulation (**Supplemental Figure 2.3,2.4).**

Differences in mastoid reference TP9 and TP10 may be due to specific NHP musculature. NHPs have large muscles on their heads in order to freely and independently move their ears (Burrows et al., 2016). This may account for the

differences in mastoid referencing and demonstrates how linking mastoids may not be optimal in all species. Investigation into other physical references (examples: FCz, Oz, linked ears, nose, and neck ring) and computational references should be investigated. Another factor that may account for the differences in results between the two animals is animal C had its recording chamber over the left hemisphere, while animal Z ha the recording chamber over the right hemisphere.

tDCS Mechanism of Action

What happens in the brain tissue after you have begun to deliver current is a matter of active research, biophysical modeling, and debate. The effects of tDCS has been shown to produce both immediate effects on neuronal excitability and long-term effects. Immediate effects, appearing at the very moment of electric field application, are related to changes in membrane polarization Kronberg, Michael A. Nitsche, 2019; Purpura & McMurtry, 1965). This can further influence neurochemical effects like dopamine release (Li et al., 2015; Tanaka et al., 2013), BDNF (Hadoush et al., 2018), and reduced oxidative stress (Lu et al., 2015). Intracellular and extracellular recordings in rats, showed that at least a 1 mV/mm voltage gradient is necessary to affect neuronal spiking and subthreshold currents (Vöröslakos et al., 2018). tDCS did not disrupt single neuron turning, it did alter population of cells during movement (Bogaard et al., 2019). Although alteration of spontaneous neural activity has been reported (Fritsch et al., 2010; Nitsche, Liebetanz, Lang, et al., 2003). tDCS has shown to entrain neural activity (Vöröslakos et al., 2018)(Ozen et al., 2010) and modulation of oscillations (Nitsche & Bikson, 2017; Reato et al., 2010).

Recently, *in vitro* experiments have shown that neuronal features such as neuronal morphology (Radman et al., 2009), position of the soma (Bikson et al., 2004) and axonal orientation (Kabakov et al., 2012) are crucial to determine the overall immediate neuronal modulation. These studies further have shown purely depolarizing or hyperpolarizing stimulation does not exist (Liu et al., 2018). Neural cell type has also been shown to influence the effects of tDCS. For example, pyramidal cells are thought to be more affected by stimulation, regardless of polarity (Bogaard et al., 2019).

On the other hand, after effects observed following current cessation require several minutes of stimulation to develop involve synaptic modification (Liu et al., 2018; Marquez-Ruiz et al., 2012) and plasticity mechanisms (Huang et al., 2017; Nitsche et al., 2008; Nitsche & Paulus, 2000; Polanía, Nitsche, et al., 2011; Polanía, Paulus, et al., 2011). For example, cathodal DCS enhanced LTP in apical dendrites while anodal DCS enhanced LTP in basal dendrites. Both anodal and cathodal stimulation reduced LTD in apical dendrites (Kronberg et al., 2017). Studies have also shown long-term effects of tDCS involved changes in GABA levels (Bachtiar et al., 2015, 2018; Patel et al., 2019; Stagg et al., 2009), BDNF levels (Ranieri et al., 2012) and various receptors such as NMDA (Fritsch et al., 2010) mGluR5 (Fritsch et al., 2010; Hadoush et al., 2018; Sun et al., 2016), AMPA (Martins et al., 2019; Stafford et al., 2018) and adenosine (Marquez-Ruiz et al., 2012). However, long-term effects of tDCS may depend on a multiplicity of stimulation factors including, but not limited to, length of stimulation, frequency, intensity of current and electrode location (Utz et al., 2010), in addition to cognitive and behavioral states (Bogaard et al., 2019). Further research is needed to solidify these mechanisms in both human and animal models.

Electrical stimulation of the scalp can affect brain activity in multiple indirect ways, including activation of peripheral nerves (Nitsche & Bikson, 2017; Zaghi et al., 2010), retina (Schwiedrzik, 2009), the vestibular apparatus, astrocytes, perivascular elements(Monai et al., 2016; Ruohonen & Karhu, 2012), and placebo effects (Horvath et al., 2015). Alternative or complementary mechanisms include vascular function (Cancel et al., 2018; Iyer & Madhavan, 2018), metabolic changes (Binkofski et al., 2011), growth and mobility (Keuters et al., 2015; Pelletier et al., 2014) or neurogenesis (Braun et al., 2016; Rueger et al., 2012).

tDCS as a Therapeutic Tool

tDCS has gained popularity as several studies suggest that it can be a valuable tool for the treatment of neuropsychiatric and neurodegenerative conditions including depression (Dell'Osso et al., 2012), stroke (Sohn et al., 2013), multiple sclerosis (Ferrucci et al., 2014), Parkinson's disease (Benninger et al., 2010), and schizophrenia (Shenoy et al., 2015). Research has also demonstrated cognitive improvement in some patients and healthy controls undergoing tDCS. Studies have shown that tDCS can enhance an individual's linguistic and mathematical abilities (Flöel et al., 2008), increase attention span (Kang, 2009), problem solving (Metuki et al., 2012), memory (Boggio et al., 2006) and coordination (Antal et al., 2004). In fact, positive effects have been described for prefrontal cortex stimulation specifically, including executive functioning, attention, working memory, memory, and language (Doruk et al., 2014; Lawrence et al., 2018; Manenti et al., 2016, 2020). Despite the promise of cognitive and behavioral improvement, the studies examining the effects of tDCS have been small and heterogeneous. Meta-analyses have failed to prove any conclusive effects.

Future Studies

tDCS is a non-invasive brain stimulation technique that can help elucidate and establish brain-behavior relationships. It allows the reversible modulation of neural activity and can targeting specific brain regions affecting a variety of cognitive, motor, social, and affective domains (for a review see Filmer et al., 2014). Furthermore, it has shown promise in both clinical and healthy populations, by modifying behavior, accelerating learning, and boosting task performance (Coffman et al., 2014; Parasuraman & McKinley, 2014) to name a few. tDCS is inexpensive, easy to use, and safe, making it attractive in many ways.

Future studies on tDCS should aim to creating universally accepted stimulation protocols and work towards receiving FDA approval. This includes optimizing tES by selecting scalp electrode placement based off behavioral or physiological means, and consideration of where current is flowing. Modeling studies of the human brain can help predict where current flows (Bikson et al., 2012) and may help account for current flow and spread changes based off of individual's brain anatomy (Miranda et al., 2006, 2009). COMETS is a recently developed MATLAB Toolbox (Jung et al., 2013) that aims to assist with electrode placement by simulating current flow amongst various electrode placements. Techniques like this may be useful for exploring tDCS current flow; however, head size, shape and anatomy still vary across individuals and allow for individual variability. More studies in this sector are largely needed. Future developments in the use of tES techniques should also combine experimental setups to examine more complex interactions of the brain. This should include pharmacological, behavioral, and cognitive domains.

Appendix

tES Safety and Ethical Considerations

tDCS is a noninvasive form of stimulation that applies weak electrical currents via the scalp in aims to modify brain activity. It has the distinct advantages compared to other forms of stimulation by being inexpensive, easy to administer, noninvasive and relatively painless. Yet, one of the main drawbacks of this technique is that it is a diffuse form of stimulation and therefore may be difficult to achieve spatial precision when aiming to activate specific brain areas or networks. To help fix this, high-definition (HD) montages are now increasingly popular and promise the ability to administer more focal current (Dmochowski et al., 2011). In fact, the Neuroelectrics system, used in Chapter 2 and 3, utilize a HD-tDCS system.

"Ring electrodes" are another way to increase focality of stimulation (see (Villamar et al., 2013), for a guide) and are comprise of five small electrodes, such as a single anode surrounded by four cathodes (DaSilva et al., 2015). Ring montages, such as this, have been shown to enhance spatial focality and also overcomes problems observed when using square sponges, in which the highest concentration of current density is observed along the straight edges (Miranda et al., 2006). MxN stimulator systems also offer other advanced HD-tDCS, that allow easy montage configuration from an array of possible electrodes, allowing each to stimulate as cathodal or anodal independently (Rostami et al., 2013). Mechanistically, the enhanced focality of ring electrodes is due to the suppression of surrounding regions by the other electrodes, constraining any modulation (Datta et al., 2009). A drawback in the use of this can be skin irritation which may result from increased electrodes, however, this can be

alleviated by increasing the distance between the positive and negative electrodes (Datta et al., 2009). Thus, before deciding upon the use of HD-tDCS or traditional montages, the trade-off between focality and participant comfort should be considered.

In addition to HD-tDCS systems, another method to reduce current spread is with novel montages. The montages in Chapter 2 and 3 only utilize one stimulating and return electrode, as traditionaly studies focus on this simplistic setup. Yet, newer studies have utilized multiple electrodes to stimulate areas using an array. One such montage was also developed (Fischer et al., 2017), uses bilateral motor cortex anodal stimulation using an array of electrodes, while cathodal stimulation was applied to non-primary motor cortex regions including frontal and parietal regions. Montages like this are thought to produce a much larger and long- lasting increase in neural excitability. Despite conventional electrical field modeling showing that both montages should produce a similar current dose to motor cortex, the novel montage was physiologically more efficacious. Recurrent connections within the motor cortex network may amplify of the administered dose (see also (Reato et al., 2010) leading to the observed enhancement. It is clear more work looking at electrode placement in addition to accounting for tDCS's diffuse characteristics is important when using tDCS in research and clinical settings.

Safety and Tolerability of tES. tES is considered to be a safe and low-risk treatment. A review of the adverse effects associated with tDCS in over 33,200 sessions and 1000 individuals reported no serious adverse effects while using tDCS (Bikson et al., 2016). Although rarely reported, mild and moderate effects have been identified including skin

irritation, headaches, fatigue, and skin burning (due to poor electrode contact), skin prickling, and headache (see (Antal et al., 2017). However, it is important to note that these effects are seen in both active and sham stimulation (Bikson et al., 2016). Furthermore, adverse effects from stimulation should be monitored and reduced including decreasing stimulation duration (<60 min), intensity (<4 mA) of stimulation, electrode size and placement to avoid increasing the temperature under the electrodes to prevent skin burns and limit irritation (Antal et al., 2017). Preparing the skin prior to electrode placement can also help improve conductivity and reduce sensation, such as trimming body hair and cleaning the skin with alcohol. A comprehensive guide to the safety considerations surrounding tES use has been published by (Rossi et al., 2009) .

Ethical Considerations. Despite growing evidence for the benefits of tES and its combination with behavioral paradigms (B. Krause & Cohen Kadosh, 2014; Santarnecchi et al., 2015), there are still some ethical considerations concerns regarding its use. An area that needs further investigation is the long-term effects and repeated use of tES on changes in cortical function and behavior. Another is its ability to easily be made and at a relatively low cost ($500). This raises the concern that it may be tried on vulnerable patient groups as a potential “improve-all” technique for cognitive enhancement without user knowledge of the ideal stimulation protocols or possible adverse side effects (Cohen Kadosh et al., 2012; Maslen et al., 2014). Additionally, stimulation parameters may not be kept within the safety guidelines, and stimulation sites may be misidentified, causing stimulation to affect different cognitive processes than those intended, leading to a decline in already worsened cognitive abilities (for a

full reviews of DIY-tES, see (Fitz & Reiner, 2014; Hamilton et al., 2011)). It is important to note that tDCS is not an FDA approved therapy and treatments are considered an 'off label' therapy.

NHP in Research

Limitations. NHP have been portrayed as ideal animal models for certain types of biomedical and cognitive research because of their similarity to humans. For this reason, we made a scaled down 10-20 human mapping system of scalp EEG to use in primates (**Supplemental Figure 5.1**).The assumption is that NHP will help us to understand the human brain; however, a few challenges exist. A major difference between human and NHP is brain size, where the human brain is 13-18 times larger than a NHP (Yin et al., 2009). For example, the neocortex is 35% larger in humans than a primate of similar size (Eshchar et al., 2016). Furthermore, the PFC, defined as the granular frontal cortex, forms 28.5% of the neocortex in the human brain but only 11.3% in the macaque brain (Elston, GN, 2007). Additionally, when related to the brain as a whole, the frontal polar cortex, area 10, is proportionately twice as large in the human brain as in that of the chimpanzee (Semendeferi, 2001). However, other model organisms, are even more problematic task in generalizing to the human brain. For example, the neocortex represents 28% of the rat brain, compared to 72% in the macaque monkey. Furthermore, supporting the use of NHP as an ideal model system. However, it is important to further recognize that an increase in brain size is not a result of simple scaling (Rilling JK, 2006). Humans have developed new brain structures and more complex functions, resulting in specialized subregions. These factors are

important when relating the results of our study to humans as we focus on brain (particularly frontal and parietal) areas that differ in size and specialization (Orban et al., 2004). Because of the differences in structure and function of NHP compared to humans, an example of what typical scalp EEG looks like is shown in **Supplemental Figure 5.2**. Limited studies exist showing this in NHP, but it is important when translating animal findings to humans (Gil-da-Costa et al., 2013; Tada et al., 2020; Woodman et al., 2007).

Another important factor is that there are consequential changes in the microstructure between humans and NHP. For example, the maximum spine density of layer III pyramidal neurons in the PFC is 70% greater in the human than in the macaque brain (Elston, GN, 2007). Another difference is cell types. For example in the ACC different cell types have been found in the but not macaque brain (Allman et al., 2002). Thus, differences between the brains of humans and NHP are apparent (Preuss, TM, 2000) and are important when interpreting results across species. Additionally, cognitive and behavioral differences (Subiaul, 2007) may further depend on these distinctions in the brain.

*Use and Importance of Non-human Primate Models***.** Nonhuman primate (NHP) model systems provide a powerful platform for investigating cognitive, behavioral, and social similarities due to their anatomical and physiological similarity to humans (Harding, 2017). NHP are particularly useful for studies aiming to understand neural mechanisms at fine spatial and temporal resolution, where single neurons and populations can be recorded. The spatial resolution of imaging methods, such as fMRI, MEG, TMS and DTI are adequate to address functions of networks and large brain areas but are limited at

the cellular level (Maestripieri, 2003). Rather, these methods reflect a more global measure of the function of a neural region or system. Most studies examining the effects of tDCS largely stem from fMRI and scalp EEG and are therefore limited in their ability to investigate neural mechanisms. With limited access to intracranial recording in humans, NHP models are a useful alternative to investigating the effects of stimulation *in vivo*. Pairing multiple methods, like simultaneous EEG and intracranial recordings, give us further power to provide new mechanistic insight and perspective onto the human literature. Additionally, understanding the relationship between neural activity across different measures may allow us to use less invasive procedures in the future to study neural activity and processing.

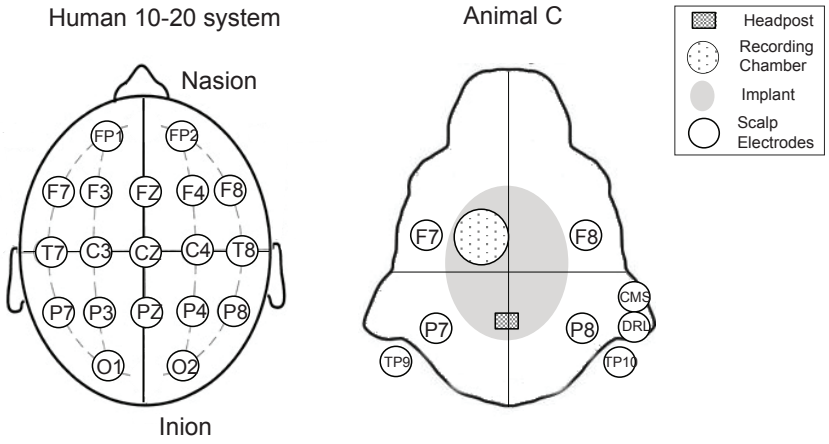

Appendix Figure 5.1: Comparison of Human and NHP tDCS Setup. NHP EEG and delivery of tDCS was based off a scaled down 10-20 human mapping system. Measurements were made from brow ridge to back of the head in the NHP, similar to nasion to inion. Approximate location frontal (F7 and F8) and parietal (P7 and P8) scalp electrodes. Electrodes were placed outside of the animals' implant housing a recording chamber, allowing simultaneous recordings. CMS/DRL electrodes are on the right earlobe and ground is TP10. This schematic is in animal C, however similar in animal Z, except the recording chamber is on the opposite hemisphere.

Assigned Intensity (mA)		Delivered Intensity (mA)	
Stimulating	Return	Stimulating	Return
0.5	0.5	0.454	0.449
1	1	0.909	0.899
1.5	1.5	1.363	1.349

Appendix Table 5.1: Intensities Delivered During tDCS. This table shows the amount of current assigned during stimulation sessions compared to what was actually delivered by the Neuroelectrics device. The values are the same for both anodal and cathodal and are V+/- as appropriate. Stimulating and return values are flipped for bilateral montage.

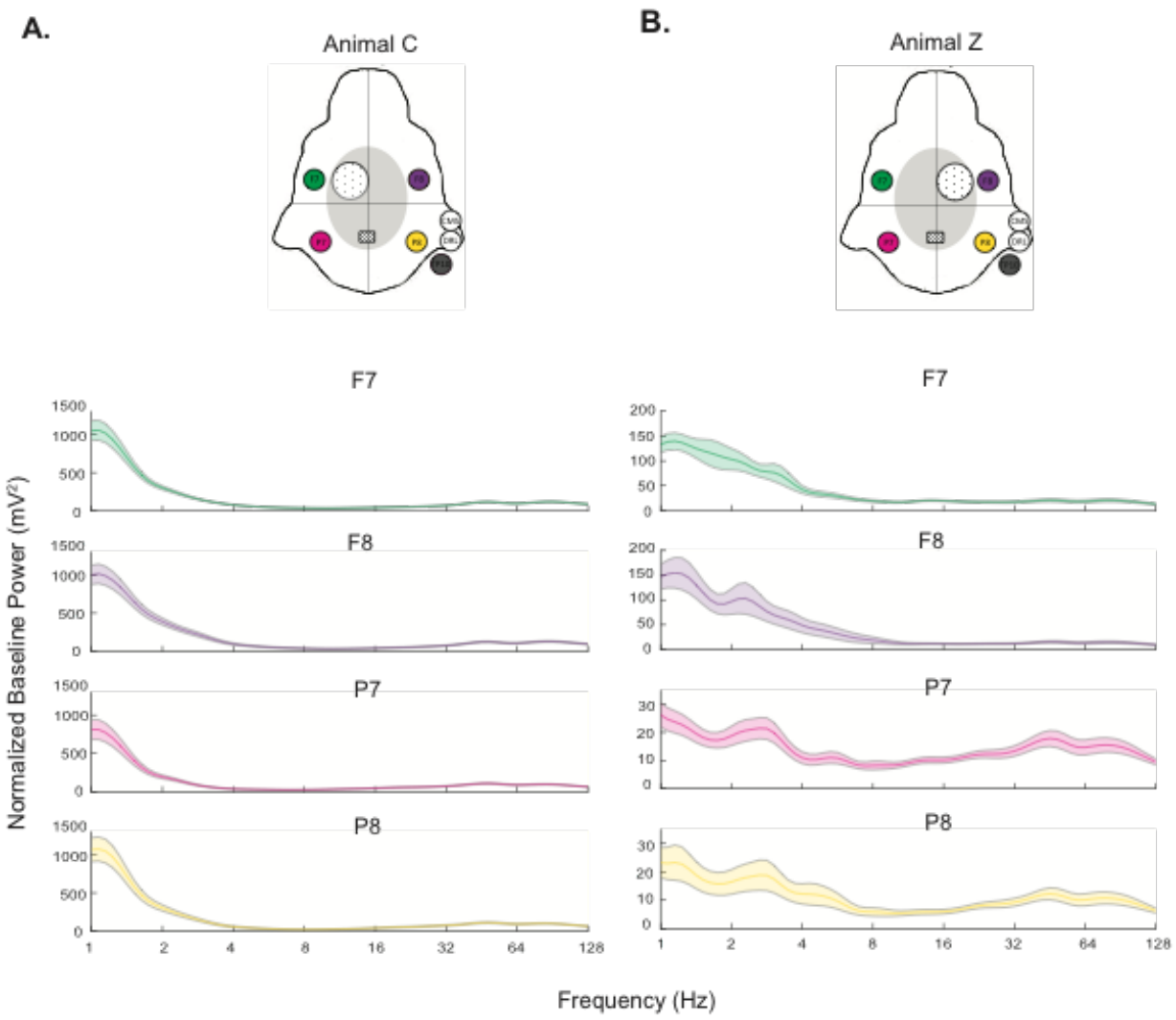

Appendix Figure 5.2: Primate Baseline Scalp EEG. Baseline scalp EEG from frontal (F7, F8) and parietal (P7, P8) electrodes from animal C (A) and Z (B). Animal C has similar baseline amplitude across scalp electrodes and is higher than animal Z. Animal Z has similar amplitude in frontal areas and parietal, but not overall.

References

Agarwal, S. M., Shivakumar, V., Bose, A., Subramaniam, A., Nawani, H., Chhabra, H., Kalmady, S. V., Narayanaswamy, J. C., & Venkatasubramanian, G. (2013). Transcranial Direct Current Stimulation in Schizophrenia. *Clinical Psychopharmacology and Neuroscience*, *11*(3), 118–125. https://doi.org/10.9758/cpn.2013.11.3.118

Alagapan, S., Schmidt, S. L., Lefebvre, J., Hadar, E., Shin, H. W., & Fröhlich, F. (2016). Modulation of Cortical Oscillations by Low-Frequency Direct Cortical Stimulation Is State-Dependent. *PLOS Biology*, *14*(3), e1002424. https://doi.org/10.1371/journal.pbio.1002424

Ali, M. M., Sellers, K. K., & Fröhlich, F. (2013). Transcranial Alternating Current Stimulation Modulates Large-Scale Cortical Network Activity by Network Resonance. *Journal of Neuroscience*, *33*(27), 11262–11275. https://doi.org/10.1523/JNEUROSCI.5867-12.2013

Allman, J., Hakeem, A., & Watson, K. (2002). Two phylogenetic specializations in the human brain. *The Neuroscientist: A Review Journal Bringing Neurobiology, Neurology and Psychiatry*, *8*(4), 335–346. https://doi.org/10.1177/107385840200800409

Ambrus, G. G., Al-Moyed, H., Chaieb, L., Sarp, L., Antal, A., & Paulus, W. (2012). The fade-in—Short stimulation—Fade out approach to sham tDCS--reliable at 1 mA for naïve and experienced subjects, but not investigators. *Brain Stimulation*, *5*(4), 499–504. https://doi.org/10.1016/j.brs.2011.12.001

Ambrus, G. G., Paulus, W., & Antal, A. (2010). Cutaneous perception thresholds of electrical stimulation methods: Comparison of tDCS and tRNS. *Clinical Neurophysiology: Official Journal of the International Federation of Clinical Neurophysiology*, *121*(11), 1908–1914. https://doi.org/10.1016/j.clinph.2010.04.020

Antal, A., Alekseichuk, I., Bikson, M., Brockmöller, J., Brunoni, A. R., Chen, R., Cohen, L. G., Dowthwaite, G., Ellrich, J., Flöel, A., Fregni, F., George, M. S., Hamilton, R., Haueisen, J., Herrmann, C. S., Hummel, F. C., Lefaucheur, J. P., Liebetanz, D., Loo, C. K., … Paulus, W. (2017). Low intensity transcranial electric stimulation: Safety, ethical, legal regulatory and application guidelines. *Clinical Neurophysiology: Official Journal of the International Federation of Clinical Neurophysiology*, *128*(9), 1774–1809. https://doi.org/10.1016/j.clinph.2017.06.001

Antal, A., & Herrmann, C. S. (2016). Transcranial Alternating Current and Random Noise Stimulation: Possible Mechanisms. *Neural Plasticity*, *2016*, e3616807. https://doi.org/10.1155/2016/3616807

Antal, A., Nitsche, M. A., Kruse, W., Kincses, T. Z., Hoffmann, K.-P., & Paulus, W. (2004). Direct current stimulation over V5 enhances visuomotor coordination by improving motion perception in humans. *Journal of Cognitive Neuroscience*, *16*(4), 521–527. http://www.mitpressjournals.org/doi/abs/10.1162/089892904323057263

Antal, A., Polania, R., Schmidt-Samoa, C., Dechent, P., & Paulus, W. (2011). Transcranial direct current stimulation over the primary motor cortex during fMRI. *NeuroImage*, *55*(2), 590–596. https://doi.org/10.1016/j.neuroimage.2010.11.085

Antzoulatos, E. G., & Miller, E. K. (2014). INCREASES IN FUNCTIONAL CONNECTIVITY BETWEEN PREFRONTAL CORTEX AND STRIATUM DURING CATEGORY LEARNING. *Neuron*, *83*(1), 216–225. https://doi.org/10.1016/j.neuron.2014.05.005

Aparício, L. V. M., Guarienti, F., Razza, L. B., Carvalho, A. F., Fregni, F., & Brunoni, A. R. (2016). A Systematic Review on the Acceptability and Tolerability of Transcranial Direct Current Stimulation Treatment in Neuropsychiatry Trials. *Brain Stimulation*, *9*(5), 671–681. https://doi.org/10.1016/j.brs.2016.05.004

Bachmann, C. G., Muschinsky, S., Nitsche, M. A., Rolke, R., Magerl, W., Treede, R.-D., Paulus, W., & Happe, S. (2010). Transcranial direct current stimulation of the motor cortex induces distinct changes in thermal and mechanical sensory percepts. *Clinical Neurophysiology: Official Journal of the International Federation of Clinical Neurophysiology*, *121*(12), 2083–2089. https://doi.org/10.1016/j.clinph.2010.05.005

Bachtiar, V., Johnstone, A., Berrington, A., Lemke, C., Johansen-Berg, H., Emir, U., & Stagg, C. J. (2018). Modulating Regional Motor Cortical Excitability with Noninvasive Brain Stimulation Results in Neurochemical Changes in Bilateral Motor Cortices. *The Journal of Neuroscience: The Official Journal of the Society for Neuroscience*, *38*(33), 7327–7336. https://doi.org/10.1523/JNEUROSCI.2853-17.2018

Bachtiar, V., Near, J., Johansen-Berg, H., & Stagg, C. J. (2015). Modulation of GABA and resting state functional connectivity by transcranial direct current stimulation. *ELife*, *4*, e08789. https://doi.org/10.7554/eLife.08789

Bastani, A., & Jaberzadeh, S. (2013). Differential modulation of corticospinal excitability by different current densities of anodal transcranial direct current stimulation. *PloS One*, *8*(8), e72254. https://doi.org/10.1371/journal.pone.0072254

Batsikadze, G., Moliadze, V., Paulus, W., Kuo, M.-F., & Nitsche, M. A. (2013). Partially non-linear stimulation intensity-dependent effects of direct current stimulation on motor cortex excitability in humans. *The Journal of Physiology*, *591*(7), 1987–2000. https://doi.org/10.1113/jphysiol.2012.249730

Battleday, R. M., Muller, T., Clayton, M. S., & Cohen Kadosh, R. (2014). Mapping the Mechanisms of Transcranial Alternating Current Stimulation: A Pathway from Network Effects to Cognition. *Frontiers in Psychiatry*, *5*, 162. https://doi.org/10.3389/fpsyt.2014.00162

Been, G., Ngo, T. T., Miller, S. M., & Fitzgerald, P. B. (2007). The use of tDCS and CVS as methods of non-invasive brain stimulation. *Brain Research Reviews*, *56*(2), 346–361. https://doi.org/10.1016/j.brainresrev.2007.08.001

Benninger, D. H., Lomarev, M., Lopez, G., Wassermann, E. M., Li, X., Considine, E., & Hallett, M. (2010). Transcranial direct current stimulation for the treatment of Parkinson's disease. *Journal of Neurology, Neurosurgery & Psychiatry*, *81*(10), 1105–1111. https://doi.org/10.1136/jnnp.2009.202556

Bikson, M. (2004). *Tjp0557-0175.pdf*. J Physiol.

Bikson, M., Datta, A., Rahman, A., & Scaturro, J. (2010). Electrode montages for tDCS and weak transcranial electrical stimulation: Role of "return" electrode's position and size. *Clinical Neurophysiology*, *121*(12), 1976–1978. https://doi.org/10.1016/j.clinph.2010.05.020

Bikson, M., Grossman, P., Thomas, C., Zannou, A. L., Jiang, J., Adnan, T., Mourdoukoutas, A. P., Kronberg, G., Truong, D., Boggio, P., Brunoni, A. R., Charvet, L., Fregni, F., Fritsch, B., Gillick, B., Hamilton, R. H., Hampstead, B. M., Jankord, R., Kirton, A., … Woods, A. J. (2016). Safety of Transcranial Direct Current Stimulation: Evidence Based Update 2016. *Brain Stimulation*, *9*(5), 641–661. https://doi.org/10.1016/j.brs.2016.06.004

Bikson, M., Inoue, M., Akiyama, H., Deans, J. K., Fox, J. E., Miyakawa, H., & Jefferys, J. G. R. (2004). Effects of uniform extracellular DC electric fields on excitability in rat hippocampal slices in vitro. *The Journal of Physiology*, *557*(Pt 1), 175–190. https://doi.org/10.1113/jphysiol.2003.055772

Bikson, M., & Rahman, A. (2013). Origins of specificity during tDCS: Anatomical, activity-selective, and input-bias mechanisms. *Frontiers in Human Neuroscience*, *7*. https://doi.org/10.3389/fnhum.2013.00688

Bikson, M., Rahman, A., & Datta, A. (2012). Computational models of transcranial direct current stimulation. *Clinical EEG and Neuroscience*, *43*(3), 176–183. https://doi.org/10.1177/1550059412445138

Bindman, L. J., Lippold, O. C. J., & Redfearn, J. W. T. (1964). The action of brief polarizing currents on the cerebral cortex of the rat (1) during current flow and (2) in the production of long-lasting after-effects. *The Journal of Physiology*, *172*(3), 369–382. https://doi.org/10.1113/jphysiol.1964.sp007425

Binkofski, F., Loebig, M., Jauch-Chara, K., Bergmann, S., Melchert, U. H., Scholand-Engler, H. G., Schweiger, U., Pellerin, L., & Oltmanns, K. M. (2011). Brain energy

consumption induced by electrical stimulation promotes systemic glucose uptake. *Biological Psychiatry*, *70*(7), 690–695. https://doi.org/10.1016/j.biopsych.2011.05.009

Bogaard, A. R., Lajoie, G., Boyd, H., Morse, A., Zanos, S., & Fetz, E. E. (2019). Cortical network mechanisms of anodal and cathodal transcranial direct current stimulation in awake primates. *BioRxiv*, 516260. https://doi.org/10.1101/516260

Boggio, P. S., Ferrucci, R., Rigonatti, S. P., Covre, P., Nitsche, M., Pascual-Leone, A., & Fregni, F. (2006). Effects of transcranial direct current stimulation on working memory in patients with Parkinson's disease. *Journal of the Neurological Sciences*, *249*(1), 31–38. https://doi.org/10.1016/j.jns.2006.05.062

Boggio, P. S., Rigonatti, S. P., Ribeiro, R. B., Myczkowski, M. L., Nitsche, M. A., Pascual-Leone, A., & Fregni, F. (2008). A randomized, double-blind clinical trial on the efficacy of cortical direct current stimulation for the treatment of major depression. *The International Journal of Neuropsychopharmacology*, *11*(2), 249–254. https://doi.org/10.1017/S1461145707007833

Boonstra, T. W., Nikolin, S., Meisener, A.-C., Martin, D. M., & Loo, C. K. (2016). Change in Mean Frequency of Resting-State Electroencephalography after Transcranial Direct Current Stimulation. *Frontiers in Human Neuroscience*, *10*. https://doi.org/10.3389/fnhum.2016.00270

Boudewyn, M., Roberts, B. M., Mizrak, E., Ranganath, C., & Carter, C. S. (2019). Prefrontal Transcranial Direct Current Stimulation (tDCS) Enhances Behavioral and EEG Markers of Proactive Control. *Cognitive Neuroscience*, *10*(2), 57–65. https://doi.org/10.1080/17588928.2018.1551869

Braun, R., Klein, R., Walter, H. L., Ohren, M., Freudenmacher, L., Getachew, K., Ladwig, A., Luelling, J., Neumaier, B., Endepols, H., Graf, R., Hoehn, M., Fink, G. R., Schroeter, M., & Rueger, M. A. (2016). Transcranial direct current stimulation accelerates recovery of function, induces neurogenesis and recruits oligodendrocyte precursors in a rat model of stroke. *Experimental Neurology*, *279*, 127–136. https://doi.org/10.1016/j.expneurol.2016.02.018

Burger, H. C., & Milaan, J. B. van. (1943). Measurements of the specific Resistance of the human Body to direct Current. *Acta Medica Scandinavica*, *114*(6), 584–607. https://doi.org/10.1111/j.0954-6820.1943.tb11253.x

Burrows, A. M., Waller, B. M., & Micheletta, J. (2016). Mimetic Muscles in a Despotic Macaque (Macaca mulatta) Differ from Those in a Closely Related Tolerant Macaque (M. nigra). *The Anatomical Record*, *299*(10), 1317–1324. https://doi.org/10.1002/ar.23393

Buzsáki, G. (2004). Large-scale recording of neuronal ensembles. *Nature Neuroscience*, *7*(5), 446–451. https://doi.org/10.1038/nn1233

Buzsáki, G., & Draguhn, A. (2004). Neuronal oscillations in cortical networks. *Science (New York, N.Y.)*, *304*(5679), 1926–1929. https://doi.org/10.1126/science.1099745

Cai, T., Xia, X., Zhang, H., Guo, Y., & Bai, Y. (2019). High-definition transcranial direct current stimulation modulates neural activities in patients with prolonged disorders of consciousness. *Brain Stimulation*, *12*(6), 1619–1621. https://doi.org/10.1016/j.brs.2019.08.017

Cancel, L. M., Arias, K., Bikson, M., & Tarbell, J. M. (2018). Direct current stimulation of endothelial monolayers induces a transient and reversible increase in transport due to the electroosmotic effect. *Scientific Reports*, *8*(1), 9265. https://doi.org/10.1038/s41598-018-27524-9

Chan, C. Y., Hounsgaard, J., & Nicholson, C. (1988). Effects of electric fields on transmembrane potential and excitability of turtle cerebellar Purkinje cells in vitro. *The Journal of Physiology*, *402*(1), 751–771. https://doi.org/10.1113/jphysiol.1988.sp017232

Chib, V. S., Yun, K., Takahashi, H., & Shimojo, S. (2013). Noninvasive remote activation of the ventral midbrain by transcranial direct current stimulation of prefrontal cortex. *Translational Psychiatry*, *3*, e268. https://doi.org/10.1038/tp.2013.44

Choe, J., Coffman, B. A., Bergstedt, D. T., Ziegler, M. D., & Phillips, M. E. (2016). Transcranial Direct Current Stimulation Modulates Neuronal Activity and Learning in Pilot Training. *Frontiers in Human Neuroscience*, *10*. https://doi.org/10.3389/fnhum.2016.00034

Clemens, B., Jung, S., Mingoia, G., Weyer, D., Domahs, F., & Willmes, K. (2014). Influence of Anodal Transcranial Direct Current Stimulation (tDCS) over the Right Angular Gyrus on Brain Activity during Rest. *PLOS ONE*, *9*(4), e95984. https://doi.org/10.1371/journal.pone.0095984

Coffman, B. A., Clark, V. P., & Parasuraman, R. (2014). Battery powered thought: Enhancement of attention, learning, and memory in healthy adults using transcranial direct current stimulation. *NeuroImage*, *85 Pt 3*, 895–908. https://doi.org/10.1016/j.neuroimage.2013.07.083

Coffman, B. A., Trumbo, M. C., Flores, R. A., Garcia, C. M., van der Merwe, A. J., Wassermann, E. M., Weisend, M. P., & Clark, V. P. (2012). Impact of tDCS on performance and learning of target detection: Interaction with stimulus characteristics and experimental design. *Neuropsychologia*, *50*(7), 1594–1602. https://doi.org/10.1016/j.neuropsychologia.2012.03.012

Cohen Kadosh, R., Levy, N., O'Shea, J., Shea, N., & Savulescu, J. (2012). The neuroethics of non-invasive brain stimulation. *Current Biology: CB*, *22*(4), R108-111. https://doi.org/10.1016/j.cub.2012.01.013

Dalong, G., Jiyuan, L., Yubin, Z., Yufei, Q., Jinghua, Y., Cong, W., & Hongbo, J. (2021). Cathodal Transcranial Direct Current Stimulation Over the Right Temporoparietal Junction Suppresses Its Functional Connectivity and Reduces Contralateral Spatial and Temporal Perception. *Frontiers in Neuroscience*, *15*. https://doi.org/10.3389/fnins.2021.629331

Das, S., Holland, P., Frens, M. A., & Donchin, O. (2016). Impact of Transcranial Direct Current Stimulation (tDCS) on Neuronal Functions. *Frontiers in Neuroscience*, *10*. https://doi.org/10.3389/fnins.2016.00550

DaSilva, A. F., Truong, D. Q., DosSantos, M. F., Toback, R. L., Datta, A., & Bikson, M. (2015). State-of-art neuroanatomical target analysis of high-definition and conventional tDCS montages used for migraine and pain control. *Frontiers in Neuroanatomy*, *9*, 89. https://doi.org/10.3389/fnana.2015.00089

DaSilva, A. F., Volz, M. S., Bikson, M., & Fregni, F. (2011). Electrode Positioning and Montage in Transcranial Direct Current Stimulation. *Journal of Visualized Experiments*, *51*. https://doi.org/10.3791/2744

Datta, A., Baker, J. M., Bikson, M., & Fridriksson, J. (2011). Individualized model predicts brain current flow during transcranial direct-current stimulation treatment in responsive stroke patient. *Brain Stimulation*, *4*(3), 169–174. https://doi.org/10.1016/j.brs.2010.11.001

Datta, A., Bansal, V., Diaz, J., Patel, J., Reato, D., & Bikson, M. (2009). Gyri-precise head model of transcranial direct current stimulation: Improved spatial focality using a ring electrode versus conventional rectangular pad. *Brain Stimulation*, *2*(4), 201–207, 207.e1. https://doi.org/10.1016/j.brs.2009.03.005

Datta, A., Krause, M. R., Pilly, P. K., Choe, J., Zanos, T. P., Thomas, C., & Pack, C. C. (2016). On comparing in vivo intracranial recordings in non-human primates to predictions of optimized transcranial electrical stimulation. *2016 38th Annual International Conference of the IEEE Engineering in Medicine and Biology Society (EMBC)*, 1774–1777. https://doi.org/10.1109/EMBC.2016.7591061

Dell'Osso, B., Zanoni, S., Ferrucci, R., Vergari, M., Castellano, F., D'Urso, N., Dobrea, C., Benatti, B., Arici, C., Priori, A., & Altamura, A. C. (2012). Transcranial direct current stimulation for the outpatient treatment of poor-responder depressed patients. *European Psychiatry*, *27*(7), 513–517. https://doi.org/10.1016/j.eurpsy.2011.02.008

Dmochowski, J. P., Datta, A., Bikson, M., Su, Y., & Parra, L. C. (2011). Optimized multi-electrode stimulation increases focality and intensity at target. *Journal of Neural Engineering*, *8*(4), 046011. https://doi.org/10.1088/1741-2560/8/4/046011

Dockery, C. A., Hueckel-Weng, R., Birbaumer, N., & Plewnia, C. (2009). Enhancement of planning ability by transcranial direct current stimulation. *The Journal of*

Neuroscience: The Official Journal of the Society for Neuroscience, *29*(22), 7271–7277. https://doi.org/10.1523/JNEUROSCI.0065-09.2009

Doruk, D., Gray, Z., Bravo, G. L., Pascual-Leone, A., & Fregni, F. (2014). Effects of tDCS on executive function in Parkinson's disease. *Neuroscience Letters*, *582*, 27–31. https://doi.org/10.1016/j.neulet.2014.08.043

Dundas, J. E., Thickbroom, G. W., & Mastaglia, F. L. (2007). Perception of comfort during transcranial DC stimulation: Effect of NaCl solution concentration applied to sponge electrodes. *Clinical Neurophysiology: Official Journal of the International Federation of Clinical Neurophysiology*, *118*(5), 1166–1170. https://doi.org/10.1016/j.clinph.2007.01.010

Elston, GN. (2007). Specialization of the neocortical pyramidal cell during primate evolution. *Elsevier*, 191–242. https://espace.library.uq.edu.au/view/UQ:317863

Eshchar, Y., Izar, P., Visalberghi, E., Resende, B., & Fragaszy, D. (2016). When and where to practice: Social influences on the development of nut-cracking in bearded capuchins (Sapajus libidinosus). *Animal Cognition*, *19*(3), 605–618. https://doi.org/10.1007/s10071-016-0965-6

Ezzyat, Y., Wanda, P. A., Levy, D. F., Kadel, A., Aka, A., Pedisich, I., Sperling, M. R., Sharan, A. D., Lega, B. C., Burks, A., Gross, R. E., Inman, C. S., Jobst, B. C., Gorenstein, M. A., Davis, K. A., Worrell, G. A., Kucewicz, M. T., Stein, J. M., Gorniak, R., … Kahana, M. J. (2018). Closed-loop stimulation of temporal cortex rescues functional networks and improves memory. *Nature Communications*, *9*(1), 365. https://doi.org/10.1038/s41467-017-02753-0

Fell, J., & Axmacher, N. (2011). The role of phase synchronization in memory processes. *Nature Reviews Neuroscience*, *12*(2), 105–118. https://doi.org/10.1038/nrn2979

Ferrucci, R., Vergari, M., Cogiamanian, F., Bocci, T., Ciocca, M., Tomasini, E., De Riz, M., Scarpini, E., & Priori, A. (2014). Transcranial direct current stimulation (tDCS) for fatigue in multiple sclerosis. *NeuroRehabilitation*, *34*(1), 121–127. http://content.iospress.com/articles/neurorehabilitation/nre1019

Fertonani, A., Ferrari, C., & Miniussi, C. (2015). What do you feel if I apply transcranial electric stimulation? Safety, sensations and secondary induced effects. *Clinical Neurophysiology: Official Journal of the International Federation of Clinical Neurophysiology*, *126*(11), 2181–2188. https://doi.org/10.1016/j.clinph.2015.03.015

Fertonani, A., Pirulli, C., & Miniussi, C. (2011). Random Noise Stimulation Improves Neuroplasticity in Perceptual Learning. *Journal of Neuroscience*, *31*(43), 15416–15423. https://doi.org/10.1523/JNEUROSCI.2002-11.2011

Filmer, H. L., Dux, P. E., & Mattingley, J. B. (2014). Applications of transcranial direct current stimulation for understanding brain function. *Trends in Neurosciences*, *37*(12), 742–753. https://doi.org/10.1016/j.tins.2014.08.003

Fischer, D. B., Fried, P. J., Ruffini, G., Ripolles, O., Salvador, R., Banus, J., Ketchabaw, W. T., Santarnecchi, E., Pascual-Leone, A., & Fox, M. D. (2017). Multifocal tDCS targeting the resting state motor network increases cortical excitability beyond traditional tDCS targeting unilateral motor cortex. *NeuroImage*, *157*, 34–44. https://doi.org/10.1016/j.neuroimage.2017.05.060

Fitz, N. S., & Reiner, P. B. (2014). The Perils of Using Electrical Stimulation to Change Human Brains. In *The Stimulated Brain* (pp. 61–83). Elsevier. https://doi.org/10.1016/B978-0-12-404704-4.00003-X

Flöel, A. (2014). TDCS-enhanced motor and cognitive function in neurological diseases. *NeuroImage*, *85 Pt 3*, 934–947. https://doi.org/10.1016/j.neuroimage.2013.05.098

Flöel, A., Rösser, N., Michka, O., Knecht, S., & Breitenstein, C. (2008). Noninvasive brain stimulation improves language learning. *Journal of Cognitive Neuroscience*, *20*(8), 1415–1422. http://www.mitpressjournals.org/doi/abs/10.1162/jocn.2008.20098

Fries, P. (2005). A mechanism for cognitive dynamics: Neuronal communication through neuronal coherence. *Trends in Cognitive Sciences*, *9*(10), 474–480. https://doi.org/10.1016/j.tics.2005.08.011

Fritsch, B., Reis, J., Martinowich, K., Schambra, H. M., Ji, Y., Cohen, L. G., & Lu, B. (2010). Direct Current Stimulation Promotes BDNF-Dependent Synaptic Plasticity: Potential Implications for Motor Learning. *Neuron*, *66*(2), 198–204. https://doi.org/10.1016/j.neuron.2010.03.035

Gandiga, P. C., Hummel, F. C., & Cohen, L. G. (2006). Transcranial DC stimulation (tDCS): A tool for double-blind sham-controlled clinical studies in brain stimulation. *Clinical Neurophysiology: Official Journal of the International Federation of Clinical Neurophysiology*, *117*(4), 845–850. https://doi.org/10.1016/j.clinph.2005.12.003

Gil-da-Costa, R., Stoner, G. R., Fung, R., & Albright, T. D. (2013). Nonhuman primate model of schizophrenia using a noninvasive EEG method. *Proceedings of the National Academy of Sciences*, *110*(38), 15425–15430. https://doi.org/10.1073/pnas.1312264110

Hadoush, H., Banihani, S. A., Khalil, H., Al-Qaisi, Y., Al-Sharman, A., & Al-Jarrah, M. (2018). Dopamine, BDNF and motor function postbilateral anodal transcranial direct current stimulation in Parkinson's disease. *Neurodegenerative Disease Management*, *8*(3), 171–179. https://doi.org/10.2217/nmt-2017-0048

Haken, H. (1996). Noise in the brain: A physical network model. *International Journal of Neural Systems*, *7*(4), 551–557. https://doi.org/10.1142/s0129065796000543

Halko, M., Datta, A., Plow, E., Scaturro, J., Bikson, M., & Merabet, L. (2011). Neuroplastic changes following rehabilitative training correlate with regional electrical field induced with tDCS. *NeuroImage*, *57*(3), 885–891. https://doi.org/10.1016/j.neuroimage.2011.05.026

Hamilton, R., Messing, S., & Chatterjee, A. (2011). Rethinking the thinking cap. *Neurology*, *76*(2), 187–193. https://doi.org/10.1212/WNL.0b013e318205d50d

Hanley, C. J., Singh, K. D., & McGonigle, D. J. (2016). Transcranial modulation of brain oscillatory responses: A concurrent tDCS-MEG investigation. *NeuroImage*, *140*, 20–32. https://doi.org/10.1016/j.neuroimage.2015.12.021

Harding, J. D. (2017). Nonhuman Primates and Translational Research: Progress, Opportunities, and Challenges. *ILAR Journal*, *58*(2), 141–150. https://doi.org/10.1093/ilar/ilx033

Harris, D. J., Wilson, M. R., Buckingham, G., & Vine, S. J. (2019). No effect of transcranial direct current stimulation of frontal, motor or visual cortex on performance of a self-paced visuomotor skill. *Psychology of Sport and Exercise*, *43*, 368–373. https://doi.org/10.1016/j.psychsport.2019.04.014

Hassanzahraee, M., Nitsche, M. A., Zoghi, M., & Jaberzadeh, S. (2020). Determination of anodal tDCS intensity threshold for reversal of corticospinal excitability: An investigation for induction of counter-regulatory mechanisms. *Scientific Reports*, *10*(1), 16108. https://doi.org/10.1038/s41598-020-72909-4

Helfrich, R. F., Schneider, T. R., Rach, S., Trautmann-Lengsfeld, S. A., Engel, A. K., & Herrmann, C. S. (2014). Entrainment of brain oscillations by transcranial alternating current stimulation. *Current Biology: CB*, *24*(3), 333–339. https://doi.org/10.1016/j.cub.2013.12.041

Herrera-Melendez, A.-L., Bajbouj, M., & Aust, S. (2020). Application of Transcranial Direct Current Stimulation in Psychiatry. *Neuropsychobiology*, *79*(6), 372–383. https://doi.org/10.1159/000501227

Horvath, J. C., Carter, O., & Forte, J. D. (2014). Transcranial direct current stimulation: Five important issues we aren't discussing (but probably should be). *Frontiers in Systems Neuroscience*, *0*. https://doi.org/10.3389/fnsys.2014.00002

Horvath, J. C., Forte, J. D., & Carter, O. (2015). Quantitative Review Finds No Evidence of Cognitive Effects in Healthy Populations From Single-session Transcranial Direct Current Stimulation (tDCS). *Brain Stimulation*, *8*(3), 535–550. https://doi.org/10.1016/j.brs.2015.01.400

Hoy, K. E., Emonson, M. R. L., Arnold, S. L., Thomson, R. H., Daskalakis, Z. J., & Fitzgerald, P. B. (2013). Testing the limits: Investigating the effect of tDCS dose on working memory enhancement in healthy controls. *Neuropsychologia*, *51*(9), 1777–1784. https://doi.org/10.1016/j.neuropsychologia.2013.05.018

Hsu, T.-Y., Juan, C.-H., & Tseng, P. (2016). Individual Differences and State-Dependent Responses in Transcranial Direct Current Stimulation. *Frontiers in Human Neuroscience*, *0*. https://doi.org/10.3389/fnhum.2016.00643

Huang, Y.-Z., Lu, M.-K., Antal, A., Classen, J., Nitsche, M., Ziemann, U., Ridding, M., Hamada, M., Ugawa, Y., Jaberzadeh, S., Suppa, A., Paulus, W., & Rothwell, J. (2017). Plasticity induced by non-invasive transcranial brain stimulation: A position paper. *Clinical Neurophysiology: Official Journal of the International Federation of Clinical Neurophysiology*, *128*(11), 2318–2329. https://doi.org/10.1016/j.clinph.2017.09.007

Imburgio, M. J., & Orr, J. M. (2018). Effects of prefrontal tDCS on executive function: Methodological considerations revealed by meta-analysis. *Neuropsychologia*, *117*, 156–166. https://doi.org/10.1016/j.neuropsychologia.2018.04.022

Iyer, P. C., & Madhavan, S. (2018). Non-invasive brain stimulation in the modulation of cerebral blood flow after stroke: A systematic review of Transcranial Doppler studies. *Clinical Neurophysiology: Official Journal of the International Federation of Clinical Neurophysiology*, *129*(12), 2544–2551. https://doi.org/10.1016/j.clinph.2018.09.019

Jackson, M. P., Rahman, A., Lafon, B., Kronberg, G., Ling, D., Parra, L. C., & Bikson, M. (2016). Animal models of transcranial direct current stimulation: Methods and mechanisms. *Clinical Neurophysiology*, *127*(11), 3425–3454. https://doi.org/10.1016/j.clinph.2016.08.016

Jacobson, L., Ezra, A., Berger, U., & Lavidor, M. (2012). Modulating oscillatory brain activity correlates of behavioral inhibition using transcranial direct current stimulation. *Clinical Neurophysiology*, *123*(5), 979–984. https://doi.org/10.1016/j.clinph.2011.09.016

Jacobson, L., Koslowsky, M., & Lavidor, M. (2012). tDCS polarity effects in motor and cognitive domains: A meta-analytical review. *Experimental Brain Research*, *216*(1), 1–10. https://doi.org/10.1007/s00221-011-2891-9

Jung, Y.-J., Kim, J.-H., & Im, C.-H. (2013). COMETS: A MATLAB toolbox for simulating local electric fields generated by transcranial direct current stimulation (tDCS). *Biomedical Engineering Letters*, *3*(1), 39–46. https://doi.org/10.1007/s13534-013-0087-x

Kabakov, A. Y., Muller, P. A., Pascual-Leone, A., Jensen, F. E., & Rotenberg, A. (2012). Contribution of axonal orientation to pathway-dependent modulation of excitatory

transmission by direct current stimulation in isolated rat hippocampus. *Journal of Neurophysiology*, *107*(7), 1881–1889. https://doi.org/10.1152/jn.00715.2011

Kanai, R., Chaieb, L., Antal, A., Walsh, V., & Paulus, W. (2008). Frequency-dependent electrical stimulation of the visual cortex. *Current Biology: CB*, *18*(23), 1839–1843. https://doi.org/10.1016/j.cub.2008.10.027

Kang, E. K. (2009). *Non-invasivecorticalstimimprovespost-strokeattentiondeclineRNN2009.pdf*. Restorative neurology and neuroscience.

Keeser, D., Meindl, T., Bor, J., Palm, U., Pogarell, O., Mulert, C., Brunelin, J., Möller, H.-J., Reiser, M., & Padberg, F. (2011). Prefrontal Transcranial Direct Current Stimulation Changes Connectivity of Resting-State Networks during fMRI. *The Journal of Neuroscience*, *31*(43), 15284–15293. https://doi.org/10.1523/JNEUROSCI.0542-11.2011

Keuters, M. H., Aswendt, M., Tennstaedt, A., Wiedermann, D., Pikhovych, A., Rotthues, S., Fink, G. R., Schroeter, M., Hoehn, M., & Rueger, M. A. (2015). Transcranial direct current stimulation promotes the mobility of engrafted NSCs in the rat brain. *NMR in Biomedicine*, *28*(2), 231–239. https://doi.org/10.1002/nbm.3244

Khadka, N., Borges, H., Paneri, B., Kaufman, T., Nassis, E., Zannou, A. L., Shin, Y., Choi, H., Kim, S., Lee, K., & Bikson, M. (2020). Adaptive current tDCS up to 4 mA. *Brain Stimulation*, *13*(1), 69–79. https://doi.org/10.1016/j.brs.2019.07.027

Kim, J.-H., Kim, D.-W., Chang, W. H., Kim, Y.-H., Kim, K., & Im, C.-H. (2014). Inconsistent outcomes of transcranial direct current stimulation may originate from anatomical differences among individuals: Electric field simulation using individual MRI data. *Neuroscience Letters*, *564*, 6–10. https://doi.org/10.1016/j.neulet.2014.01.054

Klem, G. H., Lüders, H. O., Jasper, H. H., & Elger, C. (1999). The ten-twenty electrode system of the International Federation. The International Federation of Clinical Neurophysiology. *Electroencephalography and Clinical Neurophysiology. Supplement*, *52*, 3–6.

Krause, B., & Cohen Kadosh, R. (2014). Not all brains are created equal: The relevance of individual differences in responsiveness to transcranial electrical stimulation. *Frontiers in Systems Neuroscience*, *8*. https://doi.org/10.3389/fnsys.2014.00025

Krause, M. R., Vieira, P. G., Csorba, B. A., Pilly, P. K., & Pack, C. C. (2019). Transcranial alternating current stimulation entrains single-neuron activity in the primate brain. *Proceedings of the National Academy of Sciences of the United States of America*, *116*(12), 5747–5755. https://doi.org/10.1073/pnas.1815958116

Krause, M. R., Zanos, T. P., Csorba, B. A., Pilly, P. K., Choe, J., Phillips, M. E., Datta, A., & Pack, C. C. (2017). Transcranial Direct Current Stimulation Facilitates

Associative Learning and Alters Functional Connectivity in the Primate Brain. *Current Biology*, *27*(20), 3086-3096.e3. https://doi.org/10.1016/j.cub.2017.09.020

Kronberg, G., Bridi, M., Abel, T., Bikson, M., & Parra, L. C. (2017). Direct Current Stimulation Modulates LTP and LTD: Activity Dependence and Dendritic Effects. *Brain Stimulation*, *10*(1), 51–58. https://doi.org/10.1016/j.brs.2016.10.001

Kuo, M.-F., Paulus, W., & Nitsche, M. A. (2014). Therapeutic effects of non-invasive brain stimulation with direct currents (tDCS) in neuropsychiatric diseases. *NeuroImage*, *85 Pt 3*, 948–960. https://doi.org/10.1016/j.neuroimage.2013.05.117

Lagopoulos, J., & Degabriele, R. (2008). Feeling the heat: The electrode–skin interface during DCS. *Acta Neuropsychiatrica*, *20*(2), 98–100. https://doi.org/10.1111/j.1601-5215.2008.00274.x

Lang, N., Siebner, H. R., Ward, N. S., Lee, L., Nitsche, M. A., Paulus, W., Rothwell, J. C., Lemon, R. N., & Frackowiak, R. S. (2005). How does transcranial DC stimulation of the primary motor cortex alter regional neuronal activity in the human brain? *The European Journal of Neuroscience*, *22*(2), 495–504. https://doi.org/10.1111/j.1460-9568.2005.04233.x

Lawrence, B. J., Gasson, N., Johnson, A. R., Booth, L., & Loftus, A. M. (2018). Cognitive Training and Transcranial Direct Current Stimulation for Mild Cognitive Impairment in Parkinson's Disease: A Randomized Controlled Trial. *Parkinson’s Disease*, *2018*, e4318475. https://doi.org/10.1155/2018/4318475

Leach, R. C., McCurdy, M. P., Trumbo, M. C., Matzen, L. E., & Leshikar, E. D. (2019). Differential Age Effects of Transcranial Direct Current Stimulation on Associative Memory. *The Journals of Gerontology: Series B*, *74*(7), 1163–1173. https://doi.org/10.1093/geronb/gby003

Li, L. M., Uehara, K., & Hanakawa, T. (2015). The contribution of interindividual factors to variability of response in transcranial direct current stimulation studies. *Frontiers in Cellular Neuroscience*, *9*. https://doi.org/10.3389/fncel.2015.00181

Liu, A., Vöröslakos, M., Kronberg, G., Henin, S., Krause, M. R., Huang, Y., Opitz, A., Mehta, A., Pack, C. C., Krekelberg, B., Berényi, A., Parra, L. C., Melloni, L., Devinsky, O., & Buzsáki, G. (2018). Immediate neurophysiological effects of transcranial electrical stimulation. *Nature Communications*, *9*(1), 5092. https://doi.org/10.1038/s41467-018-07233-7

London, R. E., & Slagter, H. A. (2021). No Effect of Transcranial Direct Current Stimulation over Left Dorsolateral Prefrontal Cortex on Temporal Attention. *Journal of Cognitive Neuroscience*, *33*(4), 756–768. https://doi.org/10.1162/jocn_a_01679

López-Alonso, V., Cheeran, B., Río-Rodríguez, D., & Fernández-Del-Olmo, M. (2014). Inter-individual variability in response to non-invasive brain stimulation paradigms. *Brain Stimulation*, *7*(3), 372–380. https://doi.org/10.1016/j.brs.2014.02.004

Lu, C., Wei, Y., Hu, R., Wang, Y., Li, K., & Li, X. (2015). Transcranial Direct Current Stimulation Ameliorates Behavioral Deficits and Reduces Oxidative Stress in 1-Methyl-4-Phenyl-1,2,3,6-Tetrahydropyridine-Induced Mouse Model of Parkinson's Disease. *Neuromodulation: Journal of the International Neuromodulation Society*, *18*(6), 442–446; discussion 447. https://doi.org/10.1111/ner.12302

Maestripieri, D. (2003). Attachment. In *Primate psychology* (pp. 108–143). Harvard University Press.

Manenti, R., Brambilla, M., Benussi, A., Rosini, S., Cobelli, C., Ferrari, C., Petesi, M., Orizio, I., Padovani, A., Borroni, B., & Cotelli, M. (2016). Mild cognitive impairment in Parkinson's disease is improved by transcranial direct current stimulation combined with physical therapy. *Movement Disorders: Official Journal of the Movement Disorder Society*, *31*(5), 715–724. https://doi.org/10.1002/mds.26561

Manenti, R., Sandrini, M., Gobbi, E., Binetti, G., & Cotelli, M. (2020). Effects of Transcranial Direct Current Stimulation on Episodic Memory in Amnestic Mild Cognitive Impairment: A Pilot Study. *The Journals of Gerontology. Series B, Psychological Sciences and Social Sciences*, *75*(7), 1403–1413. https://doi.org/10.1093/geronb/gby134

Marquez-Ruiz, J., Leal-Campanario, R., Sanchez-Campusano, R., Molaee-Ardekani, B., Wendling, F., Miranda, P. C., Ruffini, G., Gruart, A., & Delgado-Garcia, J. M. (2012). Transcranial direct-current stimulation modulates synaptic mechanisms involved in associative learning in behaving rabbits. *Proceedings of the National Academy of Sciences*, *109*(17), 6710–6715. https://doi.org/10.1073/pnas.1121147109

Marshall, T. R., Esterer, S., Herring, J. D., Bergmann, T. O., & Jensen, O. (2016). On the relationship between cortical excitability and visual oscillatory responses—A concurrent tDCS–MEG study. *NeuroImage*, *140*, 41–49. https://doi.org/10.1016/j.neuroimage.2015.09.069

Martins, C. W., de Melo Rodrigues, L. C., Nitsche, M. A., & Nakamura-Palacios, E. M. (2019). AMPA receptors are involved in prefrontal direct current stimulation effects on long-term working memory and GAP-43 expression. *Behavioural Brain Research*, *362*, 208–212. https://doi.org/10.1016/j.bbr.2019.01.023

Maslen, H., Earp, B. D., Cohen Kadosh, R., & Savulescu, J. (2014). Brain stimulation for treatment and enhancement in children: An ethical analysis. *Frontiers in Human Neuroscience*, *0*. https://doi.org/10.3389/fnhum.2014.00953

Matsunaga, K., Nitsche, M. A., Tsuji, S., & Rothwell, J. C. (2004). Effect of transcranial DC sensorimotor cortex stimulation on somatosensory evoked potentials in humans. *Clinical Neurophysiology*, *115*(2), 456–460. https://doi.org/10.1016/S1388-2457(03)00362-6

McDermott, T. J., Wiesman, A. I., Mills, M. S., Spooner, R. K., Coolidge, N. M., Proskovec, A. L., Heinrichs-Graham, E., & Wilson, T. W. (2019). TDCS modulates behavioral performance and the neural oscillatory dynamics serving visual selective attention. *Human Brain Mapping*, *40*(3), 729–740. https://doi.org/10.1002/hbm.24405

McFadden, J. L., Borckardt, J. J., George, M. S., & Beam, W. (2011). Reducing Procedural Pain and Discomfort Associated with Transcranial Direct Current Stimulation. *Brain Stimulation*, *4*(1), 38–42. https://doi.org/10.1016/j.brs.2010.05.002

Metuki, N., Sela, T., & Lavidor, M. (2012). Enhancing cognitive control components of insight problems solving by anodal tDCS of the left dorsolateral prefrontal cortex. *Brain Stimulation*, *5*(2), 110–115. https://doi.org/10.1016/j.brs.2012.03.002

Miniussi, C., & Ruzzoli, M. (2013). Transcranial stimulation and cognition. *Handbook of Clinical Neurology*, *116*, 739–750. https://doi.org/10.1016/B978-0-444-53497-2.00056-5

Miranda, P. C., Faria, P., & Hallett, M. (2009). What does the ratio of injected current to electrode area tell us about current density in the brain during tDCS? *Clinical Neurophysiology: Official Journal of the International Federation of Clinical Neurophysiology*, *120*(6), 1183–1187. https://doi.org/10.1016/j.clinph.2009.03.023

Miranda, P. C., Lomarev, M., & Hallett, M. (2006). Modeling the current distribution during transcranial direct current stimulation. *Clinical Neurophysiology: Official Journal of the International Federation of Clinical Neurophysiology*, *117*(7), 1623–1629. https://doi.org/10.1016/j.clinph.2006.04.009

Moliadze, V., Antal, A., & Paulus, W. (2010). Electrode-distance dependent after-effects of transcranial direct and random noise stimulation with extracephalic reference electrodes. *Clinical Neurophysiology*, *121*(12), 2165–2171. https://doi.org/10.1016/j.clinph.2010.04.033

Monai, H., Ohkura, M., Tanaka, M., Oe, Y., Konno, A., Hirai, H., Mikoshiba, K., Itohara, S., Nakai, J., Iwai, Y., & Hirase, H. (2016). Calcium imaging reveals glial involvement in transcranial direct current stimulation-induced plasticity in mouse brain. *Nature Communications*, *7*(1), 11100. https://doi.org/10.1038/ncomms11100

Monte-Silva, K., Kuo, M.-F., Hessenthaler, S., Fresnoza, S., Liebetanz, D., Paulus, W., & Nitsche, M. A. (2013). Induction of late LTP-like plasticity in the human motor

cortex by repeated non-invasive brain stimulation. *Brain Stimulation*, *6*(3), 424–432. https://doi.org/10.1016/j.brs.2012.04.011

Mordillo-Mateos, L., Turpin-Fenoll, L., Millán-Pascual, J., Núñez-Pérez, N., Panyavin, I., Gómez-Argüelles, J. M., Botia-Paniagua, E., Foffani, G., Lang, N., & Oliviero, A. (2012). Effects of simultaneous bilateral tDCS of the human motor cortex. *Brain Stimulation*, *5*(3), 214–222. https://doi.org/10.1016/j.brs.2011.05.001

Moreno-Duarte, I., Morse, L. R., Alam, M., Bikson, M., Zafonte, R., & Fregni, F. (2014). Targeted therapies using electrical and magnetic neural stimulation for the treatment of chronic pain in spinal cord injury. *NeuroImage*, *85 Pt 3*, 1003–1013. https://doi.org/10.1016/j.neuroimage.2013.05.097

Morrell, F. (1962). [Anodic surface polarization effect on motor response and on the nature of discharges from individual cortical cells]. *Fiziologicheskii zhurnal SSSR imeni I. M. Sechenova*, *48*, 251–263.

Neuling, T., Rach, S., & Herrmann, C. S. (2013). Orchestrating neuronal networks: Sustained after-effects of transcranial alternating current stimulation depend upon brain states. *Frontiers in Human Neuroscience*, *7*. https://doi.org/10.3389/fnhum.2013.00161

Nimmrich, V., Draguhn, A., & Axmacher, N. (2015). Neuronal Network Oscillations in Neurodegenerative Diseases. *NeuroMolecular Medicine*, *17*(3), 270–284. https://doi.org/10.1007/s12017-015-8355-9

Nitsche, M. A., & Bikson, M. (2017). Extending the parameter range for tDCS: Safety and tolerability of 4 mA stimulation. *Brain Stimulation*, *10*(3), 541–542. https://doi.org/10.1016/j.brs.2017.03.002

Nitsche, M. A., Cohen, L. G., Wassermann, E. M., Priori, A., Lang, N., Antal, A., Paulus, W., Hummel, F., Boggio, P. S., Fregni, F., & Pascual-Leone, A. (2008). Transcranial direct current stimulation: State of the art. *Brain Stimulation*, *1*(3), 206–223. https://doi.org/10.1016/j.brs.2008.06.004

Nitsche, M. A., Liebetanz, D., Antal, A., Lang, N., Tergau, F., & Paulus, W. (2003). Modulation of cortical excitability by weak direct current stimulation—Technical, safety and functional aspects. *Supplements to Clinical Neurophysiology*, *56*, 255–276. https://doi.org/10.1016/s1567-424x(09)70230-2

Nitsche, M. A., Liebetanz, D., Lang, N., Antal, A., Tergau, F., & Paulus, W. (2003). Safety criteria for transcranial direct current stimulation (tDCS) in humans. *Clinical Neurophysiology*, *114*(11), 2220–2222.

Nitsche, M. A., Nitsche, M. S., Klein, C. C., Tergau, F., Rothwell, J. C., & Paulus, W. (2003). Level of action of cathodal DC polarisation induced inhibition of the human motor cortex. *Clinical Neurophysiology*, *114*(4), 600–604. https://doi.org/10.1016/S1388-2457(02)00412-1

Nitsche, M. A., & Paulus, W. (2000). Excitability changes induced in the human motor cortex by weak transcranial direct current stimulation. *The Journal of Physiology*, *527*(3), 633–639. http://onlinelibrary.wiley.com/doi/10.1111/j.1469-7793.2000.t01-1-00633.x/full

Nitsche, M. A., & Paulus, W. (2001). Sustained excitability elevations induced by transcranial DC motor cortex stimulation in humans. *Neurology*, *57*(10), 1899–1901. https://doi.org/10.1212/wnl.57.10.1899

Nitsche, M. A., & Paulus, W. (2011). Transcranial direct current stimulation–update 2011. *Restorative Neurology and Neuroscience*, *29*(6), 463–492. http://content.iospress.com/articles/restorative-neurology-and-neuroscience/rnn618

Nunez, P. L., & Srinivasan, R. (2006). A theoretical basis for standing and traveling brain waves measured with human EEG with implications for an integrated consciousness. *Clinical Neurophysiology: Official Journal of the International Federation of Clinical Neurophysiology*, *117*(11), 2424–2435. https://doi.org/10.1016/j.clinph.2006.06.754

Opitz, A., Paulus, W., Will, S., Antunes, A., & Thielscher, A. (2015). Determinants of the electric field during transcranial direct current stimulation. *NeuroImage*, *109*, 140–150. https://doi.org/10.1016/j.neuroimage.2015.01.033

Orban, G. A., Van Essen, D., & Vanduffel, W. (2004). Comparative mapping of higher visual areas in monkeys and humans. *Trends in Cognitive Sciences*, *8*(7), 315–324. https://doi.org/10.1016/j.tics.2004.05.009

Ozen, S., Sirota, A., Belluscio, M. A., Anastassiou, C. A., Stark, E., Koch, C., & Buzsaki, G. (2010). Transcranial Electric Stimulation Entrains Cortical Neuronal Populations in Rats. *Journal of Neuroscience*, *30*(34), 11476–11485. https://doi.org/10.1523/JNEUROSCI.5252-09.2010

Parasuraman, R., & McKinley, R. A. (2014). Using noninvasive brain stimulation to accelerate learning and enhance human performance. *Human Factors*, *56*(5), 816–824. https://doi.org/10.1177/0018720814538815

Parazzini, M., Fiocchi, S., Liorni, I., Rossi, E., Cogiamanian, F., Vergari, M., Priori, A., & Ravazzani, P. (2014). Modeling the current density generated by transcutaneous spinal direct current stimulation (tsDCS). *Clinical Neurophysiology: Official Journal of the International Federation of Clinical Neurophysiology*, *125*(11), 2260–2270. https://doi.org/10.1016/j.clinph.2014.02.027

Parkin, B. L., Ekhtiari, H., & Walsh, V. F. (2015). Non-invasive Human Brain Stimulation in Cognitive Neuroscience: A Primer. *Neuron*, *87*(5), 932–945. https://doi.org/10.1016/j.neuron.2015.07.032

Patel, H. J., Romanzetti, S., Pellicano, A., Nitsche, M. A., Reetz, K., & Binkofski, F. (2019). Proton Magnetic Resonance Spectroscopy of the motor cortex reveals long term GABA change following anodal Transcranial Direct Current Stimulation. *Scientific Reports*, *9*(1), 2807. https://doi.org/10.1038/s41598-019-39262-7

Paulus, W. (2011). Transcranial electrical stimulation (tES - tDCS; tRNS, tACS) methods. *Neuropsychological Rehabilitation*, *21*(5), 602–617. https://doi.org/10.1080/09602011.2011.557292

Pelletier, S. J., Lagacé, M., St-Amour, I., Arsenault, D., Cisbani, G., Chabrat, A., Fecteau, S., Lévesque, M., & Cicchetti, F. (2014). The morphological and molecular changes of brain cells exposed to direct current electric field stimulation. *The International Journal of Neuropsychopharmacology*, *18*(5). https://doi.org/10.1093/ijnp/pyu090

Petti, M., Astolfi, L., Masciullo, M., Clausi, S., Pichiorri, F., Cincotti, F., Mattia, D., & Molinari, M. (2017). Transcranial cerebellar direct current stimulation: Effects on brain resting state oscillatory and network activity. *2017 39th Annual International Conference of the IEEE Engineering in Medicine and Biology Society (EMBC)*, 4359–4362. https://doi.org/10.1109/EMBC.2017.8037821

Pirulli, C., Fertonani, A., & Miniussi, C. (2013). The Role of Timing in the Induction of Neuromodulation in Perceptual Learning by Transcranial Electric Stimulation. *Brain Stimulation*, *6*(4), 683–689. https://doi.org/10.1016/j.brs.2012.12.005

Pirulli, C., Fertonani, A., & Miniussi, C. (2014). Is neural hyperpolarization by cathodal stimulation always detrimental at the behavioral level? *Frontiers in Behavioral Neuroscience*, *8*, 226. https://doi.org/10.3389/fnbeh.2014.00226

Polanía, R., Nitsche, M. A., & Paulus, W. (2011). Modulating functional connectivity patterns and topological functional organization of the human brain with transcranial direct current stimulation. *Human Brain Mapping*, *32*(8), 1236–1249. https://doi.org/10.1002/hbm.21104

Polanía, R., Paulus, W., Antal, A., & Nitsche, M. A. (2011). Introducing graph theory to track for neuroplastic alterations in the resting human brain: A transcranial direct current stimulation study. *NeuroImage*, *54*(3), 2287–2296. https://doi.org/10.1016/j.neuroimage.2010.09.085

Preuss, TM. (2000). *Taking the Measure of Diversity: Comparative Alternatives to the Model-Animal Paradigm in Cortical Neuroscience*. *55*, 287–299.

Priori, A., Berardelli, A., Rona, S., Accornero, N., & Manfredi, M. (1998). Polarization of the human motor cortex through the scalp. *Neuroreport*, *9*(10), 2257–2260. https://doi.org/10.1097/00001756-199807130-00020

Puig, M. V., Antzoulatos, E. G., & Miller, E. K. (2014). Prefrontal dopamine in associative learning and memory. *Neuroscience*, *282*, 217–229. https://doi.org/10.1016/j.neuroscience.2014.09.026

Puig, M. V., & Miller, E. K. (2012). The Role of Prefrontal Dopamine D1 Receptors in the Neural Mechanisms of Associative Learning. *Neuron*, *74*(5), 10.1016/j.neuron.2012.04.018. https://doi.org/10.1016/j.neuron.2012.04.018

Purpura, D. P., & McMurtry, J. G. (1965). Intracellular activities and evoked potential changes during polarization of motor cortex. *Journal of Neurophysiology*, *28*(1), 166–185. http://jn.physiology.org/content/28/1/166.short

Radman, T., Ramos, R. L., Brumberg, J. C., & Bikson, M. (2009). Role of cortical cell type and morphology in subthreshold and suprathreshold uniform electric field stimulation in vitro. *Brain Stimulation: Basic, Translational, and Clinical Research in Neuromodulation*, *2*(4), 215-228.e3. https://doi.org/10.1016/j.brs.2009.03.007

Ranieri, F., Podda, M. V., Riccardi, E., Frisullo, G., Dileone, M., Profice, P., Pilato, F., Di Lazzaro, V., & Grassi, C. (2012). Modulation of LTP at rat hippocampal CA3-CA1 synapses by direct current stimulation. *Journal of Neurophysiology*, *107*(7), 1868–1880. https://doi.org/10.1152/jn.00319.2011

Reato, D., Rahman, A., Bikson, M., & Parra, L. C. (2010). Low-Intensity Electrical Stimulation Affects Network Dynamics by Modulating Population Rate and Spike Timing. *Journal of Neuroscience*, *30*(45), 15067–15079. https://doi.org/10.1523/JNEUROSCI.2059-10.2010

Reato, D., Rahman, A., Bikson, M., & Parra, L. C. (2013). Effects of weak transcranial alternating current stimulation on brain activity—A review of known mechanisms from animal studies. *Frontiers in Human Neuroscience*, *0*. https://doi.org/10.3389/fnhum.2013.00687

Reinhart, R. M. G., Cosman, J. D., Fukuda, K., & Woodman, G. F. (2017). Using transcranial direct-current stimulation (tDCS) to understand cognitive processing. *Attention, Perception & Psychophysics*, *79*(1), 3–23. https://doi.org/10.3758/s13414-016-1224-2

Reinhart, R. M. G., & Woodman, G. F. (2015). The surprising temporal specificity of direct-current stimulation. *Trends in Neurosciences*, *38*(8), 459–461. https://doi.org/10.1016/j.tins.2015.05.009

Reinhart, R. M. G., Zhu, J., Park, S., & Woodman, G. F. (2015). Synchronizing theta oscillations with direct-current stimulation strengthens adaptive control in the human brain. *Proceedings of the National Academy of Sciences*, *112*(30), 9448–9453. https://doi.org/10.1073/pnas.1504196112

Rilling JK. (2006). *Human and nonhuman primate brains: Are they allometrically scaled versions of the same design? 15*(2), 65–77. https://onlinelibrary.wiley.com/doi/abs/10.1002/evan.20095

Rossi, S., Hallett, M., Rossini, P. M., & Pascual-Leone, A. (2009). Safety, ethical considerations, and application guidelines for the use of transcranial magnetic stimulation in clinical practice and research. *Clinical Neurophysiology*, *120*(12), 2008–2039. https://doi.org/10.1016/j.clinph.2009.08.016

Rostami, M., Golesorkhi, M., & Ekhtiari, H. (2013). Methodological Dimensions of Transcranial Brain Stimulation with the Electrical Current in Human. *Basic and Clinical Neuroscience*, *4*, 8–26.

Rueger, M. A., Keuters, M. H., Walberer, M., Braun, R., Klein, R., Sparing, R., Fink, G. R., Graf, R., & Schroeter, M. (2012). Multi-session transcranial direct current stimulation (tDCS) elicits inflammatory and regenerative processes in the rat brain. *PloS One*, *7*(8), e43776. https://doi.org/10.1371/journal.pone.0043776

Ruohonen, J., & Karhu, J. (2012). TDCS possibly stimulates glial cells. *Clinical Neurophysiology: Official Journal of the International Federation of Clinical Neurophysiology*, *123*(10), 2006–2009. https://doi.org/10.1016/j.clinph.2012.02.082

Rush, S., & Driscoll, D. A. (1968). Current distribution in the brain from surface electrodes. *Anesthesia and Analgesia*, *47*(6), 717–723.

Russell, M. J., Goodman, T. A., Visse, J. M., Beckett, L., Saito, N., Lyeth, B. G., & Recanzone, G. H. (2017). Sex and Electrode Configuration in Transcranial Electrical Stimulation. *Frontiers in Psychiatry*, *8*. https://doi.org/10.3389/fpsyt.2017.00147

Russell, M. J., Goodman, T., Pierson, R., Shepherd, S., Wang, Q., Groshong, B., & Wiley, D. F. (2013). Individual differences in transcranial electrical stimulation current density. *Journal of Biomedical Research*, *27*(6), 495–508. https://doi.org/10.7555/JBR.27.20130074

Russo, R., Wallace, D., Fitzgerald, P. B., & Cooper, N. R. (2013). Perception of comfort during active and sham transcranial direct current stimulation: A double blind study. *Brain Stimulation*, *6*(6), 946–951. https://doi.org/10.1016/j.brs.2013.05.009

Sánchez-León, C. A., Cordones, I., Ammann, C., Ausín, J. M., Gómez-Climent, M. A., Carretero-Guillén, A., Campos, G. S.-G., Gruart, A., Delgado-García, J. M., Cheron, G., Medina, J. F., & Márquez-Ruiz, J. (2020). Immediate and long-term effects of transcranial direct-current stimulation in the mouse primary somatosensory cortex. *BioRxiv*, 2020.07.02.184788. https://doi.org/10.1101/2020.07.02.184788

Sánchez-León, C. A., Cordones, I., Ammann, C., Ausín, J. M., Gómez-Climent, M. A., Carretero-Guillén, A., Sánchez-Garrido Campos, G., Gruart, A., Delgado-García, J. M., Cheron, G., Medina, J. F., & Márquez-Ruiz, J. (2021). Immediate and after effects of transcranial direct-current stimulation in the mouse primary somatosensory cortex. *Scientific Reports*, *11*(1), 3123. https://doi.org/10.1038/s41598-021-82364-4

Santarnecchi, E., Brem, A.-K., Levenbaum, E., Thompson, T., Kadosh, R. C., & Pascual-Leone, A. (2015). Enhancing cognition using transcranial electrical stimulation. *Current Opinion in Behavioral Sciences*, *4*, 171–178. https://doi.org/10.1016/j.cobeha.2015.06.003

Sarmiento, C. I., San-Juan, D., & Prasath, V. B. S. (2016). Letter to the Editor: Brief history of transcranial direct current stimulation (tDCS): from electric fishes to microcontrollers. *Psychological Medicine*, *46*(15), 3259–3261. https://doi.org/10.1017/S0033291716001926

Schestatsky, P., Morales-Quezada, L., & Fregni, F. (2013). Simultaneous EEG Monitoring During Transcranial Direct Current Stimulation. *Journal of Visualized Experiments*, *76*. https://doi.org/10.3791/50426

Schnitzler, A., & Gross, J. (2005). Normal and pathological oscillatory communication in the brain. *Nature Reviews Neuroscience*, *6*(4), 285–296. https://doi.org/10.1038/nrn1650

Schwiedrzik, C. M. (2009). Retina or visual cortex? The site of phosphene induction by transcranial alternating current stimulation. *Frontiers in Integrative Neuroscience*, *3*, 6. https://doi.org/10.3389/neuro.07.006.2009

Selemon, L. D., & Goldman-Rakic, P. S. (1985). Longitudinal topography and interdigitation of corticostriatal projections in the rhesus monkey. *The Journal of Neuroscience: The Official Journal of the Society for Neuroscience*, *5*(3), 776–794.

Semendeferi. (2001). Prefrontal cortex in humans and apes: A comparative study of area 10. *American Journal of Physical Anthropology*. https://onlinelibrary.wiley.com/doi/abs/10.1002/1096-8644(200103)114:3%3C224::AID-AJPA1022%3E3.0.CO;2-I

Shenoy, S., Bose, A., Chhabra, H., Dinakaran, D., Agarwal, S., Shivakumar, V., Narayanaswamy, J., Sivakumar, P., & Venkatasubramanian, G. (2015). Transcranial direct current stimulation (tDCS) for auditory verbal hallucinations in schizophrenia during pregnancy: A case report. *Brain Stimulation*, *8*(1), 163–164. https://doi.org/10.1016/j.brs.2014.10.010

Silvanto, J., Muggleton, N., & Walsh, V. (2008). State-dependency in brain stimulation studies of perception and cognition. *Trends in Cognitive Sciences*, *12*(12), 447–454. https://doi.org/10.1016/j.tics.2008.09.004

Smith, R. C., Boules, S., Mattiuz, S., Youssef, M., Tobe, R. H., Sershen, H., Lajtha, A., Nolan, K., Amiaz, R., & Davis, J. M. (2015). Effects of transcranial direct current stimulation (tDCS) on cognition, symptoms, and smoking in schizophrenia: A randomized controlled study. *Schizophrenia Research*, *168*(1–2), 260–266. https://doi.org/10.1016/j.schres.2015.06.011

Sohn, M. K., Jee, S. J., & Kim, Y. W. (2013). Effect of Transcranial Direct Current Stimulation on Postural Stability and Lower Extremity Strength in Hemiplegic Stroke Patients. *Annals of Rehabilitation Medicine*, *37*(6), 759. https://doi.org/10.5535/arm.2013.37.6.759

Stafford, J., Brownlow, M. L., Qualley, A., & Jankord, R. (2018). AMPA receptor translocation and phosphorylation are induced by transcranial direct current stimulation in rats. *Neurobiology of Learning and Memory*, *150*, 36–41. https://doi.org/10.1016/j.nlm.2017.11.002

Stagg, C. J., Best, J. G., Stephenson, M. C., O'Shea, J., Wylezinska, M., Kincses, Z. T., Morris, P. G., Matthews, P. M., & Johansen-Berg, H. (2009). Polarity-Sensitive Modulation of Cortical Neurotransmitters by Transcranial Stimulation. *Journal of Neuroscience*, *29*(16), 5202–5206. https://doi.org/10.1523/JNEUROSCI.4432-08.2009

Stagg, C. J., & Nitsche, M. A. (2011). Physiological basis of transcranial direct current stimulation. *The Neuroscientist: A Review Journal Bringing Neurobiology, Neurology and Psychiatry*, *17*(1), 37–53. https://doi.org/10.1177/1073858410386614

Subiaul, F. (2007). The imitation faculty in monkeys: Evaluating its features, distribution and evolution. *JASs Invited Reviews Journal of Anthropological Sciences*, *85*, 35–62.

Sun, Y., Lipton, J. O., Boyle, L. M., Madsen, J. R., Goldenberg, M. C., Pascual-Leone, A., Sahin, M., & Rotenberg, A. (2016). Direct current stimulation induces mGluR5-dependent neocortical plasticity. *Annals of Neurology*, *80*(2), 233–246. https://doi.org/10.1002/ana.24708

Tada, M., Suda, Y., Kirihara, K., Koshiyama, D., Fujioka, M., Usui, K., Araki, T., Kasai, K., & Uka, T. (2020). Translatability of Scalp EEG Recordings of Duration-Deviant Mismatch Negativity Between Macaques and Humans: A Pilot Study. *Frontiers in Psychiatry*, *11*, 874. https://doi.org/10.3389/fpsyt.2020.00874

Tanaka, T., Takano, Y., Tanaka, S., Hironaka, N., Kobayashi, K., Hanakawa, T., Watanabe, K., & Honda, M. (2013). Transcranial direct-current stimulation increases extracellular dopamine levels in the rat striatum. *Frontiers in Systems Neuroscience*, *7*, 6. https://doi.org/10.3389/fnsys.2013.00006

Tavakoli, A. V., & Yun, K. (2017). Transcranial Alternating Current Stimulation (tACS) Mechanisms and Protocols. *Frontiers in Cellular Neuroscience*, *11*, 214. https://doi.org/10.3389/fncel.2017.00214

Teo, F., Hoy, K. E., Daskalakis, Z. J., & Fitzgerald, P. B. (2011). Investigating the Role of Current Strength in tDCS Modulation of Working Memory Performance in Healthy Controls. *Frontiers in Psychiatry*, *2*, 45. https://doi.org/10.3389/fpsyt.2011.00045

Terney, D., Chaieb, L., Moliadze, V., Antal, A., & Paulus, W. (2008). Increasing human brain excitability by transcranial high-frequency random noise stimulation. *The Journal of Neuroscience: The Official Journal of the Society for Neuroscience*, *28*(52), 14147–14155. https://doi.org/10.1523/JNEUROSCI.4248-08.2008

Utz, K. S., Dimova, V., Oppenländer, K., & Kerkhoff, G. (2010). Electrified minds: Transcranial direct current stimulation (tDCS) and Galvanic Vestibular Stimulation (GVS) as methods of non-invasive brain stimulation in neuropsychology—A review of current data and future implications. *Neuropsychologia*, *48*(10), 2789–2810. https://doi.org/10.1016/j.neuropsychologia.2010.06.002

Villamar, M. F., Volz, M. S., Bikson, M., Datta, A., DaSilva, A. F., & Fregni, F. (2013). Technique and Considerations in the Use of 4x1 Ring High-definition Transcranial Direct Current Stimulation (HD-tDCS). *Journal of Visualized Experiments : JoVE*, *77*. https://doi.org/10.3791/50309

Vöröslakos, M., Takeuchi, Y., Brinyiczki, K., Zombori, T., Oliva, A., Fernández-Ruiz, A., Kozák, G., Kincses, Z. T., Iványi, B., Buzsáki, G., & Berényi, A. (2018). Direct effects of transcranial electric stimulation on brain circuits in rats and humans. *Nature Communications*, *9*(1), 483. https://doi.org/10.1038/s41467-018-02928-3

Wagner, T., Fregni, F., Fecteau, S., Grodzinsky, A., Zahn, M., & Pascual-Leone, A. (2007). Transcranial direct current stimulation: A computer-based human model study. *NeuroImage*, *35*(3), 1113–1124. https://doi.org/10.1016/j.neuroimage.2007.01.027

Wang, X., Wong, W. -w, Fang, Y., CHU, W. C. -w, Wong, K. -s, & Tong, R. K. -y. (2018). Dynamic Influence of Ongoing Brain Stimulation on Resting State fMRI Connectivity: A Concurrent tDCS-fMRI Study. *2018 40th Annual International Conference of the IEEE Engineering in Medicine and Biology Society (EMBC)*, 1037–1040. https://doi.org/10.1109/EMBC.2018.8512430

Weiss, M., & Lavidor, M. (2012). When Less Is More: Evidence for a Facilitative Cathodal tDCS Effect in Attentional Abilities. *Journal of Cognitive Neuroscience*, *24*(9), 1826–1833. https://doi.org/10.1162/jocn_a_00248

Wilson, T. W., McDermott, T. J., Mills, M. S., Coolidge, N. M., & Heinrichs-Graham, E. (2018). tDCS Modulates Visual Gamma Oscillations and Basal Alpha Activity in

Occipital Cortices: Evidence from MEG. *Cerebral Cortex*, *28*(5), 1597–1609. https://doi.org/10.1093/cercor/bhx055

Woodman, G. F., Kang, M.-S., Rossi, A. F., & Schall, J. D. (2007). Nonhuman primate event-related potentials indexing covert shifts of attention. *Proceedings of the National Academy of Sciences of the United States of America*, *104*(38), 15111–15116. https://doi.org/10.1073/pnas.0703477104

Woods, A. J., Antal, A., Bikson, M., Boggio, P. S., Brunoni, A. R., Celnik, P., Cohen, L. G., Fregni, F., Herrmann, C. S., Kappenman, E. S., Knotkova, H., Liebetanz, D., Miniussi, C., Miranda, P. C., Paulus, W., Priori, A., Reato, D., Stagg, C., Wenderoth, N., & Nitsche, M. A. (2016). A technical guide to tDCS, and related non-invasive brain stimulation tools. *Clinical Neurophysiology*, *127*(2), 1031–1048. https://doi.org/10.1016/j.clinph.2015.11.012

Woods, A. J., Bryant, V., Sacchetti, D., Gervits, F., & Hamilton, R. (2015). Effects of Electrode Drift in Transcranial Direct Current Stimulation. *Brain Stimulation*, *8*(3), 515–519. https://doi.org/10.1016/j.brs.2014.12.007

Wu, Y.-J., Chien, M.-E., Chiang, C.-C., Huang, Y.-Z., Durand, D. M., & Hsu, K.-S. (2021). Delta oscillation underlies the interictal spike changes after repeated transcranial direct current stimulation in a rat model of chronic seizures. *Brain Stimulation*, *14*(4), 771–779. https://doi.org/10.1016/j.brs.2021.04.025

Wu, Y.-J., Lin, C.-C., Yeh, C.-M., Chien, M.-E., Tsao, M.-C., Tseng, P., Huang, C.-W., & Hsu, K.-S. (2017). Repeated transcranial direct current stimulation improves cognitive dysfunction and synaptic plasticity deficit in the prefrontal cortex of streptozotocin-induced diabetic rats. *Brain Stimulation*, *10*(6), 1079–1087. https://doi.org/10.1016/j.brs.2017.08.007

Yin, D., Valles, F. E., Fiandaca, M. S., Forsayeth, J., Larson, P., Starr, P., & Bankiewicz, K. S. (2009). Striatal Volume Differences Between Non-human and Human Primates. *Journal of Neuroscience Methods*, *176*(2), 200–205. https://doi.org/10.1016/j.jneumeth.2008.08.027

Zaghi, S., Acar, M., Hultgren, B., Boggio, P. S., & Fregni, F. (2010). Noninvasive brain stimulation with low-intensity electrical currents: Putative mechanisms of action for direct and alternating current stimulation. *The Neuroscientist: A Review Journal Bringing Neurobiology, Neurology and Psychiatry*, *16*(3), 285–307. https://doi.org/10.1177/1073858409336227